

**Development of Titania-Supported Iridium
Catalysts for the Green Synthesis of
Nitrogen-Containing Chemicals**

Han Yu



March 2022

Table of content

Chapter I General Introduction	1
1.1 Green chemistry	1
1.1.1 Development of green chemistry	1
1.1.2 Conception of green chemistry	5
1.1.3 Green chemistry in practice	5
1.2 Transition metal catalyst	9
1.2.1 Transition metal catalysts in organic synthesis	10
1.2.2 Iridium homogeneous and heterogeneous catalysts	11
1.3 Synthesis of nitrogen-containing chemicals	17
1.3.1 Synthesis of amines	17
1.3.2 Synthesis of benzimidazoles	26
1.3.3 Synthesis of benzoxazoles	34
1.4 Supports in the heterogeneous catalysis	35
1.4.1 Overview of Supports for heterogeneous catalyst	35
1.4.2 Strong metal support interaction (SMSI)	38
1.4.3 Titania as catalyst support	39
1.5 Purposes of present study	42
1.6 References	44
Chapter II Rapid Multialkylation of Aqueous Ammonia with Alcohols by Heterogeneous Iridium Catalyst under Simple Conditions	61

2.1	Introduction	61
2.2	Experimental section	62
2.2.1	General information	62
2.2.2	Preparation of supported iridium catalyst	63
2.2.3	General procedure for the catalytic runs	64
2.2.4	Physical and analytical measurements	64
2.3	Results and discussion	66
2.4	Conclusion	84
2.5	References	84

Chapter III Effect of Phosphorus-Modification of Titania Supports on the

Iridium-Catalyzed Synthesis of Benzimidazoles 61

3.1	Introduction	89
3.2	Experiment section	90
3.2.1	General information	90
3.2.2	Preparation of phosphorus-doped rutile titania by a hydrothermal method	91
3.2.3	Preparation of phosphorus-modified TiO ₂ by an impregnation method	91
3.2.4	Preparation of supported iridium catalyst	91
3.2.5	General procedure for the catalytic runs	92
3.2.6	Hot filtration tests	93
3.2.7	Physical and analytical measurements	93
3.3	Results and discussion	94
3.3.1	Effects of phosphorus-doped rutile prepared by the hydrothermal method	94
3.3.2	Effects of phosphorus-modification of titania by the impregnation method	100

3.4	Conclusion	112
3.5	References	113
Chapter IV Development of Titania-Supported Iridium Catalysts for the		
Acceptor-Less Dehydrogenative Synthesis of Benzoxazoles		
4.1	Introduction	119
4.2	Experiment section	120
4.2.1	General information	120
4.2.2	Preparation of supported iridium catalyst	121
4.2.3	General procedure for catalytic runs	122
4.2.4	Physical and analytical measurements	122
4.3	Results and discussion	123
4.3.1	Effects of titania support on the dehydrogenative synthesis of 2-phenyl benzoxazole	123
4.3.2	Effect of $[\text{Ir}(\text{cod})\text{Cl}]_2$ as an Ir precursor on the catalytic activity	129
4.4	Conclusion	138
4.5	References	138
Chapter V Summary		
Publications		
Publications in journal		
Conference		
Acknowledgment		

Chapter I General Introduction

1.1 Green chemistry

1.1.1 Development of green chemistry

Chemistry is an essential branch of science with a long history from prehistoric times [1]. Based on the rapid development of theory and experiment, chemistry has become one of the cornerstones of human civilization in the recent two hundred years [2]. On account of chemical technology, many problems that limit human development have been effectively solved.

However, while bringing people great benefits, the chemical industry has also brought severe environmental problems such as air and freshwater pollution, acid rain, global warming, etc. [3]. These issues affected the world in climate change, sharp drop in forest resources, land resources degradation, and biodiversity reduction. As early as the 1960s, chemical pollution began to show its adverse effects on human settlements, and people were gradually becoming aware of the existence of environmental hazards. For example, dichlorodiphenyltrichloroethane (DDT) solved the problem of pests and diseases, but it also brought a blow to the ecological food chain due to extensive use. This persistent organic pollutant still affects us today [4].

Since then, people have deepened their understanding of the environmental impacts of chemical products and paid a great effort to environmental governance. In 1962, the marine biologist Rachel Carson (1907-1964) published her famous book *Silent Spring*, endorsed by US supreme court justice William O. Douglas (1898-1980). This book urged public awareness of pesticides and environmental pollution [5]. In

1970, the establishment of EPA (Environment Protection Agency) in US brought the environmental problems under the government's control [4]. Subsequently, major international economic cooperation organizations also put environmental issues into the agenda [6]. With the in-depth understanding of environmental problems, the conventional strategy of end-of-pipeline control turned gradually to an approach of front-end pollution prevention [7].

In 1990, US Congress passed the "Pollution Prevention Act" at President George H.W. Bush (1924-2018) [7]. It demands that pollution be prevented or reduced at the source or recycled in an environmentally safe approach [8]. In the following years, the EPA led the development of pollution prevention programs [9]. Meanwhile, Barry M. Trost, an American organic chemist, introduced the concept of atom economy (atom utilization rate) in the same year [10]. It is equal to the ratio of the desired product to the total mass of the products in mass, which describes the conversion efficiency of a chemical process. The proposal of this crucial basic concept has attracted people's great attention and grew the bud of green chemistry. It is noteworthy that the term green chemistry is thrown around repeatedly in the second symposium held by EPA in 1994 [6]. The following year, the Green Chemistry Challenge Award program was announced to promote the prevention of chemical pollution and industrial ecology research [11].

In 1998, Paul T. Anastas and John C. Warner published the well-known book, *Green Chemistry: Theory and Practice* [12]. They proposed the famous "12 principles of green chemistry", making this book the classic green chemistry work. The details of the 12 principles are as follow:

① **Prevention**

It is better to prevent waste than to treat or clean up waste after it is formed.

② **Atom economy**

Synthetic methods should be designed to maximize the incorporation of all materials used in the process into the final product.

③ **Less hazardous chemical syntheses**

Wherever practicable, synthetic methodologies should be designed to use and generate substances that possess little or no toxicity to human health and the environment.

④ **Designing safer chemicals**

Chemical products should be designed to preserve the efficacy of function while reducing toxicity.

⑤ **Safer Solvents and Auxiliaries**

The use of auxiliary substances (e.g., solvents, separation agents, etc.) should be made unnecessary wherever possible and innocuous when used.

⑥ **Design for energy efficiency**

Energy requirements should be recognized for their environmental and economic impacts and should be minimized. Synthetic methods should be conducted at ambient temperature and pressure.

⑦ **Use of renewable feedstock**

A raw material or feedstock should be renewable rather than depleting wherever technically and economically practicable.

⑧ **Reduce derivatives**

Unnecessary derivatization (blocking group, protection/ deprotection, temporary modification) should be avoided whenever possible. Catalytic reagents (as selective as possible) are superior to stoichiometric reagents.

⑨ **Catalysis**

Catalytic reagents (as selective as possible) are superior to stoichiometric reagents.

⑩ **Design for degradation**

Chemical products should be designed so that at the end of their function they do not persist in the environment and break down into innocuous degradation products.

⑪ **Real-time analysis for pollution prevention** Analytical methodologies need to be further developed to allow for real-time, in-process monitoring and control prior to the formation of hazardous substances.

⑫ **Inherently safer chemistry for accident prevention**

Substances and the form of a substance used in a chemical process should be chosen to minimize the potential for chemical accidents, including releases, explosions, and fires.

As a guideline to the development of environmentally benign products and processes, these principles cover all aspects of synthesis and operations, and build up the basic conceptual framework of green chemistry.

After this, green chemistry has emerged in various countries around the world [13]. In UK, the Royal Society of Chemistry established the first international journal Green Chemistry in 1999, marking that green chemistry has become the forefront of chemistry. The Green Chemistry award was launched in 2000. Meanwhile, Japan put forward the concept of “green and sustainable development chemistry (GSC)”. This concept guarantees “human and environmental health and safety” and “energy and resource-saving” through a technological revolution, including product design, raw material

selection, manufacturing method, usage method and recycling [14]. Other countries and major international organizations have also established green chemistry organizations and relevant awards in succession. Since then, the development of green chemistry has entered a new stage [13].

1.1.2 Conception of green chemistry

Green chemistry utilizes a set of principles that reduces or eliminates the use or generation of hazardous substances in the design, manufacture, and application of chemical products [15]. It is now widely applied in organic chemistry, inorganic chemistry, biochemistry, analytical chemistry, and even physical chemistry [16]. Green chemistry is a philosophy and to be a goal that people are striving for [17].

In a scientific view, green chemistry is the innovation and development of thinking in conventional chemistry [18]. While from the economic point of view, green chemistry provides rational utilization of resources and energy and reduces production costs, which is in line with the sustainable economic development [19].

1.1.3 Green chemistry in practice

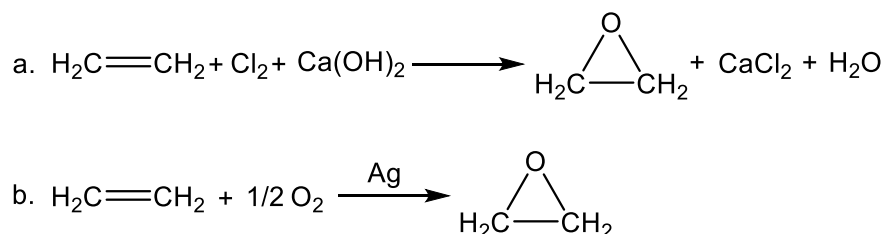
As discussed above, green chemistry is expected to achieve the lowest pollution coefficient and minimum resource consumption per unit product [16]. It fundamentally reduces pollution from the chemical reaction rather than the specialized treatment of terminal waste. In general, a chemical reaction is mainly affected by four aspects: properties of the raw material or starting material, features of synthetic route, reaction conditions, and characteristics of the product or target molecule. To solve the problem of pollution, we have to start from the consideration of these issues.

1. Design reactions in terms of the atom economy

As described above, in 1991, B. Trost first proposed the concept of atom economy: how many per cent of the atoms in the raw materials exactly are converted into products [20]. The ideal atom economy is 100% converting the atoms in the raw material molecules into products with no by-products or waste, thus achieving “Zero-emission” of waste. By designing a reaction via an atomic efficient route, one can consider both resource utilization and environmental protection. Especial for the production of bulk basic organic materials, the application of atom economy is significant for both economic benefits and environmental safety [21].

$$\text{Atom economy} = \frac{\text{Molecular weight of desired products}}{\text{Molecular weight of all products}} * 100\%$$

For example, ethylene oxide is a chemical raw material produced in large quantities, widely applied in the synthesis of antifreeze, surfactants, and polymers [17]. As shown in Scheme 1-a, the reaction has waste calcium chloride and water in the conventional route to synthesize ethylene oxide. In this case, the atom economy is 17%. On the other hand, the silver-catalyzed oxidation of ethylene realized the conversion of all reactants to the desired product and produced no byproduct and the atom economy was greatly increased to 70%.

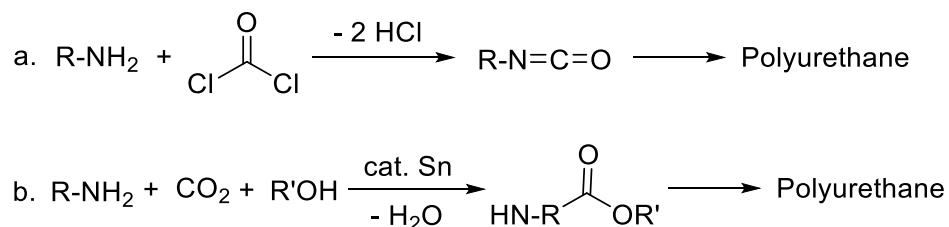


Scheme 1. Synthesis of Ethylene Oxide

2. Utilization of green raw materials

The type of chemical reaction or the nature of the synthetic route depends mainly on the starting material. The choice of initial raw material often determines the hazards and risks in transportation, handling, production processes, and final products [22]. In the current chemical processes, it is inevitable to use toxic and harmful raw materials, such as organic halogen, formaldehyde, ethylene oxide, etc., which seriously pollute the environment and endanger human health and community safety [17]. One of the essential tasks of green chemistry is to replace them with non-toxic and harmless raw materials to produce various chemical products.

For example, in the conventional production of polyurethane, an important industrial raw material [23], isocyanate derived from a primary amine and phosgene is often utilized as a starting material, as shown in Scheme 2-a. There are two potential environmental risks: One is the use of highly toxic and corrosive phosgene, another is the production of hydrogen chloride. To solve this problem, T. Sakakura and coauthor developed a halogen-free catalytic synthetic method using carbon dioxide, alcohols and primary amines catalyzed by Sn catalyst [24]. The use of CO₂ and alcohol is safer and environmentally benign, and the byproduct is only water.

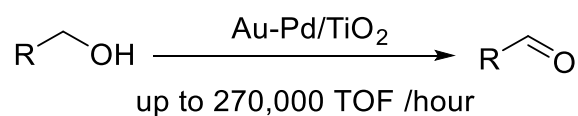


Scheme 2. Synthesis of polyurethane

3. Utilization of green solvent or the operation under the solvent-free conditions

Environmental pollution is derived not only from raw materials and products but also from the substances used in the process of manufacture [25]. The most important one is a solvent used in the synthetic reaction, separation and formulation. Currently, the used solvents mainly belong to volatile organic compounds (VOC), which may harm human health and cause carcinogens, reproductive hazards, and neurotoxins, or pollute the atmosphere and water during use [26]. Therefore, using non-toxic solvents such as water, supercritical fluid, polymers, ionic liquid instead of conventional harmful solvents is significant. The operation under solvent-free conditions is more favorable.

For example, a solvent-free reaction is a clean, economical, efficient and safe procedure [27]. The oxidation of alcohols to aldehydes is an important reaction in the synthesis of fine chemicals. G. J. Hutchings and coauthor uncovered the core-shell type Au-Pd/TiO₂ catalyst exhibit unprecedented activity in the oxidation of alcohols, including primary aliphatic alcohols, in the absence of other solvents [28].



Scheme 3. Oxidation of alcohols

4. Utilization of a catalyst

In chemical synthesis, high-performance catalysts can alter the chemical reaction pathway, lower the reaction's activation energy, increase the product's selectivity, promote the production yield, and reduce energy consumption [19]. Also, the use of stoichiometric reagents can be avoided. As shown in Figure 1, catalysts speed up a reaction by reducing the activation energy and/or changing the reaction mechanism [29]

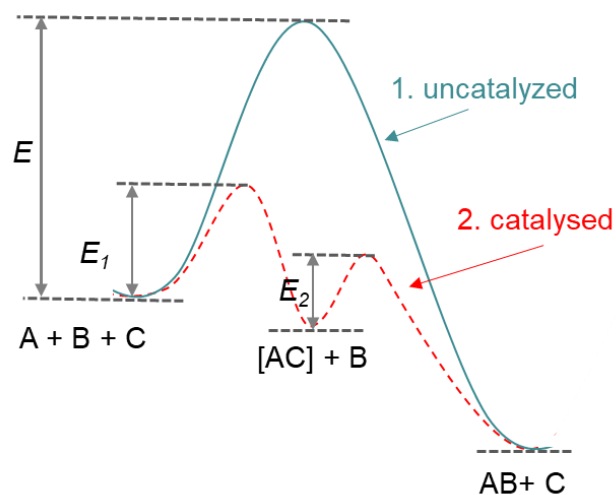


Figure 1. Schematic energy diagrams of the reaction

1.2 Transition metal catalyst

International Union of Pure and Applied Chemistry (IUPAC) defines transition elements as “an element whose atom has an incomplete d sub-shell, or which can give rise to cations with an incomplete d sub-shell [30].” Based on this definition, elements in the d-block elements of the periodic table without group 12 are assigned to the transition metals.

Transition metals exhibit varieties of oxidation states in their compounds, one of their marked features (Table 1). The difference in oxidation states is dependent on the electron configurations of their atoms.

Table 1. Stable oxidation states of the third transition series

Elements	Oxidation States
La	0, +1, +2, +3
Hf	-2, 0, +1, +2, +3, +4
Ta	-3, -1, 0, +1, +2, +3, +4, +5

W	-4, -2, -1, 0, +1, +2, +3, +4, +5, +6
Re	-3, -1, 0, +1, +2, +3, +4, +5, +6, +7
Os	-4, -2, -1, 0, +1, +2, +3, +4, +5, +6, +7, +8
Ir	-3, -1, +1, +2, +3, +4, +5, +6, +7, +8, +9
Pt	-3, -2, -1, 0, +1, +2, +3, +4, +5, +6
Au	-3, -2, -1, 0, +1, +2, +3, +5

Transition metals can form an extensive range of complex ions. A complex ion usually has a metal ion at its center surrounded by molecules or ions. The surrounded molecules or ions are known as ligands or complexing agents. These ligands have lone electron pairs that can be used to form coordination bonds with metal ions.

1.2.1 Transition metal catalysts in organic synthesis

As described above, catalysts provide an alternative route for the reaction to occur. Catalysts affect the transition state of the reaction by providing a low-energy activation pathway. The catalyst affects the reaction rate without affecting the overall standard Gibbs energy change [30].

The excellent catalytic performance of transition metals is mainly dependent on their characteristics: Due to the incompletely filled d orbitals, they can switch between different valence states. Transition metals often form unstable complexes with the reactants because of their variable valence states. The thus formed complex intermediates can find a reaction pathway with lower activation energy. The decrease in activation energy accelerates the reaction rate. These unstable intermediates are then decomposed to form the final product, and the catalyst is regenerated at the end of the reaction.

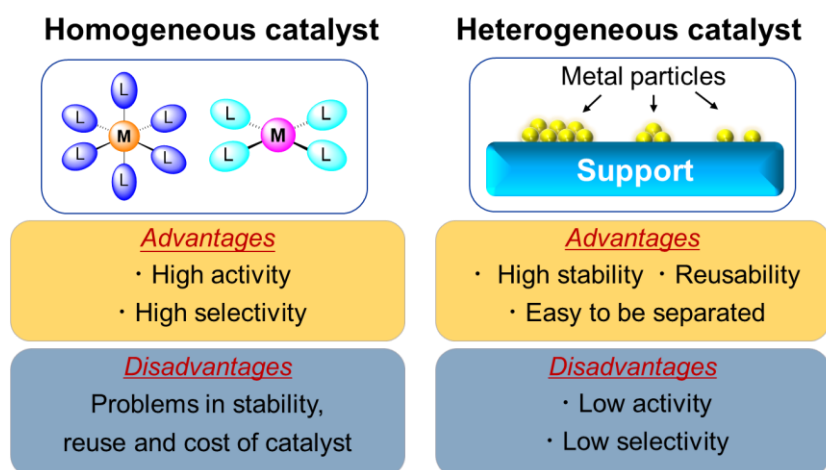


Figure 2. The difference in homogeneous and heterogeneous catalyst.

In general, catalysts can be categorized into two types, heterogeneous and homogeneous. Figure 2 compared the difference between homogeneous and heterogeneous catalysts. In homogeneous catalysis, reactant and catalyst are in the same phase (for example, in liquid phase), while for the heterogeneous catalysts, reactant and catalyst are in different phases (for example, liquid-solid). Homogeneous catalyst is applied, especially in the fine chemical industry. Its advantages are high activity and selectivity, but its disadvantages are stability issues, reuse, and cost of catalyst [31]. Besides, heterogeneous catalysis is advantageous in terms of high stability, reusability, and separation ease [32]. However, often its low activity and selectivity are still a problem.

1.2.2 Iridium homogeneous and heterogeneous catalysts

Iridium is an element in the third transition series of the periodic table. Iridium can possess a valent state ranging from +9 to -3, as shown in Table 2[33,34]. Numerous iridium complexes such as IrCl_3 , IrCl_4 , H_2IrCl_6 , and a serial of organic complex have been reported to show high activities for various reactions as homogeneous catalysts [35–43]. On the other hand, small and stable iridium clusters could be formed on the

surface of specific supports [44]. Nanoscale particles of iridium with a large surface area also exhibit interesting physics and catalytic properties [45,46], similar to those with gold and platinum nanoparticles [47,48]. To date, systematic studies have been made to develop both homogeneous and heterogeneous iridium catalysts [49–54].

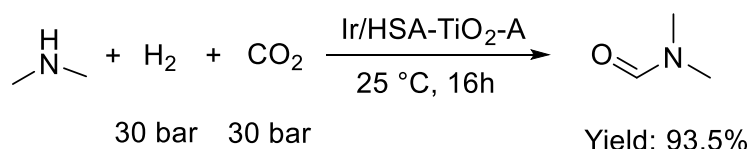
Table 2. Oxidation states of iridium with example [55]

Oxidation states	Example
-3	$[\text{Ir}(\text{CO})_3]^{3-}$
-1	$[\text{Ir}(\text{CO})_3(\text{PPh}_3)]^-$
+0	$[\text{Ir}_4(\text{CO})_{12}]$
+1	$[\text{Ir}(\text{CO})\text{Cl}(\text{PPh}_3)_2]$
+2	$[\text{IrCl}_2]$
+3	$[\text{IrCl}_3]$
+4	$[\text{IrO}_2]$
+5	$[\text{Ir}_4\text{F}_{20}]$
+6	$[\text{IrF}_6]$
+7	$[(\text{n}^2-\text{O}_2)\text{IrO}_2]^+$
+8	$[\text{IrO}_4]$
+9	$[\text{IrO}_4]^+$

Recent progress in the development of heterogeneous iridium catalyst is review as follow:

a. Hydrogenation/ Dehydrogenation

Y. Cao and coauthor prepared bifunctional iridium catalyst supported on high surface area anatase TiO_2 with excellent performance for synthesizing DMF from CO_2 , H_2 , and NHMe_2 under mild aqueous conditions [56]. The study shows that partially reduced iridium oxide (Ir/IrO_x) clusters are responsible for the reductive activation of CO_2 under an H_2 atmosphere.



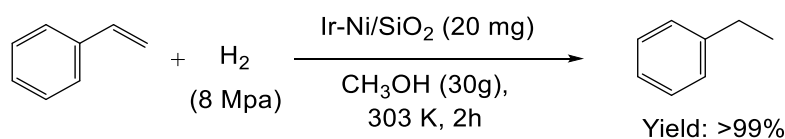
One-step ligand-free method was applied to prepare ceria support iridium (Ir/CeO₂) catalysts for the catalytic carbon dioxide hydrogenation [57]. By changing the loading amount of iridium, the valence state of Ir species can be finely tuned. Thus, the strong metal-support interaction (SMSI) between iridium species and ceria support played a crucial role in selectivity in CO₂ hydrogenation (Table 3). The effect of Ir loading amount on the reaction selectivity was also reported by M. Luo et al. [58]. In the Ir/TiO₂ catalyzed hydrogenation of crotonaldehyde, both the activity (TOF) and selectivity to crotyl alcohol increased as the Ir loading amount increased from 0.5 to 3 wt%, while slightly decreasing with further increasing from 3 to 5 wt%.

Table 3. Catalytic performance of Ir/CeO₂ in CO₂ hydrogenation

Entry	Catalyst	Ir (wt %)	CO ₂ Conversion (%)	CH ₄ Selectivity (%)	CO Selectivity (%)	Activity (mol _{CO2} mol _{Ir} ⁻¹ h ⁻¹)
1	20 Ir/CeO ₂	19.7	8.8	88	12	8.7
2	15 Ir/CeO ₂	15	6.9	56	44	9
3	5 Ir/CeO ₂	5.9	6.8	trace	>99	22.5
4	0.7 Ir/CeO ₂	0.7	2.9	trace	>99	81.1

Recently, M. Tamura and K. Tomishige developed a silica-supported nickel-iridium catalyst for the efficient hydrogenation of olefins with high selectivity [59]. They prepared the catalyst by a simple sequential impregnation method of Ir and Ni species followed by the reduction. The catalyst with the Ni/Ir molar ratio of 1 gave the

desired products high yields over 99% in 2 hours reaction and is applicable in the hydrogenation of various olefins.

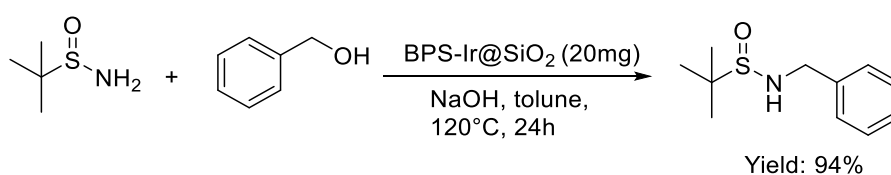


As discussed in the following section, K. Wada and co-workers developed a series of titania-supported iridium catalysts to synthesize benzimidazoles and related compounds via the dehydrogenative pathways [42,60].

b. Hydrogen auto-transfer (Borrowing Hydrogen)

D. Wang and co-workers developed a novel benzothiazole-doped porous organic polymers (POP) supported iridium catalysts with high catalytic activity for borrowing hydrogen and dehydrogenation reactions in water with good recovery performance [61]. The authors show that the present catalyst is superior to the previously reported catalyst in ten reactions, including alcohol, amine, amide, ketone, and biguanides. The catalyst exhibits a high surface area, hierarchical porosity, and thermodynamic stability.

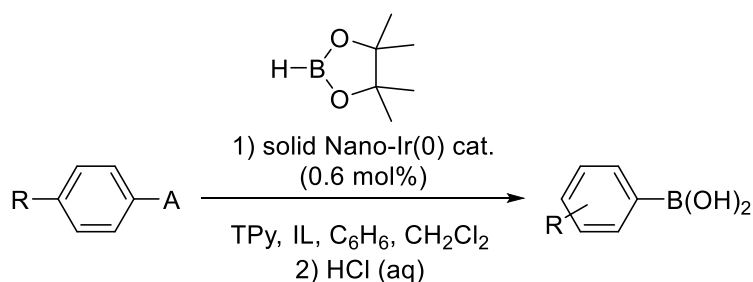
Meanwhile, the author D. Wang and co-workers developed silica-supported iridium catalyst BPS-Ir@SiO₂ using benzotriazole-pyridinyl-silane (BPS) ligand [62]. The obtained catalyst exhibited high activity in the borrowing hydrogen reaction of tert-butanefulfonamide with various benzyl alcohols. The catalyst could be run at least six cycles without significant loss of activity.



Again, titania-supported iridium catalysts for the synthesis of benzimidazoles via the hydrogen auto-transfer have been developed by K. Wada and co-workers [41,43].

c. Functionalization of C–H Bonds (Borylation)

Y. Zhu and co-workers developed a kind of well-dispersed iridium(0) nanoparticles by reduction of the precursor hydrido-iridium carborane, $(\text{Ph}_3\text{P})_2\text{Ir}(\text{H})-(7,8\text{-nido-C}_2\text{B}_9\text{H}_{11})$. They stabilized the iridium(0) nanoparticles with the ionic liquid, trihexyltetradecylphosphonium methyl sulfonate, $[\text{THTdP}][\text{MS}]$ [63]. This catalytic system was effective for aryl-borylation of unsubstituted and monosubstituted benzenes with pinacolborane to form boric acids. A high yield of 91% was achieved in a microwave reactor. The catalyst could be reused at least six times with activity loss of less than 0.5%.



Since then, a series of heterogeneous iridium catalysts was developed for the borylation. A. Nishida developed a heterogeneous iridium catalyst with $[2,2'$ -bipyridine]-4,4'-dicarboxylic acid for the C–H borylation of arenes with bis(pinacolato)diboron (B_2pin_2) [64,65]. The catalyst shows superior performance for the functionalization of disubstituted aromatics, both in terms of yield (83–95%) and good selectivity. Further study suggests that the catalyst worked heterogeneously and can be reused more than ten times. M. Sawamura and coworkers developed silica-

supported iridium catalysts for the borylation of aromatic C–H bonds with B_2pin_2 . This present catalyst was effective for the activation of unactivated $C(sp^3)$ –H bonds in 2-alkylpyridines to form primary and secondary alkylboronates [66,67].

d. Fuel cell reaction

In 1987, iridium was firstly reported to be effective as an electrode for the electrooxidation of methanol in H_2SO_4 and $HClO_4$ solutions [68]. It shows higher activity than platinum at low positive potential regions.

H. Zhang and coauthor reported a new preparation method of high active iridium catalysts for fuel cells and water electrolyzers [46]. They use a quite small but suitable amount of Nafion to control the particle size of iridium species. The obtained catalyst shows higher activity in both oxygen reduction reaction (ORR) and oxygen evolution reaction (OER). After dialysis treatment, the catalyst can be used to prepare catalyst layers (CLs) with high performance for fuel cells and water electrolyzers.

Recently, a series of Ir-based composite nanomaterials such as Ir/Ir-Sn/ SnO_2 [69] and Ir–Ru alloyed nanoparticles [70], carbon-supported bimetallic Pd-Ir [71] for the ethanol oxidation reaction. There are reports on the carbon-supported Ir–Rh nanoparticles for ammonia oxidation and corresponding fuel cell system [72] and the supported PtSnIr/C and IrSn/C catalysts [73]. Note that in the early stage, there are several reports of Ir electrocatalyst using the mixture of Pt black and Ir black [74] and Pt-Ir binary alloy [75,76] for the ammonia oxidation.

e. Reduction of NO

NO is one of the most significant automobile exhaust pollutions. The reduction of NO is of great significance. P. G  lin and coauthor developed supported Ir catalysts to enable selective catalytic reduction (SCR) of NO into N₂ by propene under lean-burn conditions [77]. W. Chen and coauthor compared the activity of planar Ir(210) and faceted Ir(210) for reported their study of NO reduction with C₂H₂ [78].

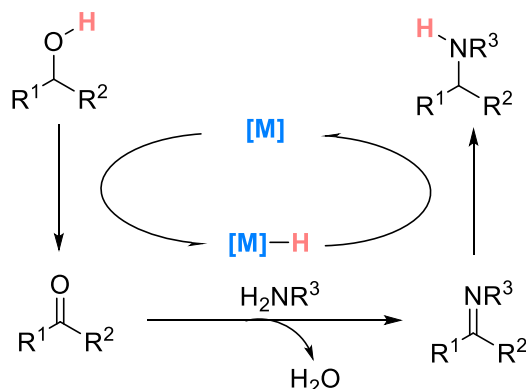
1.3 Synthesis of nitrogen-containing chemicals

Nitrogen-containing compounds are widely found in nature, which are important components of natural products and bioactive molecules [79–81]. The first synthetic organic compound in the history of chemistry was urea containing nitrogen [82]. The U.S. Food and Drug Administration (FDA) approved drugs show that 59 % of unique small-molecule drugs contain a nitrogen heterocycle [83]. Nitrogen-containing compounds such as amines, amides, nitrogen-containing heterocyclic, and derivatives are key building blocks in the current chemical industry as chemical raw materials and drug intermediates [84]. Therefore, establishing efficient catalytic systems to achieve clean conversion and synthesis of nitrogenous chemicals is of great significance for efficient resource utilization and green chemistry [85,86].

1.3.1 Synthesis of amines

Ammonia is one of the most produced chemicals in the world [87]. The use of ammonia for the synthesis of amines is of great significance [88]. Amines are often produced by the reaction of ammonia with alkyl halides [89–93]. However, these reactions produce waste materials such as halide salt harmful to human health and the

environment. Recently, alcohols as substrates have attracted extensive attention because of their advantages of readily available, easy handling, and environmentally benign features [94]. The N-alkylation reaction of ammonia by alcohols is often considered a hydrogen auto-transfer (borrowing hydrogen) reaction (Scheme 1). The process shows high atom efficiency and theoretically produces only water as a byproduct, which meets the requirements of green chemistry [95]. However, its disadvantage is still needing harsh conditions. Often the reaction requires a significant energy input, additives, high pressure of the reductive gases, and so on [96,97]. However, with the development of catalysis technology, several effective catalysis systems for the N-alkylation of alcohols and ammonia have been reported in recent decades. The reaction conditions are milder with improved yields.



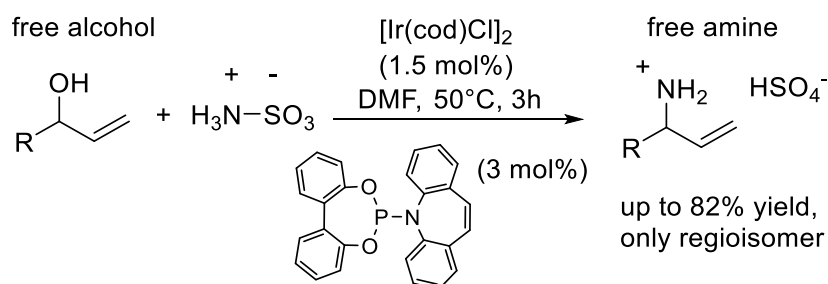
Scheme 1. Mechanism for the N-alkylation of ammonia and alcohol

Homogeneous catalyst system

Ir catalysis system

In 2007, E. M. Carreira and coauthors reported the first direct iridium-catalyzed synthesis of primary allylic amines from allylic alcohols and sulfamic acid [98]. This system uses commercially available iridium complex [Ir(cod)Cl]₂ with a

phosphoramidite-based bidentate phosphorus–olefin ligand. The sulfamic acid is an ammonia equivalent and an in-situ activator of hydroxy groups.



K. Fujita and R. Yamaguchi developed a water-soluble and air-stable iridium catalyst [Cp*Ir(NH₃)₃][I]₂ for multialkylation of aqueous ammonia with a variety of primary and secondary alcohols. The present reaction converts aqueous ammonia selectively to the corresponding tertiary and secondary amines, respectively [99]. The catalyst could be recycled by a facile procedure and maintained high activity for at least three cycles. Recently, K. Fujita and co-workers reported water-soluble iridium catalysts, dicationic complexes of iridium bearing N-heterocyclic carbene and diamine ligands. These complexes show high catalytic activity for N-monoalkylation of aqueous ammonia with various alcohols to give the corresponding primary amines [100].

Pt catalysis system

T. Ohshima and K. Mashima demonstrated the first sample of direct catalytic amination of various allylic alcohols with aqueous ammonia by using Pt/DPEphos catalyst system without the prior activation of the allylic alcohol [101]. Meanwhile, these authors also developed Pt-Xantphos and Pt-DPEphos catalysts for the direct alkylation of ammonia and various amines by aryl- or alkyl-substituted allylic alcohols [102].

Ru catalysis system

D. Milstein and coauthor discovered an air-stable Ru pincer complex $[\text{RuHCl}(\text{A-iPr-PNP})(\text{CO})]$ for N-monoalkylation of ammonia with alcohols to primary amines [103]. The treatment of $[\text{RuHCl}(\text{PPh}_3)_3(\text{CO})]$ with a new electron-rich tridentate PNP ligand gave the catalysts. The catalytic reactions proceed in toluene or even in the absence of solvent or “on water”. Based on the methodology discussed above, the authors developed a series of relevant Ru homogeneous catalysts to synthesize amines from alcohols and ammonia [104–106].

Based on Milstein’s report, P. Hofmann and coauthor synthesized the new Ru complex with from $(\text{PPh}_3)_3\text{Ru}(\text{H})(\text{Cl})(\text{CO})$ and 4,5-bis(dicyclohexylphosphinomethyl)-acridine (Figure 3) [107].

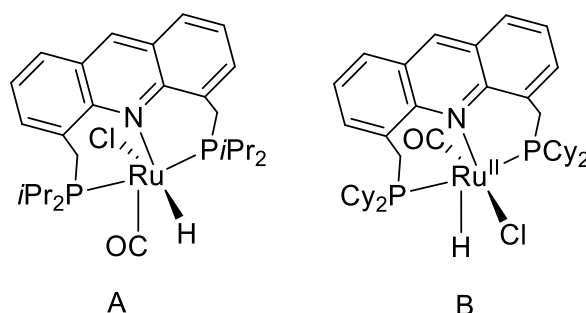
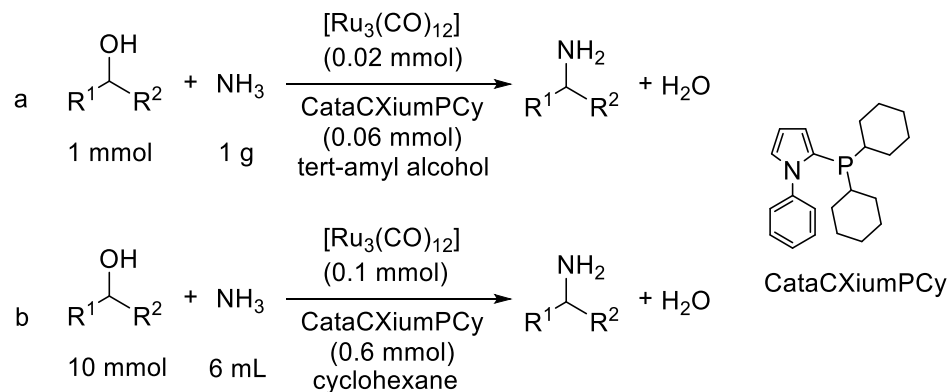


Figure 3. Ru complex developed by (A) D. Milstein and (B) P. Hofmann

D. Vogt and coauthor disclosed a homogeneous ruthenium catalysis system of $[\text{Ru}_3(\text{CO})_{12}]$ combined with the pyrrole phosphine ligand (discovered by M. Beller [108,109], see below). This catalyst could directly synthesize primary amines from secondary alcohols and ammonia without protecting groups [110]. This protocol is well applicable for cyclic and acyclic aliphatic substrates, as well as unsaturated and aryl-substituted alcohols.



Scheme 2. Ru catalysis system reported by (a) M. Beller and (b) D. Vogt.

Interestingly, at the same time, M. Beller, who developed the pyrrole phosphine ligand described above, also reported the same Ru homogeneous system (Scheme 2) [111]. They used $[\text{Ru}_3(\text{CO})_{12}]$ as a homogeneous catalyst combined with CataCXiumPCy (the pyrrole phosphine) ligand to achieve the amination of secondary alcohols to give primary amines in an ammonia atmosphere without hydrogen sources. Soon after that, the authors developed $[\text{Ru}(\text{CO})\text{Cl}(\text{PPh}_3)_3]$ /Xantphos catalyst system for the first time. This catalyzed the amination of primary and secondary diols with ammonia to give the corresponding diamines. The catalyst is also applicable for the efficient synthesis of primary amines from primary and secondary alcohols bearing hydroxy-substituted esters [112]. Similarly, a commercially available $[\text{Ru}_3(\text{CO})_{12}]$ /DCPE catalyst system for the catalytic amination of α -hydroxy amides with ammonia and various amines was developed by the same authors [113].

Heterogeneous catalyst system

Ir catalysis system

Y. Uozumi and Y. M. A. Yamada reported a boron-iridium heterobimetallic

polymeric catalyst for the in-water dehydrative alkylation of ammonia and amines with alcohols [114]. The catalyst acted as a heterogeneous active catalyst, which could be reused at least twice with stable activity. The reactions in the presence of the catalyst (1 mol% Ir) gave the corresponding alkylated amines in high yields at 100 °C without organic solvents under aerobic and aqueous conditions [115].

Ru catalysis system

The synthesis of tertiary and secondary amines from various primary and secondary alcohols with urea catalyzed by the titania-supported ruthenium hydroxide catalyst $\text{Ru}(\text{OH})_x/\text{TiO}_2$ was reported by N. Mizuno and co-workers [116]. Further experiments and characterization evidenced that the catalysts act heterogeneously and could be reused without significant activity loss. Soon after, the authors reported the details of the N-alkylation reaction and expanded the nitrogen sources to ammonia and its surrogates, such as inorganic salt and organic amines [117]. The catalyst shows high activity in synthesizing various symmetrically and unsymmetrically substituted amines and oxidative synthesis of nitriles in air.

D. Y. Murzin and coauthors compared carbon-supported ruthenium, palladium, platinum, iridium, and osmium catalysts for the amination of dodecanol with ammonia to dodecyl amine [118]. The results revealed that Ru/C and Pd/C catalyst showed the highest activity in the present reaction, and the presence of hydrogen in the system benefited the conversion and selectivity.

M. Rose and co-workers investigated the amination of biogenic diol isomannide with ammonia in aqueous solutions by the Ru/C catalyst [119]. They examined the effect of various supports and dopant metals on Ru catalysts as well. They optimized the reaction conditions for various other primary and secondary alcohols and evidenced

that water is a suitable solvent for the sustainable production of biogenic amines.

A zeolite-supported Ru catalyst, Ru/HBEA, was developed by L. Fang and M. Pera-Titus to synthesize primary amines from long-chain fatty alcohols and ammonia [120]. The support strongly affects the activity of the catalyst. With Ru catalyst (5 wt%) supported on HBEA of Si/Al = 25, the reaction at 180 °C in a batch reactor gave the desired product with selectivity over 90 % at the conversion over 90 %.

Recently, S. Wang and N. Yan reported the crucial behavior of ammonia on the surface of Ru/TiO₂ catalyst for the amination of alcohol [121]. The DRIFT study showed the formation of NH_x species on Ru/TiO₂ nanoparticles. These NH_x species were found to interact with adsorbed alcohol to promote the activity of the catalyst in the dehydrogenation of alcohol, the rate-determining step of the amination. Moreover, the formed N species were moderately bound with Ru to inhibit further multialkylation.

Au catalysis system

J. A. Dumesic and coauthor used controlled surface reactions to prepare bimetallic Au-Pd/TiO₂ catalyst for the amination of 1-hexanol with ammonia [122]. The bimetallic Au and Pd supported on titania exhibited a remarkable synergetic effect. As the Pd/Au atomic ratio increased from 0 to 0.06, the conversion rate of hexanol increased from 8.7 μmol ks⁻¹ (μmol total Pd)⁻¹ to 42 μmol ks⁻¹ (μmol total Pd)⁻¹.

Titania-supported gold catalyst realized the selective synthesis of tertiary or secondary amines via amination of stoichiometric alcohols [123]. Urea was used as an alternative N source to ammonia because urea is more advantageous for safe storage, handling, and transportation. The highlight of this catalytic system is that an excellent yield of 93% was achieved in 100 times scale-up reaction under solvent-free conditions, with a very small amount of Au/TiO₂ catalyst (0.03 mol% Au).

Pt catalyst system

Pt/NiCuAlO_x catalyst was developed for the direct amino cyclization of 2,5-tetrahydrofurandimethanol (THFDM) with ammonia. The product, 8-oxa-3-azabicyclo[3.2.1] octane, is a valuable building block for synthesizing bioactive molecules [124].

Rh-In catalysis system

Y. Nakagawa and K. Tomishige reported the role of indium in the Rh-In catalyst supported on activated carbon FAC-10 for the in-water amination of various C3 alcohols such as 1,2-propanediol with ammonia [125]. Indium effectively promoted the activity of Rh for the dehydrogenation of alcohol, which is the rate-determining step of amination.

Co catalysis system

A. Y. Khodakov and V. V. Ordonsky revealed the promotional effect of deposited carbon on the selectivity of alumina-supported cobalt catalyst for the amination of alcohols to primary amines [126]. Usually, the deposited carbon on the catalyst surface hampers the catalyst performance. However, in the present case, the authors employed the carbon deposition procedure to pretreat the Co/ γ -Al₂O₃ catalyst to increase the selectivity for primary amines from 30-50 to 80-90%. The steric hindrance by the deposited carbon on the cobalt nanoparticles was considered to suppress the further reaction of primary amines.

Ni catalysis system

K. Shimizu and co-workers developed the non-noble metal heterogeneous catalyst, namely the alumina-supported nickel nanoparticles, to synthesize primary amines from alcohols and ammonia without additional hydrogen sources under relatively mild

conditions [127]. The catalyst showed a higher activity on turnover numbers (TON) than Ru-based homogeneous catalysts ever reported at that time and was applicable for various aliphatic alcohols. The study revealed that the metallic Ni⁰ species are account for the high activity, and the presence of both acidic and basic sites on the alumina support surfaces is also an essential factor. In the following study, the author employed another support calcium silicate to prepare a nickel-based catalyst Ni/CaSiO₃ by ion-exchange method [128]. Various aliphatic alcohols can be catalytically converted to corresponding primary amines with high TON by using this catalyst.

Unprecedented activity and selectivity to primary amine in the direct amination of aliphatic alcohols with ammonia were reported for the nickel catalysts on cerium-aluminum mixed oxides with low loading levels [129]. These catalysts achieved 80% n-octanol conversion with 78% selectivity to n-octylamine, far better than the catalysts with high Ni loading. The presence of ceria promoted the formation of highly reducible nickel species with very small particle sizes (2-3 nm).

K. Hellgardt and K. K. “Mimi” Hii developed a continuous flow catalysis system for the highly selective synthesis of primary amines from alcohols and ammonia by using commercially-available nickel catalyst (65 wt % Ni-Al₂O₃/SiO₂) [130]. The accumulation of water and produced amine in the reactor could hamper the activity of the catalyst. Therefore, the continuous supply of anhydrous NH₃ in the flow system dramatically promoted the production of desired primary amines.

A commercial Raney Ni catalyst could be used for the efficient N-alkylation of ammonia by a variety of benzylic alcohols and bio-based, aliphatic alcohols, and aromatic diols. The reactions selectively produced primary benzylamines [131]. The

author reported efficient amination of vanillyl alcohol with ammonia to phenolic primary vanillyl amine.

Nanoceria-supported bimetallic Pd–Ni catalysts with low metal loadings (0.5 wt% Ni and 0.5 wt% Pd) showed excellent activity for the synthesis of diamines from aliphatic alcohols and ammonia [132]. One could control the activity and selectivity by adjusting the preparation method and the composition of the catalyst and by tuning the interaction between Pd, Ni, and nanoceria.

Cu catalyst system

N. Mizuno's group reported the effectiveness of the $\text{Cu}(\text{OH})_x/\text{Al}_2\text{O}_3$ catalyst for the N-alkylation of ammonia (generated ins situ from urea or aqueous ammonia) to secondary amines [133]. The reactions of urea and aqueous ammonia with benzyl alcohol for 12 h at 135 °C gave the desired dibenzyl amine in 85% and 80% yields, respectively. The present catalysts also enabled the reaction of primary amines with primary alcohols to secondary amines

1.3.2 Synthesis of benzimidazoles

Benzimidazole is a heterocyclic aromatic organic compound and is particularly important in pharmaceutical chemistry [134,135]. Numbers of methods have been applied for the synthesis of benzimidazole derivatives so far [136–139], including reactions of 1,2-phenylenediamines with carboxylic acids, its derivatives [140], or aldehydes [141]. In contrast, there are serious problems such as the co-production of toxic wastes and low atom efficiencies. Methods using transition metal-catalyzed reactions such as carbonylation of 1,2-phenylenediamine followed by cyclodehydration [142], and intramolecular N-arylation reaction of (o-bromophenyl)-amidines were also

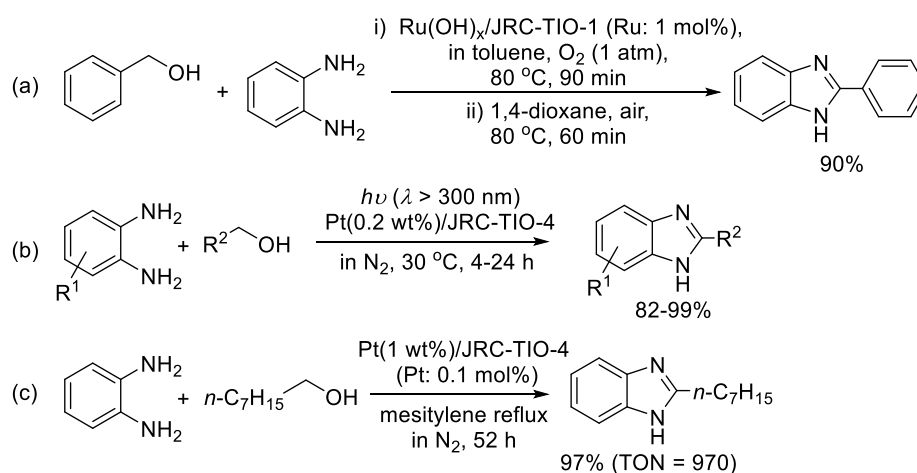
reported [143]. Among these methods, the use of primary alcohols and derivatives of 1,2-phenylenediamine or 2-nitroaniline via dehydrogenation or hydrogen transfer are more straightforward and environmentally benign routes because of their green output and high atom efficiency (see above discussions).

Dehydrogenation route

Kondo and co-workers reported a successful example catalyzed by a ruthenium phosphine complex, namely $\text{RuCl}_2(\text{PPh}_3)_3$ [144]. However, this process required harsh conditions, such as a high reaction temperature of 200 °C. Afterward, the reaction catalyzed by $\text{Ru}(\text{PPh}_3)_3(\text{CO})\text{H}_2$ in combination with a Xantphos ligand was reported to proceed in refluxing toluene smoothly. Still, an excess amount of crotononitrile was required as a hydrogen acceptor [145]. Acceptor-less reactions were reported to be realized in the presence of an iridium complex stabilized by a tridentate P^NP ligand together with a stoichiometric amount of strong base [146]. Recently, Milstein and co-workers reported cobalt-catalyzed acceptor-less reactions operated at 150 °C [147]. However, homogeneous catalysts have several inherent disadvantages in developing environmentally benign processes, such as the difficulty of recovering and recycling the catalysts after the reaction.

The use of solid catalysts, especially supported metal catalysts, can overcome these problems. Therefore, much attention has been focused on synthetic processes with supported metal catalysts [148–153]. In this context, several supported transition metal catalysts have been developed so far to synthesize benzimidazoles. The oxidative synthesis of 2-phenylbenzimidazole was achieved at 80 °C via tandem reactions of the oxidation of benzyl alcohol, double condensation with

phenylenediamine, and amine oxidation in the presence of a ruthenium hydroxide catalyst supported on anatase (JRC-TIO-1, supplied from the Catalysis Society of Japan) [154] (Scheme 3(a)). The synthesis of benzimidazoles by simultaneous photocatalytic oxidation of alcohol and catalytic dehydrogenation of the intermediates on Pt-modified titania nanoparticles (JRC-TIO-4, equivalent to Degussa P25) has been demonstrated at room temperature under UV irradiation ($\lambda > 300$ nm) [155] (Scheme 3(b)). Various primary alcohols including ethanol and benzyl alcohol were applicable and the desired products were selectively produced.



Scheme 3. Examples of the synthesis of benzimidazoles by supported transition metal catalysts.

Remarkably, Shimizu and co-workers have compared the activity of various supported transition metal catalysts for the dehydrogenative synthesis of 2-substituted benzothiazoles and benzimidazoles directly from primary alcohols in refluxing mesitylene without acceptors and additives. They reported the excellent activity of Pt/TiO₂(JRC-TIO-4) catalyst [156] (Scheme 3(c)): Ir/TiO₂ was also effective under

these conditions. However, the effects of kinds of titania supports were not well investigated in these reports.

Following these reports, successful examples using solid catalysts, such as $\text{Co}_3\text{O}_4@\text{Al}_2\text{O}_3/\text{SiO}_2$ in the air or O_2 [157], Pd/Cu-MOF with a base [158], Ru/N-doped carbon with KOH [159], Mg-modified Cu-Pd/ γ - Al_2O_3 [160], and polystyrene supported rhodium with a base [161], were reported. A review by Shimizu et al. [162] summarizes recent progress.

Our lab is focusing our efforts on developing supported transition-metal catalysts that realize the acceptor-less dehydrogenative (see section 1.2.2a). As discussed above, iridium owns variable valence in both oxidation and reduction states. On account of the well-known SMSI effect, iridium interacts strongly with titania support in the reduction atmosphere, thus promoting the formation of small and stable particles with a large surface area and surface energy. The thus-formed small particles would provide more active sites and exhibit physics and catalytic properties that are potentially favorable for the catalytic process.

As shown in Figure 4, the comparison of the activity of the supported catalysts revealed the dominance of iridium catalysts to Pd, Rh, and Ru ones at 120 °C. As a support for the iridium catalyst, titania (JRC-TIO-4) was the most excellent [60]. Table 2 further proved that titania used as support significantly affects the low-temperature activity of the iridium catalyst. While the catalysts supported on anatase showed moderate to poor activity at 100 °C, the reaction in the presence of rutile-supported catalysts smoothly proceeded to give the desired product in high yields. In the dehydrogenative conversion of 2-(2-aminophenyl)ethanol to indole, a similar trend of dependency on titania was also observed.

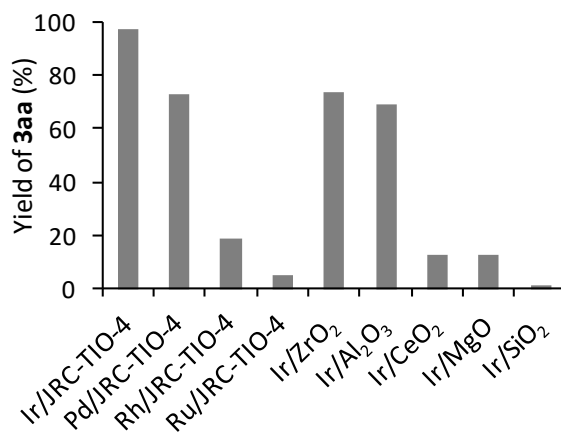
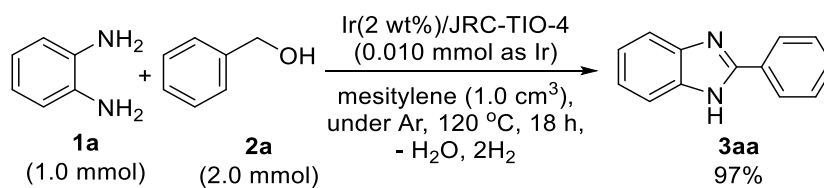


Figure 4. Effects of metallic species and supports on the synthesis of 2-phenyl benzimidazole at 120 °C, 18 h [60].

Table 4. Effects of JRC titania supports^a

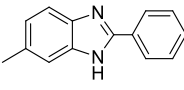
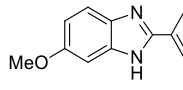
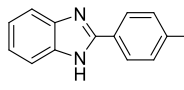
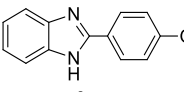
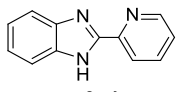
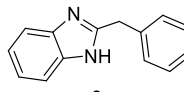
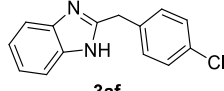
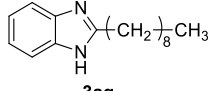
Entry	TiO ₂ support ^b	Yield of 3aa at 120 °C 18 h (%)	Yield of 3aa at 100 °C 18 h (%)
1	JRC-TiO-4 (A+R)	96	24
2	JRC-TiO-6 (R)	96	59
3	JRC-TiO-7 (A)	29	17
4	JRC-TiO-8 (A)	55	19
5	JRC-TiO-9 (A)	59	27

^aReaction conditions are shown in eq.1. ^b(A): Anatase-rich and (R) rutile-rich titanias.

In the reaction at a higher substrate-to-catalyst ratio (S/C = 1,000), a high turnover number (TON) over 800 was achieved. This titania-supported iridium catalyst was applicable to the reactions of various primary alcohols and derivatives of 1,2-

phenylenediamine as shown in Table 5. Not only benzylic alcohols but simple aliphatic alcohols could be used also. Further characterization of CO uptake and XPS study suggest the formation of well-reduced iridium species on rutile would be one reason for the predominant catalytic activity (Figure 5).

Table 5 Scope of substrates catalyzed by Ir(2.0 wt%)/JRC-TIO-4^a

		
>99%	7%	87%
		
>99%	54% (150 °C)	99% (150 °C)
		
> 99% (150 °C)		99%

^aReaction conditions are shown in eq.1.

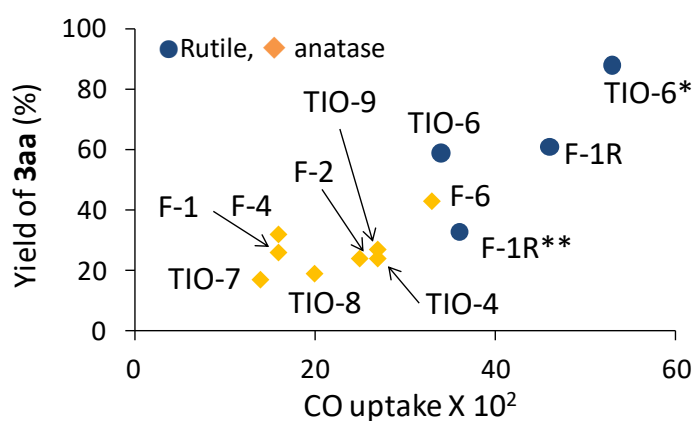


Figure 5. Relationship between CO uptake (mol/Ir-mol) by the catalysts and the yield of **3aa** at 100 °C. *Prepared without calcination. **Prepared using [(COD)IrCl]₂ as an iridium source.

Hydrogen transfer route

The hydrogen transfer (borrowing hydrogen) reaction is another convenient and sustainable approach for synthesizing benzimidazoles.

Several homogeneous base metal catalysts were reported, but they often required the presence of excess bases. Using a commercially available cheap cobalt catalyst such as $\text{Co}(\text{acac})_2$ was reported to produce a wide variety of 2-substituted benzimidazoles by hydrogen auto transfer route. However, a stoichiometric amount of a strong base was required [163].

An iron catalysis system for one-pot synthesis of benzimidazoles from 2-nitroanilines and alcohols via hydrogen transfer route was reported by H. Huang and co-workers [164]. By screening various iron salt, dppf [1,1'-bis(diphenylphosphino)ferrocene] showed the best activity in toluene solvent. The catalytic reaction gave the products moderate to good yields with various 2-nitroanilines and substituted benzylic alcohols under the optimized conditions. The reaction pathway was proposed via a cascade of alcohol oxidation, nitro reduction, condensation, and dehydrogenation.

The the Knölker complex, an iron complex, showed excellent performance for the selective reduction of nitroarenes with various alcohols [165]. This system delivered an excellent functional group tolerance to various nitroarenes and aza heterocyclic derivatives. It produced imines, quinoxalines, and benzimidazoles in moderate to good yields in the presence of Me_3NO , whereas it needed the addition of an excess amount of base.

The activity of homogeneous palladium catalysts to synthesize 2-substituted benzimidazoles via a hydrogen-transfer strategy was reported [166]. In this study,

$\text{Pd}(\text{dppf})\text{Cl}_2$ [1,1'-Bis(diphenylphosphino)ferrocene] dichloro-palladium(II) showed the highest activity. The catalysis system showed good tolerance to functional groups. Various 2-substituted benzimidazoles reacted to give corresponding 2-substituted benzimidazoles with moderate to high yields.

On the other hand, a few of heterogeneous catalysis system for the hydrogen transfer synthesis of benzimidazoles have been reported due to their high reusability.

The titania-supported gold catalyst selectively synthesized benzimidazoles from cheap and readily available nitro compounds and alcohols via hydrogen-transfer processes [167]. The catalyst exhibited high activity and selectivity was easy to be reused. Moreover, the catalysis system showed good tolerance to air and water with a broad substrate scope without additional additives, oxidants, and reductants.

Efficient carbon-supported palladium catalysts were also developed to synthesize benzimidazoles from the low-cost substrate via a hydrogen-transfer pathway [168]. The reaction could be carried out with a variety of N-substituted 2-nitroanilines smoothly to give the corresponding benzimidazoles with good to excellent yields under mild conditions. The Pd/C catalyst could be recovered easily and reused six times with a stable high activity.

Previous works in our lab [41,43] revealed that titania-supported iridium catalysts enable the synthesis of benzimidazoles from 2-nitroaniline and primary alcohols under mild conditions via the hydrogen transfer route. Different from the case of the dehydrogenative reactions (see the previous section), the iridium catalysts supported on anatase JRC-TIO-7 with a large surface showed the highest activity. Further study revealed there is a positive correlation between BET surface area and the activity of iridium catalysts. Moreover, {010}/{101}-faceted anatase (PA-135-3.5) showed

excellent performance as support in spite of its moderate surface areas. As expected, TEM analysis sustained the formation of small iridium nanoparticles on titania supports, which would be one reason for the excellent catalytic activity.

1.3.3 Synthesis of benzoxazoles

Benzoxazoles are five-membered heterocycles in the benzazole family. They are important aromatic heterocyclic nitrogen-containing compounds and are widely found in natural products. Because of various biological activities, benzoxazoles have become important intermediates in pharmaceutical and chemical industries [169,170], and their synthesis routes have been studied extensively [171,172]. The most common routes are reactions of 2-aminophenols condensation with carboxylic acid derivatives [173], oxidation with aldehydes [174] [175], or oxidative coupling with amine [176]. On the other hand, the conversion of 2-nitrophenol and alcohols into benzazoles via a hydrogen transfer pathway has been reported in the presence of homogeneous iridium complex catalysts, namely $[\text{Cp}^*\text{IrI}_2]_2$ [145].

Subsequently, the dehydrogenative synthesis of benzothiazoles by heterogeneous Pt/Al₂O₃ catalysts was reported [156]. However, very few examples of effective heterogeneous catalysis through the acceptor-less dehydrogenative synthesis of benzoxazoles are known. Solid-immobilized ruthenium complex catalysts have been developed to synthesize benzoxazoles from primary alcohols and 2-aminophenol via the acceptor-less dehydrogenation [177]. The phosphine-functionalized magnetic nanoparticles (PFMNPs; Fe₃O₄@SiO₂@PPh₂) were combined with the ruthenium

carbonyl chloride complex $\text{Ru}_2\text{Cl}_4(\text{CO})_6$. The obtained catalysts could be reused at least five times without a significant loss of activity.

A heterogeneous catalyst PdOMS, composed of palladium oxide nanoparticles intercalated mesoporous silica, showed promising activity in the acceptor-less dehydrogenative synthesis of benzoxazoles and benzimidazoles [178]. The PdOMS catalyst successfully enabled the formation of 2-substituted benzoxazole or benzimidazole with high yields (72–95%). The characterization revealed the formation of well-dispersed palladium oxide nanoparticles at the walls of mesoporous silica, and the catalyst could be reused at least five times.

1.4 Supports in the heterogeneous catalysis

1.4.1 Overview of Supports for heterogeneous catalyst

IUPAC defines “support of a catalyst” as “in multiphase catalysts, the active catalytic material is often present as the minor component dispersed upon a support sometimes called a carrier. The support may be catalytically inert but it may contribute to the overall catalytic activity” [30][179]. The catalyst support is the support body, dispersant, and binder of the active component of catalyst, which may have a catalytic activity sometimes or interact with the active component. The support plays a crucial role for the catalyst since it can promote the stability of the catalyst, reduce the use of noble metal species, thus improve the economy of the catalyst [180] [181]. The special features of support such as porosity, large surface area, tunable morphology promote dispersion of metal particles and inhibit the aggregation of active metal particles, thereby enhancing the activity of catalyst [182] [183]. According to the properties of materials, the catalyst support can be categorized into four groups.

1. Metal oxide

Metal oxides are widely applied as catalysts in various industrial processes such as refining and petrochemical processes [184]. Meanwhile, metal oxides may also be used simply as support of the catalysts [185]. In general, there are two types of metal oxides, non-reducible oxides and reducible oxides. The functionality of the latter oxides is based on the removability of oxygen atoms from the structure to form oxygen-deficient structures [186]. The properties of these two groups of oxides are intrinsically different.

The oxidation states of non-reducible oxides do not easily change. They possess wide band gaps and show low reactivity. Therefore, they play the role of inert support in catalysis [187]. The typical examples are Al_2O_3 (8.7 eV), SiO_2 (10 eV), MgO (7.8 eV), and ZrO_2 (5.0 eV) (numbers in the parentheses show typical bandgaps). With decreasing the size to nanoscale, the oxides remarkably changes their morphology and exposes steps, kinks, and corners. Thus the electronic structure of oxide changes drastically due to electronic confinement effects within oxide nanoparticle [188].

Reducible oxides mainly include transition metal and rare earth elements (TiO_2 , NiO , WO_3 , CeO_2 , and so on), which can readily accept electronic charges from donors. Therefore, these oxides easily adopt various oxidation states and show rich redox chemistry [189]. The oxygen anions of reducible metal oxides consequently show some oxidizing power [32]. In addition, the enhanced ion conductivity enables the encapsulation of metal clusters with oxide layers, the transport of active oxygen atoms of oxide supports, and the diffusion of oxygen defects [190].

2. Organic polymer

The immobilization of homogeneous asymmetric catalysts on a polymer support

is obviously advantageous. It enables the separation and the recovery of the catalysts from the reaction mixture, while promoting the recovery and reuse of chiral components, which are often the most expensive components in the system [191] [192].

a. Dendrimer support. Dendrimers are three-dimensional polymeric materials consisting of the core, the branching groups, and the terminal groups, and were widely used for stabilizing transition metals [193,194]. For example, the iridium catalysts bearing BINAP-based ligands immobilized on the core of Frechet type dendrimers were reported to show enhanced catalytic activity for the Ir-catalyzed asymmetric hydrogenation of quinolones without compromising the enantioselectivity.

b. Macroporous polymers support. Diffusion limitation of the supported catalysts can be reduced by using macroporous polymers with tunable porosity. For example, macroporous polymer-supported chiral ruthenium(II)/ phenyloxazoline (Ru-PHEOX) complexes showed a higher activity than the homogeneous catalysts in the cyclopropanation of styrene with ethyl diazoacetate (EDA) [195].

c. Soluble polymer supports. Soluble polymers can minimize diffusion issues. By using controlled polymerization, Soluble polymers can a facile control incorporate of catalytic sites and easily adjust the nature of the polymer matrix and the catalyst loading. For example, a soluble polymer containing BINAP subunits could be applied for the Ru-catalyzed asymmetric hydrogenation synthesis of naproxen [196]

3. Carbon

Carbon-based materials include activated carbons and the nanostructured carbons including fullerene, carbon nanotubes (CNTs) and nanofibers (CNFs), graphene and mesoporous carbons. These materials are often used as support of the heterogeneous catalysts due to their high availability, low cost, large surface areas, tunable porosity, various surface functionalites [197], as well as other emarkable physical properties such

as good electronic conductivity and good chemical inertness [198].

4. Metal-organic frameworks (MOF)

Recently, MOFs are rapidly recognized as one of the most attractive support because of their distinctive properties such as high porosity, diverse composition, tunable pore structure and versatile functionality [199]. The use of MOFs porous materials effectively prevents particle nucleation and aggregation of the immobilized metal nanoparticles even in the absence of surfactants [200].

1.4.2 Strong metal support interaction (SMSI)

In 1978, S. J. Tauster and coauthor discovered the strong metal support interaction (SMSI) between titania support and incorporated group 8 noble metals [201]. The reduction in hydrogen at high temperature drastically changed the catalytic performance of titania-supported noble metal catalysts [202], which were caused by electronic or geometrical interaction as well as charge transfer between metallic nanoparticles and support [203–205]. During the high temperature reduction process, the TiO_x species migrate to the surface of the noble metal nanoparticles and cover them to form capping layer that changes the performance of the catalyst [206–208]. Moreover, it also controls the growth of the metal nanoparticles [208].

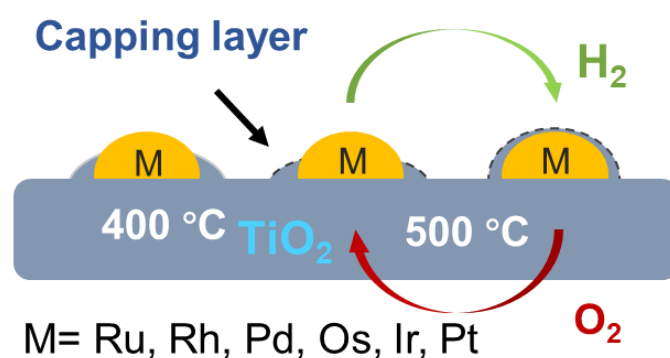


Figure 5. Schematic illustration of SMSI

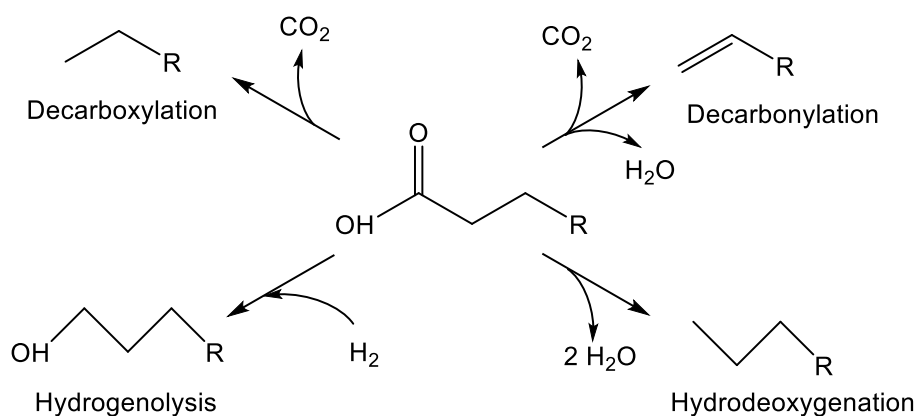
1.4.3 Titania as catalyst support

Since SMSI was reported in 1978, TiO_2 attracted great interest and has been intensively researched as catalyst support, a promoter, or additive to the catalysts [32]. The advantage of TiO_2 support is mainly due to its unique chemical and physical properties, for example:

1. High chemical and thermal stability [209].
2. Resistance towards corrosion [210,211].
3. SMSI for stability, activity, and selectivity [212–214].
4. Proton conductivity [215].
5. Crystal facet effect [216,217].
6. Commercial availability and low cost.

1. Deoxygenation

Deoxygenation reactions involve decarboxylation, decarbonylation, hydrodeoxygenation, and hydrogenolysis as shown in Scheme 4. It is an important process in organic synthesis and is utilized in biofuels production [218].



Scheme 4. Possible types of deoxygenation pathways

So far, various titanium dioxide-supported metal catalysts have been developed for deoxygenation reactions. For example, C. H. Ko and coauthor reported Ru-Fe/TiO₂ catalyzed hydrodeoxygenation of anisole as a model of upgrading bio-oil [219]. X. Wang and coauthor developed Pt/TiO₂ for the highly effective hydrodeoxygenation of guaiacol [220]. The other titania-supported metal catalysts such as Cu-Ni/TiO₂ [221], NiMo/TiO₂ [222], AuRh/TiO₂ [223], Mo/TiO₂ [224] were also reported for the deoxygenation reaction.

2. Hydrogenation

Titania is widely employed as support of the heterogeneous transition metal catalysts for hydrogenation reactions. Most of the authors attribute the excellent support of titania to the strong interaction of titania support with metal particles and yielding highly dispersed nanoparticles. For example, C. Hardacre and coauthor developed Pt/TiO₂ catalyst for the highly selective and efficient hydrogenation of carboxylic acids to alcohols and alkanes [225]. The hydrogenation of stearic acid and cyclohexene catalyzed by Pt/TiO₂ also have been reported [225,226]. Pd/TiO₂ is utilized for the selective hydrogenation of acetylene in ethylene [227,228]. Ni/TiO₂ is reported for the hydrogenation of benzaldehyde, acetophenone, ethanol, and so on [229,230]. Cu/TiO₂ was utilized for the CO₂ hydrogenation to methanol [231].

3. Esterification and transesterification

Esterification and transesterification are important in the chemical and fuel industries. J. J. Leahy and coauthor developed ZrO₂/TiO₂ catalyst enhanced catalytic activity for the esterification reaction between levulinic acid and ethanol [206]. C. H. Christensen and coauthor employed Au/TiO₂ catalyst for the esterification of a primary alcohol in hydroxymethylfurfural (HMF) [232]. Although the experiment results

indicates support does not play a direct role in the reaction, titania supported catalyst shows the highest activity. Furan-2,5-dimethylcarboxylate (FDMC) was formed directly with an excellent yield of 98% at 130 °C. while the oxidation of HMF at room temperature (22 °C) under an oxygen atmosphere give a 90% yield of 5-hydroxymethylfuroate (HMMF). Au/TiO₂ offers an alternative to other oxidation catalysts for esterification and transesterification[233].

4. Water–gas shift reaction

The water-gas shift reaction (WGS) describes the reaction of carbon monoxide and water vapor to form carbon dioxide and hydrogen. It is mainly used in the hydrogen and ammonia synthesis industries. As the demand for clean fuels and hydrogen fuel cells increases, the development of WGS catalysts is one of the current research interests. TiO₂-supported noble metals have been sustained to be promising candidates for the catalysts of the low-temperature WGS reaction for fuel cell applications [231,234]. Various transition metals was employed for the titania supported catalyst with high performance for WGS such as Pt/TiO₂ [235], Ni@TiO_{2-x} [236], Au/TiO₂ [237], Ru/TiO₂ [236], Pd/TiO₂ [234], Rh/TiO₂ [234].

5. Desulfurization (SO_x) reaction

Desulfurization or desulphurization is an important process in oil refinery streams. J. Ramirez and L. Cedeño investigated the effect of TiO₂ support on the Mo-Based catalyst towards hydrodesulfurization of thiophene [236]. This study revealed that the titanium species act as a promoter of the Mo phase due to the electronic properties of the partially reduced and/or sulfided TiO₂ surface.

6. Other reactions

Titania is also applied as catalyst support for other important green chemical

reactions such as oxidation of NO by ozone [231], oxidation of HCl [231], reduction of NO with NH₃ [231], titania-supported cobalt Fischer–Tropsch reaction [231], etc.

1.5 Purposes of present study

As described above, the growing development of the chemical industry has provided a material guarantee for the improvement of people's living, but it has also caused tremendous pollution to the environment. In this context, the development of green chemistry has become an important way to solve this problem. Obviously, the highly selective and efficient catalytic reaction is in line with the principle of green chemistry.

Nitrogen-containing chemicals such as amines and nitrogen-containing heterocyclic compounds are key building blocks in the current chemical industry as chemical raw materials and drug intermediates. Over 59 % of unique small-molecule drugs contain a nitrogen heterocycle [83]. Therefore, establishing efficient catalytic systems to achieve clean conversion and synthesis of nitrogenous chemicals is of great significance for efficient resource utilization and green chemistry.

The excellent catalytic performance of transition metals is mainly dependent on their own characteristics. Iridium is one of the best candidates of transition metal catalyst that has been intensively studied because of its unique properties. For example, iridium can possess various oxidation states. It can form small and stable clusters on various supports. And the thus formed particles with a large surface area and surface energy expose more active sites and exhibits interesting physical and catalytic properties. On the other hand, a reducible oxide such as titania has been disclosed to be

a good catalyst support in many applications. The SMSI of titania strongly affect the dispersion of noble metal particle on the titania support, the geometry of adsorption, the electronic structures of composite, and significantly changes the catalytic performance.

In the present dissertation, we focus on developing titania-supported iridium catalysts and their application in various potential reactions towards the synthesis of nitrogen-containing chemicals from ammonia/amines with alcohols. In the previous study, it has been evidenced titania supported iridium catalysts possess excellent catalytic activity in the oxidation of alcohols [238,239]. Our lab successfully developed rutile or anatase-supported iridium catalysts to efficiently convert o-phenylenediamine or o-nitroaniline with alcohols to benzimidazoles via dehydrogenation or hydrogen transfer route, respectively [41,42,60]. On the basis of these results, the application of titania-supported iridium to relevant new catalytic reactions is highly expected.

In chapter II, we developed titania-supported iridium catalysts with a high loading level for the synthesis of tertiary and secondary amines from aqueous ammonia and various benzylic alcohols. The reaction conditions meet most requirements of green chemistry principles. The developed heterogeneous catalysts were recyclable and smoothly gave the desired products high yields at relatively low temperatures without any additional solvents even in an air atmosphere.

In chapter III, we investigated the effect of phosphorus modification on titania supports for iridium catalysts. We developed two series of phosphorus-modified titania: phosphorus-doped rutile, which was obtained by hydrothermal method, and P-modified anatase by the impregnation method. The results show the presence of phosphorus greatly enhanced the activity of catalyst for the synthesis of benzimidazoles via

hydrogen transfer.

Chapter IV expands the application of iridium catalysts supported on anatase in the acceptor-less dehydrogenation synthesis of benzoxazoles. The catalytic activity was greatly affected by the crystal structure of titania supports, iridium precursors, and the loading of iridium species. We developed recyclable iridium catalysts supported on anatase enabled the reaction of 2-aminophenol and with various primary alcohols to give corresponding benzoxazoles in high to moderate yields.

In chapter V, the conclusions of the present study are summarized. The recyclable titania-supported iridium catalysts are successfully applied in various reactions for the synthesis of nitrogen-containing chemicals via the green route, which can give us the desired products. Further study on the application of titania-supported iridium catalysts is prospected.

1.6 References

- [1] M. Ridenour, *A brief history of chemistry*, Waldorf Education, 2004.
- [2] E.W. Morley, *A history of chemistry*, *J. Am. Chem. Soc.* 29 (1907) 946–947.
- [3] D.L. Hjeresen, J.M. Boese, D.L. Schutt, *Green Chemistry and Education*, *J. Chem. Educ.* 77 (2000) 1543.
- [4] K.K. Rana, S. Rana, *Fundamentals, Representative Applications and Future Perspectives of Green Chemistry: A Short Review*, *OALib.* 01 (2014) 1–16.
- [5] R. Carson, *Silent spring*, Houghton Mifflin Harcourt, 2012.
- [6] J.A. Linthorst, *An overview: Origins and development of green chemistry*, *Found. Chem.* 12 (2010) 55–68.
- [7] J. Lee, *Engineering the Environment: Regulatory Engineering at the U.S. Environmental Protection Agency, 1970-1980*, Virginia Polytechnic Institute and State University, 2013.
- [8] A.W. Lindsey, B.J. Campbell, *Pollution Prevention-US Environmental Policy*, in: *Stud. Environ. Sci.*, Elsevier, 1991: pp. 1–17.
- [9] M.E. Kraft, *U.S. Environmental Policy and Politics: From the 1960s to the 1990s*, *J. Policy Hist.* 12 (2000) 17–42.

- [10] B.M. Trost, The atom economy - A search for synthetic efficiency, *Science* (80-.). 254 (1991) 1471–1477.
- [11] M. Kidwai, R. Mohan, Green chemistry: an innovative technology, *Found. Chem.* 7 (2005) 269–287.
- [12] C. Anastas, T. Warner, *Green chemistry: theory and practice*, Oxford University Press Inc., New York, 1998.
- [13] A.A. Jensen, Establishment of a European Green and Sustainable Chemistry Award, (2000).
- [14] T. Ushikubo, Green Chemistry in Japan, *Chem. Int. -- Newsmag. IUPAC.* 35 (2014) 9–11.
- [15] P.T. Anastas, L.B. Bartlett, M.M. Kirchhoff, T.C. Williamson, The role of catalysis in the design, development, and implementation of green chemistry, *Catal. Today.* 55 (2000) 11–22.
- [16] J. Clark, D. Macquarrie, *Handbook of Green Chemistry and Technology*, John Wiley & Sons, 2007.
- [17] P. Anastas, N. Eghbali, Green chemistry: principles and practice, *Chem. Soc. Rev.* 39 (2010) 301–312.
- [18] J.B. Zimmerman, P.T. Anastas, H.C. Erythropel, W. Leitner, Designing for a green chemistry future, *Science* (80-.). 367 (2020) 397–400.
- [19] R.A. Sheldon, Metrics of Green Chemistry and Sustainability: Past, Present, and Future, *ACS Sustain. Chem. Eng.* 6 (2018) 32–48.
- [20] B.M. Trost, On inventing reactions for atom economy, *Acc. Chem. Res.* 35 (2002) 695–705.
- [21] B.M. Choudary, M.L. Kantam, P.L. Santhi, New and ecofriendly options for the production of speciality and fine chemicals, *Catal. Today.* 57 (2000) 17–32.
- [22] N. Winterton, The green solvent: a critical perspective, *Clean Technol. Environ. Policy.* 23 (2021) 2499–2522.
- [23] J.O. Akindoyo, M.D.H. Beg, S. Ghazali, M.R. Islam, N. Jeyaratnam, A.R. Yuvaraj, Polyurethane types, synthesis and applications-a review, *RSC Adv.* 6 (2016) 114453–114482.
- [24] M. Abla, J.C. Choi, T. Sakakura, Halogen-free process for the conversion of carbon dioxide to urethanes by homogeneous catalysis, *Chem. Commun.* 1 (2001) 2238–2239.
- [25] F.P. Byrne, S. Jin, G. Paggiola, T.H.M. Petchey, J.H. Clark, T.J. Farmer, A.J. Hunt, C.R. McElroy, J. Sherwood, Tools and techniques for solvent selection: green solvent selection guides, *Sustain. Chem. Process.* 4 (2016) 1–24.
- [26] M. Sarmah, M. Mondal, U. Bora, Agro-waste extract based solvents: emergence of novel green solvent for the design of sustainable processes in catalysis and organic chemistry, *ChemistrySelect.* 2 (2017) 5180–5188.
- [27] A. Whitehead, S.R. Sieck, S. Mukherjee, P.R. Hanson, *Solvent-Free Reactions*, 2005.
- [28] D.I. Enache, J.K. Edwards, P. Landon, B. Solsona-Espriu, A.F. Carley, A.A.

- Herzing, M. Watanabe, C.J. Kiely, D.W. Knight, G.J. Hutchings, Solvent-free oxidation of primary alcohols to aldehydes using Au-Pd/TiO₂ catalyst, *Science* (80-.). 311 (2006) 362–365.
- [29] G.D. Peckham, I.J. McNaught, Chemical principles revisited: Applications of Maxwell-Boitzmann distribution diagrams, *J. Chem. Educ.* 69 (1992) 554–558.
- [30] V. Gold, ed., *The IUPAC Compendium of Chemical Terminology*, International Union of Pure and Applied Chemistry (IUPAC), Research Triangle Park, NC, 2019.
- [31] B.M. Bhanage, M. Arai, *Catalyst product separation techniques in heck reaction*, Taylor & Francis Group, 2001.
- [32] M.J. Ndolomingo, N. Bingwa, R. Meijboom, Review of supported metal nanoparticles: synthesis methodologies, advantages and application as catalysts, *J. Mater. Sci.* 55 (2020) 6195–6241.
- [33] G. Wang, M. Zhou, J.T. Goettel, G.J. Schrobilgen, J. Su, J. Li, T. Schlöder, S. Riedel, Identification of an iridium-containing compound with a formal oxidation state of IX, *Nature*. 514 (2014) 475–477.
- [34] P. Pyykkö, W.H. Xu, The formal oxidation states of iridium now run from -III to +IX, *Angew. Chemie - Int. Ed.* 54 (2015) 1080–1081.
- [35] Y.B. Jang, T.H. Kim, M.H. Sun, J. Lee, S.J. Cho, Preparation of iridium catalyst and its catalytic activity over hydrazine hydrate decomposition for hydrogen production and storage, *Catal. Today*. 146 (2009) 196–201.
- [36] A.J. Saadun, G. Zichittella, V. Paunović, B.A. Markaide-Aiastui, S. Mitchell, J. Pérez-Ramírez, Epitaxially Directed Iridium Nanostructures on Titanium Dioxide for the Selective Hydrodechlorination of Dichloromethane, *ACS Catal.* 10 (2020) 528–542.
- [37] Q.Y. Bi, J.D. Lin, Y.M. Liu, S.H. Xie, H.Y. He, Y. Cao, Partially reduced iridium oxide clusters dispersed on titania as efficient catalysts for facile synthesis of dimethylformamide from CO₂, H₂ and dimethylamine, *Chem. Commun.* 50 (2014) 9138–9140.
- [38] E.W. Zhao, H. Zheng, K. Ludden, Y. Xin, H.E. Hagelin-Weaver, C.R. Bowers, Strong Metal-Support Interactions Enhance the Pairwise Selectivity of Parahydrogen Addition over Ir/TiO₂, *ACS Catal.* 6 (2016) 974–978.
- [39] H. Vuori, A. Pasanen, M. Lindblad, M. Valden, M.V. Niemelä, A.O.I. Krause, The effect of iridium precursor on oxide-supported iridium catalysts prepared by atomic layer deposition, *Appl. Surf. Sci.* 257 (2011) 4204–4210.
- [40] S. Schlicht, P. Büttner, J. Bachmann, Highly Active Ir/TiO₂ Electrodes for the Oxygen Evolution Reaction Using Atomic Layer Deposition on Ordered Porous Substrates, *ACS Appl. Energy Mater.* 2 (2019) 2344–2349.
- [41] T. Fukutake, K. Wada, H. Yu, S. Hosokawa, Q. Feng, Development of titania-supported iridium catalysts with excellent low-temperature activities for the synthesis of benzimidazoles via hydrogen transfer, *Mol. Catal.* 477 (2019) 110550.

- [42] T. Fukutake, K. Wada, G.C. Liu, S. Hosokawa, Q. Feng, Striking effects of a titania support on the low-temperature activities of Ir catalysts for the dehydrogenative synthesis of benzimidazole and indole, *Catal. Today*. 303 (2018) 235–240.
- [43] K. Wada, H. Yu, Q. Feng, Titania-supported iridium catalysts for dehydrogenative synthesis of benzimidazoles, *Chinese Chem. Lett.* 31 (2020) 605–608.
- [44] A. Uzun, D.A. Dixon, B.C. Gates, Prototype Supported Metal Cluster Catalysts: Ir₄ and Ir₆, *ChemCatChem*. 3 (2011) 95–107.
- [45] S. Kundu, H. Liang, Shape-selective formation and characterization of catalytically active iridium nanoparticles, *J. Colloid Interface Sci.* 354 (2011) 597–606.
- [46] Y. Zhang, H. Zhang, Y. Zhang, Y. Ma, H. Zhong, H. Ma, Facile synthesis of Nafion-stabilized iridium nanoparticles and their direct use for fuel cells and water electrolyzers, *Chem. Commun.* (2009) 6589–6591.
- [47] T.K. Sau, A.L. Rogach, Nonspherical Noble Metal Nanoparticles: Colloid-Chemical Synthesis and Morphology Control, *Adv. Mater.* 22 (2010) 1781–1804.
- [48] S. Guo, E. Wang, Noble metal nanomaterials: Controllable synthesis and application in fuel cells and analytical sensors, *Nano Today*. 6 (2011) 240–264.
- [49] J.F. Hartwig, M.J. Pouy, Iridium-catalyzed allylic substitution, 2011.
- [50] J. Choi, A.S. Goldman, Ir-catalyzed functionalization of C-H bonds, *Top. Organomet. Chem.* 34 (2011) 139–167.
- [51] J. Choi, A.H.R. MacArthur, M. Brookhart, A.S. Goldman, Dehydrogenation and related reactions catalyzed by iridium pincer complexes, *Chem. Rev.* 111 (2011) 1761–1779.
- [52] T. Suzuki, Organic synthesis involving iridium-catalyzed oxidation, *Chem. Rev.* 111 (2011) 1825–1845.
- [53] S. Pan, T. Shibata, Recent advances in iridium-catalyzed alkylation of C-H and N-H bonds, *ACS Catal.* 3 (2013) 704–712.
- [54] Q. Cheng, H.F. Tu, C. Zheng, J.P. Qu, G. Helmchen, S.L. You, Iridium-Catalyzed Asymmetric Allylic Substitution Reactions, *Chem. Rev.* (2018).
- [55] S.B. SINGH, Iridium Chemistry and Its Catalytic Applications: a Brief, *Green Chem. Technol. Lett.* 2 (2016) 206–210.
- [56] Q.Y. Bi, J.D. Lin, Y.M. Liu, S.H. Xie, H.Y. He, Y. Cao, Partially reduced iridium oxide clusters dispersed on titania as efficient catalysts for facile synthesis of dimethylformamide from CO₂, H₂ and dimethylamine, *Chem. Commun.* 50 (2014) 9138–9140.
- [57] S. Li, Y. Xu, Y. Chen, W. Li, L. Lin, M. Li, Y. Deng, X. Wang, B. Ge, C. Yang, S. Yao, J. Xie, Y. Li, X. Liu, D. Ma, Tuning the Selectivity of Catalytic Carbon Dioxide Hydrogenation over Iridium/Cerium Oxide Catalysts with a Strong Metal–Support Interaction, *Angew. Chemie - Int. Ed.* 56 (2017) 10761–

- 10765.
- [58] P. Chen, J. Lu, G. Xie, L. Zhu, M. Luo, Characterizations of Ir/TiO₂ catalysts with different Ir contents for selective hydrogenation of crotonaldehyde, *React. Kinet. Mech. Catal.* 106 (2012) 419–434.
- [59] J. qi Bai, M. Tamura, Y. Nakagawa, K. Tomishige, A nickel-iridium alloy as an efficient heterogeneous catalyst for hydrogenation of olefins, *Chem. Commun.* 55 (2019) 10519–10522.
- [60] K. Tateyama, K. Wada, H. Miura, S. Hosokawa, R. Abe, M. Inoue, Dehydrogenative synthesis of benzimidazoles under mild conditions with supported iridium catalysts, *Catal. Sci. Technol.* 6 (2016) 1677–1684.
- [61] J. Li, H. Liu, H. Zhu, W. Yao, D. Wang, Highly Efficient and Recyclable Porous Organic Polymer Supported Iridium Catalysts for Dehydrogenation and Borrowing Hydrogen Reactions in Water, *ChemCatChem.* (2021).
- [62] G. Zhu, Z.C. Duan, H. Zhu, M. Qi, D. Wang, Iridium and copper supported on silicon dioxide as chemoselective catalysts for dehydrogenation and borrowing hydrogen reactions, *Mol. Catal.* 505 (2021) 111516.
- [63] Z. Yinghuai, K. Chenyan, T.P. Ang, A. Emi, W. Monalisa, L.K.J. Louis, N.S. Hosmane, J.A. Maguire, Catalytic phenylborylation reaction by iridium(0) nanoparticles produced from hydridoiridium carborane, *Inorg. Chem.* 47 (2008) 5756–5761.
- [64] T. Tagata, M. Nishida, A. Nishida, Development of recyclable iridium catalyst for C–H borylation, *Tetrahedron Lett.* 50 (2009) 6176–6179.
- [65] T. Tagata, M. Nishida, A. Nishida, Continuous-Flow C–H borylation of arene derivatives, *Adv. Synth. Catal.* 352 (2010) 1662–1666.
- [66] S. Kawamorita, H. Ohmiya, K. Hara, A. Fukuoka, M. Sawamura, Directed ortho borylation of functionalized Arenes catalyzed by a silica-supported compact phosphine-iridium system, *J. Am. Chem. Soc.* 131 (2009) 5058–5059.
- [67] S. Kawamorita, R. Murakami, T. Iwai, M. Sawamura, Synthesis of primary and secondary alkylboronates through site-selective C(sp³)-H activation with silica-supported monophosphine-Ir catalysts, *J. Am. Chem. Soc.* 135 (2013) 2947–2950.
- [68] A. Aramata, T. Yamazaki, K. Kunimatsu, M. Enyo, Electrooxidation of methanol on iridium in acidic solutions: Electrocatalysis and surface characterization by infrared spectroscopy, *J. Phys. Chem.* 91 (1987) 2309–2314.
- [69] W. Du, Q. Wang, D. Saxner, N.A. Deskins, D. Su, J.E. Krzanowski, A.I. Frenkel, X. Teng, Highly active Iridium/Iridium-tin/tin oxide heterogeneous nanoparticles as alternative electrocatalysts for the ethanol oxidation reaction, *J. Am. Chem. Soc.* 133 (2011) 15172–15183.
- [70] W. Du, N.A. Deskins, D. Su, X. Teng, Iridium-ruthenium alloyed nanoparticles for the ethanol oxidation fuel cell reactions, *ACS Catal.* 2 (2012) 1226–1231.
- [71] S.Y. Shen, T.S. Zhao, J.B. Xu, Carbon-supported bimetallic PdIr catalysts for

- ethanol oxidation in alkaline media, *Electrochim. Acta.* 55 (2010) 9179–9184.
- [72] J.C.M. Silva, M.H.M.T. Assumpção, P. Hammer, A.O. Neto, E. V. Spinacé, E.A. Baranova, Iridium–Rhodium Nanoparticles for Ammonia Oxidation: Electrochemical and Fuel Cell Studies, *ChemElectroChem.* 4 (2017) 1101–1107.
- [73] A. Bonesi, M. Asteazaran, M.S. Moreno, G. Zampieri, S. Bengio, W. Triaca, A.M. Castro Luna, Preparation and evaluation of carbon-supported catalysts for ethanol oxidation, *J. Solid State Electrochem.* 17 (2013) 1823–1829.
- [74] B.A. López De Mishima, D. Lescano, T. Molina Holgado, H.T. Mishima, Electrochemical oxidation of ammonia in alkaline solutions: its application to an amperometric sensor, *Electrochim. Acta.* 43 (1998) 395–404.
- [75] K. Endo, K. Nakamura, Y. Katayama, T. Miura, Pt–Me (Me = Ir, Ru, Ni) binary alloys as an ammonia oxidation anode, *Electrochim. Acta.* 49 (2004) 2503–2509.
- [76] K. Endo, Y. Katayama, T. Miura, Pt–Ir and Pt–Cu binary alloys as the electrocatalyst for ammonia oxidation, *Electrochim. Acta.* 49 (2004) 1635–1638.
- [77] E. Iojoiu, P. Gélin, H. Praliaud, M. Primet, Reduction of NO by propene over supported iridium catalysts under lean-burn conditions: An in situ FTIR study, *Appl. Catal. A Gen.* 263 (2004) 39–48.
- [78] W. Chen, Q. Shen, R.A. Bartynski, P. Kaghazchi, T. Jacob, Reduction of nitric oxide by acetylene on Ir surfaces with different morphologies: Comparison with reduction of NO by CO, *Langmuir.* 29 (2013) 1113–1121.
- [79] T. Xiong, Q. Zhang, New amination strategies based on nitrogen-centered radical chemistry, *Chem. Soc. Rev.* 45 (2016) 3069–3087.
- [80] B. Zhang, A. Studer, Recent advances in the synthesis of nitrogen heterocycles via radical cascade reactions using isonitriles as radical acceptors, *Chem. Soc. Rev.* 44 (2015) 3505–3521.
- [81] H. Kim, S. Chang, The use of ammonia as an ultimate amino source in the transition metal-catalyzed C–H amination, *Acc. Chem. Res.* 50 (2017) 482–486.
- [82] F. Wöhler, Ueber künstliche Bildung des Harnstoffs, *Ann. Phys.* 88 (1828) 253–256.
- [83] E. Vitaku, D.T. Smith, J.T. Njardarson, Analysis of the structural diversity, substitution patterns, and frequency of nitrogen heterocycles among U.S. FDA approved pharmaceuticals, *J. Med. Chem.* 57 (2014) 10257–10274.
- [84] N. Kerru, L. Gummidi, S. Maddila, K.K. Gangu, S.B. Jonnalagadda, A review on recent advances in nitrogen-containing molecules and their biological applications, *Molecules.* 25 (2020).
- [85] N. Jiao, Nitrogenation strategy for the synthesis of N-containing compounds, 2016.
- [86] J. He, L. Chen, S. Liu, K. Song, S. Yang, A. Riisager, Sustainable access to

- renewable N-containing chemicals from reductive amination of biomass-derived platform compounds, *Green Chem.* 22 (2020) 6714–6747.
- [87] V. Pattabathula, J. Richardson, Introduction to ammonia production, *Chem. Eng. Prog.* 112 (2016) 69–75.
- [88] D.M. Roundhill, Transition Metal and Enzyme Catalyzed Reactions involving Reactions with Ammonia and Amines, *Chem. Rev.* 92 (1992) 1–27.
- [89] M.C. Willis, Palladium-catalyzed coupling of ammonia and hydroxide with aryl halides: The direct synthesis of primary anilines and phenols, *Angew. Chemie - Int. Ed.* 46 (2007) 3402–3404.
- [90] Q. Shen, J.F. Hartwig, Palladium-catalyzed coupling of ammonia and lithium amide with aryl halides, *J. Am. Chem. Soc.* 128 (2006) 10028–10029.
- [91] N. Xia, M. Taillefer, A very simple copper-catalyzed synthesis of anilines by employing aqueous ammonia, *Angew. Chemie - Int. Ed.* 48 (2009) 337–339.
- [92] G.D. Vo, J.F. Hartwig, Palladium-catalyzed coupling of ammonia with aryl chlorides, bromides, iodides, and sulfonates: A general method for the preparation of primary arylamines, *J. Am. Chem. Soc.* 131 (2009) 11049–11061.
- [93] X.F. Wu, C. Darcel, Ligand-free iron/copper-cocatalyzed amination of aryl iodides, *European J. Org. Chem.* 3 (2009) 4753–4756.
- [94] S. Bähn, S. Imm, L. Neubert, M. Zhang, H. Neumann, M. Beller, The catalytic amination of alcohols, *ChemCatChem.* 3 (2011) 1853–1864.
- [95] J.I. Van der Vlugt, Advances in selective activation and application of ammonia in homogeneous catalysis, *Chem. Soc. Rev.* 39 (2010) 2302–2322.
- [96] J.L. Klinkenberg, J.F. Hartwig, Catalytic organometallic reactions of ammonia, *Angew. Chemie - Int. Ed.* 50 (2011) 86–95.
- [97] G. Guillena, D.J. Ramón, M. Yus, Hydrogen autotransfer in the N-alkylation of amines and related compounds using alcohols and amines as electrophiles, *Chem. Rev.* 110 (2010) 1611–1641.
- [98] C. Defieber, M.A. Ariger, P. Moriel, E.M. Carreira, Iridium-Catalyzed Synthesis of Primary Allylic Amines from Allylic Alcohols: Sulfamic Acid as Ammonia Equivalent, *Angew. Chemie Int. Ed.* 46 (2007) 3139–3143.
- [99] R. Kawahara, K.I. Fujita, R. Yamaguchi, Multialkylation of aqueous ammonia with alcohols catalyzed by water-soluble Cp*Ir-amine complexes, *J. Am. Chem. Soc.* 132 (2010) 15108–15111.
- [100] K.I. Fujita, S. Furukawa, N. Morishima, M. Shimizu, R. Yamaguchi, N-Alkylation of Aqueous Ammonia with Alcohols Leading to Primary Amines Catalyzed by Water-Soluble N-Heterocyclic Carbene Complexes of Iridium, *ChemCatChem.* 10 (2018) 1993–1997.
- [101] K. Das, R. Shibuya, Y. Nakahara, N. Germain, T. Ohshima, K. Mashima, Platinum-catalyzed direct amination of allylic alcohols with aqueous ammonia: Selective synthesis of primary allylamines, *Angew. Chemie - Int. Ed.* 51 (2012) 150–154.

- [102] T. Ohshima, K. Mashima, Platinum-Catalyzed Direct Amination of Allylic Alcohols, *J. Synth. Org. Chem. Japan.* 70 (2012) 1145–1156.
- [103] C. Gunanathan, D. Milstein, Selective Synthesis of Primary Amines Directly from Alcohols and Ammonia, *Angew. Chemie.* 120 (2008) 8789–8792.
- [104] E. Khaskin, M.A. Iron, L.J.W. Shimon, J. Zhang, D. Milstein, N-H activation of amines and ammonia by Ru via metal-ligand cooperation, *J. Am. Chem. Soc.* 132 (2010) 8542–8543.
- [105] E. Balaraman, D. Srimani, Y. Diskin-Posner, D. Milstein, Direct Synthesis of Secondary Amines From Alcohols and Ammonia Catalyzed by a Ruthenium Pincer Complex, *Catal. Letters.* 145 (2015) 139–144.
- [106] P. Daw, Y. Ben-David, D. Milstein, Acceptorless Dehydrogenative Coupling Using Ammonia: Direct Synthesis of N-Heteroaromatics from Diols Catalyzed by Ruthenium, *J. Am. Chem. Soc.* 140 (2018) 11931–11934.
- [107] X. Ye, P.N. Plessow, M.K. Brinks, M. Schelwies, T. Schaub, F. Rominger, R. Paciello, M. Limbach, P. Hofmann, Alcohol amination with ammonia catalyzed by an acridine-based ruthenium pincer complex: A mechanistic study, *J. Am. Chem. Soc.* 136 (2014) 5923–5929.
- [108] A. Tillack, D. Hollmann, K. Mevius, D. Michalik, S. Bähn, M. Beller, Salt-Free Synthesis of Tertiary Amines by Ruthenium-Catalyzed Amination of Alcohols, *European J. Org. Chem.* 2008 (2008) 4745–4750.
- [109] D. Hollmann, A. Tillack, D. Michalik, R. Jackstell, M. Beller, An improved ruthenium catalyst for the environmentally benign amination of primary and secondary alcohols, *Chem. - An Asian J.* 2 (2007) 403–410.
- [110] D. Pinggen, C. Müller, D. Vogt, Direct amination of secondary alcohols using ammonia, *Angew. Chemie - Int. Ed.* 49 (2010) 8130–8133.
- [111] S. Imm, L. Neubert, H. Neumann, M. Beller, An efficient and general synthesis of primary amines by ruthenium-catalyzed amination of secondary alcohols with ammonia, *Angew. Chemie - Int. Ed.* 49 (2010) 8126–8129.
- [112] S. Imm, S. Bähn, M. Zhang, L. Neubert, H. Neumann, F. Klasovsky, J. Pfeffer, T. Haas, M. Beller, Improved Ruthenium-Catalyzed Amination of Alcohols with Ammonia: Synthesis of Diamines and Amino Esters, *Angew. Chemie - Int. Ed.* 50 (2011) 7599–7603.
- [113] M. Zhang, S. Imm, S. Bähn, H. Neumann, M. Beller, Synthesis of α -Amino Acid Amides: Ruthenium-Catalyzed Amination of α -Hydroxy Amides, *Angew. Chemie Int. Ed.* 50 (2011) 11197–11201.
- [114] H. Ohta, Y. Yuyama, Y. Uozumi, Y.M.A. Yamada, In-water dehydrative alkylation of ammonia and amines with alcohols by a polymeric bimetallic catalyst, *Org. Lett.* 13 (2011) 3892–3895.
- [115] Y.A. Yamada, H. Ohta, Y. Yuyama, Y. Uozumi, Polymeric bimetallic catalyst-promoted in-water dehydrative alkylation of ammonia and amines with alcohols, *Synth.* 45 (2013) 2093–2100.
- [116] J. He, J.W. Kim, K. Yamaguchi, N. Mizuno, Efficient catalytic synthesis of

- tertiary and secondary amines from alcohols and urea, *Angew. Chemie - Int. Ed.* 48 (2009) 9888–9891.
- [117] K. Yamaguchi, J. He, T. Oishi, N. Mizuno, The “borrowing hydrogen strategy” by supported ruthenium hydroxide catalysts: Synthetic scope of symmetrically and unsymmetrically substituted amines, *Chem. - A Eur. J.* 16 (2010) 7199–7207.
- [118] D. Ruiz, A. Aho, T. Saloranta, K. Eränen, J. Wärnå, R. Leino, D.Y. Murzin, Direct amination of dodecanol with NH₃ over heterogeneous catalysts. Catalyst screening and kinetic modelling, *Chem. Eng. J.* 307 (2017) 739–749.
- [119] J. Niemeier, R. V. Engel, M. Rose, Is water a suitable solvent for the catalytic amination of alcohols?, *Green Chem.* 19 (2017) 2839–2845.
- [120] L. Fang, Z. Yan, J. Wu, A. Bugaev, C. Lamberti, M. Pera-Titus, Highly selective Ru/HBEA catalyst for the direct amination of fatty alcohols with ammonia, *Appl. Catal. B Environ.* 286 (2021).
- [121] X.P. Fu, P. Han, Y.Z. Wang, S. Wang, N. Yan, Insight into the roles of ammonia during direct alcohol amination over supported Ru catalysts, *J. Catal.* 399 (2021) 121–131.
- [122] M.R. Ball, T.S. Wesley, K.R. Rivera-Dones, G.W. Huber, J.A. Dumesic, Amination of 1-hexanol on bimetallic AuPd/TiO₂ catalysts, *Green Chem.* 20 (2018) 4695–4709.
- [123] L. He, Y. Qian, R.S. Ding, Y.M. Liu, H.Y. He, K.N. Fan, Y. Cao, Highly efficient heterogeneous gold-catalyzed direct synthesis of tertiary and secondary amines from alcohols and urea, *ChemSusChem.* 5 (2012) 621–624.
- [124] X. Cui, H. Yuan, J.P. Li, F. De Campo, M. Pera-Titus, Y. Deng, F. Shi, Novel route for the synthesis of 8-oxa-3-azabicyclo[3.2.1]octane: One-pot aminocyclization of 2,5-tetrahydrofurandimethanol catalyzed by Pt/NiCuAlO_x, *Catal. Commun.* 58 (2015) 195–199.
- [125] T. Takanashi, Y. Nakagawa, K. Tomishige, Amination of alcohols with ammonia in water over Rh catalyst, *Chem. Lett.* 43 (2014) 822–824.
- [126] F. Niu, S. Xie, M. Bahri, O. Ersen, Z. Yan, B.T. Kusuma, M. Pera-Titus, A.Y. Khodakov, V. V. Ordonsky, Catalyst Deactivation for Enhancement of Selectivity in Alcohols Amination to Primary Amines, *ACS Catal.* 9 (2019) 5986–5997.
- [127] K.I. Shimizu, K. Kon, W. Onodera, H. Yamazaki, J.N. Kondo, Heterogeneous Ni catalyst for direct synthesis of primary amines from alcohols and ammonia, *ACS Catal.* 3 (2013) 112–117.
- [128] K.I. Shimizu, S. Kanno, K. Kon, S.M.A. Hakim Siddiki, H. Tanaka, Y. Sakata, N-alkylation of ammonia and amines with alcohols catalyzed by Ni-loaded CaSiO₃, *Catal. Today.* 232 (2014) 134–138.
- [129] A. Tomer, Z. Yan, A. Ponchel, M. Pera-Titus, Mixed oxides supported low-nickel formulations for the direct amination of aliphatic alcohols with ammonia, *J. Catal.* 356 (2017) 133–146.

- [130] A.Y.K. Leung, K. Hellgardt, K.K.M. Hii, Catalysis in Flow: Nickel-Catalyzed Synthesis of Primary Amines from Alcohols and NH₃, *ACS Sustain. Chem. Eng.* 6 (2018) 5479–5484.
- [131] Y. Liu, A. Afanasenko, S. Elangovan, Z. Sun, K. Barta, Primary Benzylamines by Efficient N-Alkylation of Benzyl Alcohols Using Commercial Ni Catalysts and Easy-to-Handle Ammonia Sources, *ACS Sustain. Chem. Eng.* 7 (2019) 11267–11274.
- [132] L. Fang, Z. Yan, K. Vits, B. Southward, M. Pera-Titus, Nanoceria-promoted low Pd-Ni catalyst for the synthesis of secondary amines from aliphatic alcohols and ammonia, *Catal. Sci. Technol.* 9 (2019) 1215–1230.
- [133] J. He, K. Yamaguchi, N. Mizuno, Selective synthesis of secondary amines via N-alkylation of primary amines and ammonia with alcohols by supported copper hydroxide catalysts, *Chem. Lett.* 39 (2010) 1182–1183.
- [134] D.A. Horton, G.T. Bourne, M.L. Smythe, The combinatorial synthesis of bicyclic privileged structures or privileged substructures, *Chem. Rev.* 103 (2003) 893–930.
- [135] Salahuddin, M. Shaharyar, A. Mazumder, Benzimidazoles: A biologically active compounds, *Arab. J. Chem.* 10 (2017) S157–S173.
- [136] J.B. wright, The chemistry of the benzimidazoles, *Chem. Rev.* 48 (1951) 397–541.
- [137] P.N. Preston, Synthesis, Reactions, and Spectroscopic Properties of Benzimidazoles, *Chem. Rev.* 74 (1974) 279–314.
- [138] M. Curini, F. Epifano, F. Montanari, O. Rosati, S. Taccone, Ytterbium triflate promoted synthesis of benzimidazole derivatives, *Synlett.* 2004 (2004) 1832–1834.
- [139] J. Zhu, Z. Zhang, C. Miao, W. Liu, W. Sun, Synthesis of benzimidazoles from o-phenylenediamines and DMF derivatives in the presence of PhSiH₃, *Tetrahedron.* 73 (2017) 3458–3462.
- [140] E. Alcalde, I. Dinares, L. Perez-Garcia, T. Roca, An advantageous synthesis of 2-substituted benzimidazoles using polyphosphoric acid. 2-(pyridyl)-1H-benzimidazoles, 1-alkyl-(1H-benzimidazol-2-yl)pyridinium salts, their homologues and vinylogues, *Synthesis (Stuttg.)*. (1992) 395–398.
- [141] P. Sun, Z. Hu, The convenient synthesis of benzimidazole derivatives catalyzed by I₂ in aqueous media, *J. Heterocycl. Chem.* 43 (2006) 773–775.
- [142] R.J. Perry, B.D. Wilson, A Novel Palladium-Catalyzed Synthesis of 2-Arylbenzimidazoles, *J. Org. Chem.* 58 (1993) 7016–7021.
- [143] C.T. Brain, S.A. Brunton, An intramolecular palladium-catalysed aryl amination reaction to produce benzimidazoles, *Tetrahedron Lett.* 43 (2002) 1893–1895.
- [144] T. Kondo, S. Yang, K.-T.T. Huh, M. Kobayashi, S. Kotachi, Y. Watanabe, Ruthenium Complex-Catalyzed Facile Synthesis of 2-Substituted Benzimidazoles, *Chem. Lett.* 20 (1991) 1275–1278.

- [145] A.J. Blacker, M.M. Farah, M.I. Hall, S.P. Marsden, O. Saidi, J.M.J. Williams, Synthesis of benzazoles by hydrogen-transfer catalysis, *Org. Lett.* 11 (2009) 2039–2042.
- [146] T. Hille, T. Irrgang, R. Kempe, The synthesis of benzimidazoles and quinoxalines from aromatic diamines and alcohols by iridium-catalyzed acceptorless dehydrogenative alkylation, *Chem. - A Eur. J.* 20 (2014) 5569–5572.
- [147] P. Daw, Y. Ben-David, D. Milstein, Direct Synthesis of Benzimidazoles by Dehydrogenative Coupling of Aromatic Diamines and Alcohols Catalyzed by Cobalt, *ACS Catal.* 7 (2017) 7456–7460.
- [148] P. Laszlo, Catalysis of Organic Reactions by Inorganic Solids, *Acc. Chem. Res.* 19 (1986) 121–127.
- [149] Y. Izumi, M. Onaka, Organic Syntheses Using Aluminosilicates, *Adv. Catal.* 38 (1992) 245–282.
- [150] L. Yin, J. Liebscher, Carbon-carbon coupling reactions catalyzed by heterogeneous palladium catalysts, *Chem. Rev.* 107 (2007) 133–173.
- [151] A. Corma, H. Garci, Supported gold nanoparticles as catalysts for organic reactions, *Chem. Soc. Rev.* 37 (2008) 2096–2126.
- [152] K. Wada, S. Hosokawa, M. Inoue, Development of Ceria-Supported Ruthenium Catalysts Effective for Various Synthetic Reactions, *Catal. Surv. from Asia.* 15 (2011) 1–11.
- [153] K. Wada, H. Miura, S. Hosokawa, M. Inoue, Development of ceria-supported ruthenium catalysts for green organic transformation processes, *J. Japan Pet. Inst.* 56 (2013) 69–79.
- [154] J.W. Kim, J. He, K. Yamaguchi, N. Mizuno, Heterogeneously catalyzed one-pot synthesis of aldimines from primary alcohols and amines by supported ruthenium hydroxides, *Chem. Lett.* 38 (2009) 920–921.
- [155] Y. Shiraishi, Y. Sugano, S. Tanaka, T. Hirai, One-pot synthesis of benzimidazoles by simultaneous photocatalytic and catalytic reactions on Pt@TiO₂ nanoparticles, *Angew. Chemie - Int. Ed.* 49 (2010) 1656–1660.
- [156] C. Chaudhari, S.M.A.H. Siddiki, K.I. Shimizu, Acceptorless dehydrogenative synthesis of benzothiazoles and benzimidazoles from alcohols or aldehydes by heterogeneous Pt catalysts under neutral conditions, *Tetrahedron Lett.* 56 (2015) 4885–4888.
- [157] P.L. Reddy, R. Arundhathi, M. Tripathi, P. Chauhan, N. Yan, D.S. Rawat, Solvent-Free Oxidative Synthesis of 2-Substituted Benzimidazoles by Immobilized Cobalt Oxide Nanoparticles on Alumina/Silica Support, *ChemistrySelect.* 2 (2017) 3889–3895.
- [158] J. Mokhtari, A. Hasani Bozcheloei, One-pot synthesis of benzoazoles via dehydrogenative coupling of aromatic 1,2-diamines/2-aminothiophenol and alcohols using Pd/Cu-MOF as a recyclable heterogeneous catalyst, *Inorganica Chim. Acta.* 482 (2018) 726–731.

- [159] B. Guo, H.X. Li, S.Q. Zhang, D.J. Young, J.P. Lang, C-N Bond Formation Catalyzed by Ruthenium Nanoparticles Supported on N-Doped Carbon via Acceptorless Dehydrogenation to Secondary Amines, Imines, Benzimidazoles and Quinoxalines, *ChemCatChem*. 10 (2018) 5627–5636.
- [160] F. Feng, Y. Deng, Z. Cheng, X. Xu, Q. Zhang, C. Lu, L. Ma, X. Li, Heterogeneous catalytic synthesis of 2-methylbenzimidazole from 2-nitroaniline and ethanol over mg modified Cu-Pd/ γ -Al₂O₃, *Catalysts*. 9 (2019) 8.
- [161] S. Sharma, A. Sharma, Yamini, P. Das, Supported Rhodium (Rh@PS) Catalyzed Benzimidazoles Synthesis Using Ethanol/Methanol as C₂H₃/CH Source, *Adv. Synth. Catal.* 361 (2019) 67–72.
- [162] S.M.A. Hakim Siddiki, T. Toyao, K.I. Shimizu, Acceptorless dehydrogenative coupling reactions with alcohols over heterogeneous catalysts, *Green Chem.* 20 (2018) 2933–2952.
- [163] S. Das, S. Mallick, S. De Sarkar, Cobalt-Catalyzed Sustainable Synthesis of Benzimidazoles by Redox-Economical Coupling of o-Nitroanilines and Alcohols, *J. Org. Chem.* 84 (2019) 12111–12119.
- [164] G. Li, J. Wang, B. Yuan, D. Zhang, Z. Lin, P. Li, H. Huang, Iron-catalyzed one-pot synthesis of benzimidazoles from 2-nitroanilines and benzylic alcohols, *Tetrahedron Lett.* 54 (2013) 6934–6936.
- [165] J. Wu, C. Darcel, Iron-Catalyzed Hydrogen Transfer Reduction of Nitroarenes with Alcohols: Synthesis of Imines and Aza Heterocycles, *J. Org. Chem.* 86 (2021) 1023–1036.
- [166] X. Li, R. Hu, Y. Tong, Q. Pan, D. Miao, S. Han, An efficient route for the synthesis of benzimidazoles via a hydrogen-transfer strategy between o-nitroanilines and alcohols, *Tetrahedron Lett.* 57 (2016) 4645–4649.
- [167] L. Tang, X. Guo, Y. Yang, Z. Zha, Z. Wang, Gold nanoparticles supported on titanium dioxide: An efficient catalyst for highly selective synthesis of benzoxazoles and benzimidazoles, *Chem. Commun.* 50 (2014) 6145–6148.
- [168] Q. Guan, Q. Sun, L. Wen, Z. Zha, Y. Yang, Z. Wang, The synthesis of benzimidazoles via a recycled palladium catalysed hydrogen transfer under mild conditions, *Org. Biomol. Chem.* 16 (2018) 2088–2096.
- [169] T. Hisano, M. Ichikawa, K. Tsumoto, M. Tasaki, Synthesis of Benzoxazoles, Benzothiazoles and Benzimidazoles and Evaluation of Their Antifungal, Insecticidal and Herbicidal Activities, *Chem. Pharm. Bull.* 30 (1982) 2996–3004.
- [170] C.S. Demmer, L. Bunch, Benzoxazoles and oxazolopyridines in medicinal chemistry studies, *Eur. J. Med. Chem.* 97 (2015) 778–785.
- [171] N. Aggarwal, A. Kaur, K. Anand, H. Kumar, S. Wakode, Biologically active Benzoxazole: A comprehensive review, *Int. J. Pharm. Sci. Res.* 2 (2017) 2455–4685.
- [172] R.V. Kumar, Synthetic strategies towards benzoxazole ring systems: A review,

- Asian J. Chem. 16 (2004) 1241–1260.
- [173] Y. Wang, K. Sarris, D.R. Sauer, S.W. Djuric, A simple and efficient one step synthesis of benzoxazoles and benzimidazoles from carboxylic acids, *Tetrahedron Lett.* 47 (2006) 4823–4826.
- [174] S.M. Inamdar, V.K. More, S.K. Mandal, CuO nano-particles supported on silica, a new catalyst for facile synthesis of benzimidazoles, benzothiazoles and benzoxazoles, *Tetrahedron Lett.* 54 (2013) 579–583.
- [175] P.B. Gorepatil, Y.D. Mane, V.S. Ingle, Samarium(III) triflate as an efficient and reusable catalyst for facile synthesis of benzoxazoles and benzothiazoles in aqueous medium, *Synlett.* 24 (2013) 2241–2244.
- [176] Y. Endo, J.E. Bäckvall, Biomimetic oxidative coupling of benzylamines and 2-aminophenols: Synthesis of benzoxazoles, *Chem. - A Eur. J.* 18 (2012) 13609–13613.
- [177] A. Khalafi-Nezhad, F. Panahi, Ruthenium-catalyzed synthesis of benzoxazoles using acceptorless dehydrogenative coupling reaction of primary alcohols with 2-aminophenol under heterogeneous conditions, *ACS Catal.* 4 (2014) 1686–1692.
- [178] P.K. Samanta, S. Ray, T. Das, S.H. Gage, M. Nandi, R.M. Richards, P. Biswas, Palladium oxide nanoparticles intercalated mesoporous silica for solvent free acceptorless dehydrogenation reactions of alcohols, *Microporous Mesoporous Mater.* 284 (2019) 186–197.
- [179] L. Robert, J. Burwell, Manual of symbols and terminology for physicochemical quantities and units—appendix II, *Pure Appl. Chem.* 46 (1976) 71–90.
- [180] H.-S. Oh, H.N. Nong, T. Reier, M. Gliech, P. Strasser, Oxide-supported Ir nanodendrites with high activity and durability for the oxygen evolution reaction in acid PEM water electrolyzers, *Chem. Sci.* 6 (2015) 3321–3328.
- [181] A. Gómez-Cortés, G. Díaz, R. Zanella, H. Ramírez, P. Santiago, J.M. Saniger, Au-ir/tio₂ prepared by deposition precipitation with urea: improved activity and stability in co oxidation, *J. Phys. Chem. C.* 113 (2009) 9710–9720.
- [182] X. Shao, X. Yang, J. Xu, S. Liu, S. Miao, X. Liu, X. Su, H. Duan, Y. Huang, T. Zhang, Iridium Single-Atom Catalyst Performing a Quasi-homogeneous Hydrogenation Transformation of CO₂ to Formate, *Chem.* 5 (2019) 693–705.
- [183] S. Bagheri, N. Muhd Julkapli, S. Bee Abd Hamid, Titanium dioxide as a catalyst support in heterogeneous catalysis, *Sci. World J.* 2014 (2014).
- [184] J.C. Védrine, Metal Oxides in Heterogeneous Oxidation Catalysis: State of the Art and Challenges for a More Sustainable World, *ChemSusChem.* 12 (2019) 577–588.
- [185] M. Sankar, Q. He, R. V. Engel, M.A. Sainna, A.J. Logsdail, A. Roldan, D.J. Willock, N. Agarwal, C.J. Kiely, G.J. Hutchings, Role of the Support in Gold-Containing Nanoparticles as Heterogeneous Catalysts, *Chem. Rev.* 120 (2020) 3890–3938.
- [186] M.V. Ganduglia-Pirovano, A. Hofmann, J. Sauer, Oxygen vacancies in

- transition metal and rare earth oxides: Current state of understanding and remaining challenges, *Surf. Sci. Rep.* 62 (2007) 219–270.
- [187] W.H. Strehlow, E.L. Cook, *Compilation of Energy Band Gaps in Elemental and Binary Compound Semiconductors and Insulators*, *J. Phys. Chem. Ref. Data.* 2 (1973) 163–200.
- [188] F. Yang, D. Deng, X. Pan, Q. Fu, X. Bao, Understanding nano effects in catalysis, *Natl. Sci. Rev.* 2 (2015) 183–201.
- [189] G. Pacchioni, H.J. Freund, Controlling the charge state of supported nanoparticles in catalysis: lessons from model systems, *Chem. Soc. Rev.* 47 (2018) 8474–8502.
- [190] Y. Guo, Y.W. Zhang, Metal Clusters Dispersed on Oxide Supports: Preparation Methods and Metal-Support Interactions, *Top. Catal.* 61 (2018) 855–874.
- [191] Q.H. Fan, Y.M. Li, A.S.C. Chan, Recoverable catalysts for asymmetric organic synthesis, *Chem. Rev.* 102 (2002) 3385–3466.
- [192] A.M.P. Salvo, F. Giacalone, M. Gruttadauria, Advances in organic and organic-inorganic hybrid polymeric supports for catalytic applications, *Molecules.* 21 (2016).
- [193] Y.G. Kim, S.K. Oh, R.M. Crooks, Preparation and Characterization of 1-2 nm Dendrimer-Encapsulated Gold Nanoparticles Having Very Narrow Size Distributions, *Chem. Mater.* 16 (2004) 167–172.
- [194] R.W.J. Scott, O.M. Wilson, R.M. Crooks, Synthesis, Characterization, and Applications of Dendrimer-Encapsulated Nanoparticles, *J. Phys. Chem. B.* 109 (2005) 692–704.
- [195] A.M. Abu-Elfotoh, K. Phomkeona, K. Shibatomi, S. Iwasa, Asymmetric inter- and intramolecular cyclopropanation reactions catalyzed by a reusable macroporous-polymer-supported chiral ruthenium(II)/phenyloxazoline complex, *Angew. Chemie - Int. Ed.* 49 (2010) 8439–8443.
- [196] Q.H. Fan, C.Y. Ren, C.H. Yeung, W.H. Hu, A.S.C. Chan, Highly effective soluble polymer-supported catalysts for asymmetric hydrogenation [2], *J. Am. Chem. Soc.* 121 (1999) 7407–7408.
- [197] E. Pérez-Mayoral, V. Calvino-Casilda, E. Soriano, Metal-supported carbon-based materials: Opportunities and challenges in the synthesis of valuable products, *Catal. Sci. Technol.* 6 (2016) 1265–1291.
- [198] M.S. Dresselhaus, G. Dresselhaus, P. Avouris, *Carbon Nanotubes: Synthesis, Structure, Properties and Applications*, Springer Berlin Heidelberg, 2001.
- [199] V. Pascanu, G. González Miera, A.K. Inge, B. Martín-Matute, Metal-Organic Frameworks as Catalysts for Organic Synthesis: A Critical Perspective, *J. Am. Chem. Soc.* 141 (2019) 7223–7234.
- [200] A.H. Chughtai, N. Ahmad, H.A. Younus, A. Laypkov, F. Verpoort, Metal-organic frameworks: Versatile heterogeneous catalysts for efficient catalytic organic transformations, *Chem. Soc. Rev.* 44 (2015) 6804–6849.
- [201] S.J. Tauster, S.C. Fung, R.L. Garten, Strong Metal-Support Interactions. Group

- 8 Noble Metals Supported on TiO₂, *J. Am. Chem. Soc.* 100 (1978) 170–175.
- [202] S.J. Tauster, Strong Metal-Support Interactions, *Acc. Chem. Res.* 20 (1987) 389–394.
- [203] S.J. Tauster, S.C. Fung, R.T.K. Baker, J.A. Horsley, Strong Interactions in Catalysts, *Science* (80-.). 211 (1981) 1121–1125.
- [204] J.C. Matsubu, S. Zhang, L. DeRita, N.S. Marinkovic, J.G. Chen, G.W. Graham, X. Pan, P. Christopher, Adsorbate-mediated strong metal-support interactions in oxide-supported Rh catalysts, *Nat. Chem.* 9 (2017) 120–127.
- [205] H. Li, X. Weng, Z. Tang, H. Zhang, D. Ding, M. Chen, H. Wan, Evidence of the Encapsulation Model for Strong Metal-Support Interaction under Oxidized Conditions: A Case Study on TiO_x/Pt(111) for CO Oxidation by in Situ Wide Spectral Range Infrared Reflection Adsorption Spectroscopy, *ACS Catal.* 8 (2018) 10156–10163.
- [206] J. Fan, X. Wu, L. Yang, D. Weng, The SMSI between supported platinum and CeO₂-ZrO₂-La₂O₃ mixed oxides in oxidative atmosphere, *Catal. Today.* 126 (2007) 303–312.
- [207] S. Yang, D.Y. Chung, Y.J. Tak, J. Kim, H. Han, J.S. Yu, A. Soon, Y.E. Sung, H. Lee, Electronic structure modification of platinum on titanium nitride resulting in enhanced catalytic activity and durability for oxygen reduction and formic acid oxidation, *Appl. Catal. B Environ.* 174–175 (2015) 35–42.
- [208] C.J. Pan, M.C. Tsai, W.N. Su, J. Rick, N.G. Akalework, A.K. Agegnehu, S.Y. Cheng, B.J. Hwang, Tuning/exploiting Strong Metal-Support Interaction (SMSI) in Heterogeneous Catalysis, *J. Taiwan Inst. Chem. Eng.* 74 (2017) 154–186.
- [209] S. Matsuda, A. Kato, Titanium oxide based catalysts - a review, *Appl. Catal.* 8 (1983) 149–165.
- [210] J. Pan, C. Leygraf, D. Thierry, A.M. Ektessabi, Corrosion resistance for biomaterial applications of TiO₂ films deposited on titanium and stainless steel by ion-beam-assisted sputtering, *J. Biomed. Mater. Res.* 35 (1997) 309–318.
- [211] I. Poullos, P. Spathis, A. Grigoriadou, K. Delidou, P. Tsoumparis, Protection of marbles against corrosion and microbial corrosion with TiO₂ coatings, *J. Environ. Sci. Heal. - Part A Toxic/Hazardous Subst. Environ. Eng.* 34 (1999) 1455–1471.
- [212] K. Foger, J.R. Anderson, Thermally stable SMSI supports: Iridium supported on TiO₂-Al₂O₃ and on Ce-stabilized anatase, *Appl. Catal.* 23 (1986) 139–155.
- [213] D. Li, N. Ichikuni, S. Shimazu, T. Uematsu, Hydrogenation of CO₂ over sprayed Ru/TiO₂ fine particles and strong metal-support interaction, *Appl. Catal. A Gen.* 180 (1999) 227–235.
- [214] A. Vázquez-Zavala, J. García-Gómez, A. Gómez-Cortés, Study of the structure and selectivity of Pt–Au catalysts supported on Al₂O₃, TiO₂, and SiO₂, *Appl. Surf. Sci.* 167 (2000) 177–183.
- [215] H. Yasutake, M.S. Islam, M.A. Rahman, J. Yagyu, M. Fukuda, Y. Shudo, K.

- Kuroiwa, Y. Sekine, S. Hayami, High proton conductivity from titanium oxide nanosheets and their variation based on crystal phase, *Bull. Chem. Soc. Jpn.* 94 (2021) 1840–1845.
- [216] A. Jia, Y. Zhang, T. Song, Z. Zhang, C. Tang, Y. Hu, W. Zheng, M. Luo, J. Lu, W. Huang, Crystal-plane effects of anatase TiO₂ on the selective hydrogenation of crotonaldehyde over Ir/TiO₂ catalysts, *J. Catal.* 395 (2021) 10–22.
- [217] A. Visikovskiy, K. Mitsuhashi, Y. Kido, Role of gold nanoclusters supported on TiO₂ (110) model catalyst in CO oxidation reaction, *J. Vac. Sci. Technol. A Vacuum, Surfaces, Film.* 31 (2013) 061404.
- [218] X.Y. Ooi, W. Gao, H.C. Ong, H.V. Lee, J.C. Juan, W.H. Chen, K.T. Lee, Overview on catalytic deoxygenation for biofuel synthesis using metal oxide supported catalysts, *Renew. Sustain. Energy Rev.* 112 (2019) 834–852.
- [219] T.N. Phan, C.H. Ko, Synergistic effects of Ru and Fe on titania-supported catalyst for enhanced anisole hydrodeoxygenation selectivity, *Catal. Today.* 303 (2018) 219–226.
- [220] Z. He, M. Hu, X. Wang, Highly effective hydrodeoxygenation of guaiacol on Pt/TiO₂: Promoter effects, *Catal. Today.* 302 (2018) 136–145.
- [221] M.M. Ambursa, T.H. Ali, H.V. Lee, P. Sudarsanam, S.K. Bhargava, S.B.A. Hamid, Hydrodeoxygenation of dibenzofuran to bicyclic hydrocarbons using bimetallic Cu-Ni catalysts supported on metal oxides, *Fuel.* 180 (2016) 767–776.
- [222] D. Kubička, J. Horáček, M. Setnička, R. Bulánek, A. Zúkal, I. Kubičková, Effect of support-active phase interactions on the catalyst activity and selectivity in deoxygenation of triglycerides, *Appl. Catal. B Environ.* 145 (2014) 101–107.
- [223] T.S. Nguyen, D. Laurenti, P. Afanasiev, Z. Konuspayeva, L. Piccolo, Titania-supported gold-based nanoparticles efficiently catalyze the hydrodeoxygenation of guaiacol, *J. Catal.* 344 (2016) 136–140.
- [224] T.K. Vo, W.S. Kim, S.S. Kim, K.S. Yoo, J. Kim, Facile synthesis of Mo/Al₂O₃-TiO₂ catalysts using spray pyrolysis and their catalytic activity for hydrodeoxygenation, *Energy Convers. Manag.* 158 (2018) 92–102.
- [225] H.G. Manyar, C. Paun, R. Pilus, D.W. Rooney, J.M. Thompson, C. Hardacre, Highly selective and efficient hydrogenation of carboxylic acids to alcohols using titania supported Pt catalysts, *Chem. Commun.* 46 (2010) 6279.
- [226] J.A. Toledo-Antonio, C. Ángeles-Chávez, M.A. Cortés-Jácome, I. Cuauhtémoc-López, E. López-Salinas, M. Pérez-Luna, G. Ferrat-Torres, Highly dispersed Pt-Ir nanoparticles on titania nanotubes, *Appl. Catal. A Gen.* 437–438 (2012) 155–165.
- [227] Y. Li, Y. Fan, H. Yang, B. Xu, L. Feng, M. Yang, Y. Chen, Strong metal-support interaction and catalytic properties of anatase and rutile supported palladium catalyst Pd/TiO₂, *Chem. Phys. Lett.* 372 (2003) 160–165.

- [228] J.H. Kang, E.W. Shin, W.J. Kim, J.D. Park, S.H. Moon, Selective Hydrogenation of Acetylene on TiO₂-Added Pd Catalysts, *J. Catal.* 208 (2002) 310–320.
- [229] K.J.A. Raj, M.G. Prakash, R. Mahalakshmy, T. Elangovan, B. Viswanathan, Selective hydrogenation of acetophenone over nickel supported on titania, *Catal. Sci. Technol.* 2 (2012) 1429.
- [230] V. Nichele, M. Signoretto, F. Menegazzo, I. Rossetti, G. Cruciani, Hydrogen production by ethanol steam reforming: Effect of the synthesis parameters on the activity of Ni/TiO₂ catalysts, *Int. J. Hydrogen Energy.* 39 (2014) 4252–4258.
- [231] I. Jögi, K. Erme, J. Raud, M. Laan, Oxidation of NO by ozone in the presence of TiO₂ catalyst, *Fuel.* 173 (2016) 45–51.
- [232] E. Taarning, I.S. Nielsen, K. Egeblad, R. Madsen, C.H. Christensen, Chemicals from renewables: Aerobic oxidation of furfural and hydroxymethylfurfural over gold catalysts, *ChemSusChem.* 1 (2008) 75–78.
- [233] B. Jørgensen, S. Egholm Christiansen, M.L. Dahl Thomsen, C.H. Christensen, Aerobic oxidation of aqueous ethanol using heterogeneous gold catalysts: Efficient routes to acetic acid and ethyl acetate, *J. Catal.* 251 (2007) 332–337.
- [234] P. Panagiotopoulou, D.I. Kondarides, Effect of morphological characteristics of TiO₂-supported noble metal catalysts on their activity for the water-gas shift reaction, *J. Catal.* 225 (2004) 327–336.
- [235] C.M. Kalamaras, P. Panagiotopoulou, D.I. Kondarides, A.M. Efstathiou, Kinetic and mechanistic studies of the water-gas shift reaction on Pt/TiO₂ catalyst, *J. Catal.* 264 (2009) 117–129.
- [236] M. Xu, S. Yao, D. Rao, Y. Niu, N. Liu, M. Peng, P. Zhai, Y. Man, L. Zheng, B. Wang, B. Zhang, D. Ma, M. Wei, Insights into Interfacial Synergistic Catalysis over Ni@TiO₂-x Catalyst toward Water-Gas Shift Reaction, *J. Am. Chem. Soc.* 140 (2018) 11241–11251.
- [237] M. Shekhar, J. Wang, W.S. Lee, W.D. Williams, S.M. Kim, E.A. Stach, J.T. Miller, W.N. Delgass, F.H. Ribeiro, Size and support effects for the water-gas shift catalysis over gold nanoparticles supported on model Al₂O₃ and TiO₂, *J. Am. Chem. Soc.* 134 (2012) 4700–4708.
- [238] A. Yoshida, Y. Mori, T. Ikeda, K. Azemoto, S. Naito, Enhancement of catalytic activity of Ir/TiO₂ by partially reduced titanium oxide in aerobic oxidation of alcohols, *Catal. Today.* 203 (2013) 153–157.
- [239] S. Ito, X. Wang, A. Waheed, G. Li, N. Maeda, D.M. Meier, S. Naito, A. Baiker, Support effects in iridium-catalyzed aerobic oxidation of benzyl alcohol studied by modulation-excitation attenuated total reflection IR spectroscopy, *J. Catal.* 393 (2021) 42–50.

Chapter II Rapid Multialkylation of Aqueous Ammonia with Alcohols by Heterogeneous Iridium Catalyst under Simple Conditions

2.1 Introduction

Ammonia is one of the chemicals products of the most output in the world with an annual production of 144 million tons [1]. On account of its readily available and low cost, ammonia has been intensively studied as a nitrogen source in the synthesis of high-value chemical products [2–4]. However, most of the reactions require the use of harmful and toxic alkyl halides as substrates [5–9]. It is noteworthy that with the rising of “green & sustainable chemistry” [10,11], the catalytic synthesis of amine from ammonia with alcohols has attracted significant attention due to its advantages of high atom efficiency and environmentally benign features [4,12–14]. The N-alkylation reaction possesses a high atomic utilization and does not produce toxic or wasteful by-products (only H₂O is outgrowth) [15–18]. Up to now, the intensive research interests focus on developing homogeneous catalyzed systems for the synthesis of organic amines using ammonia or its solution, and transition-metal homogeneous catalysis systems utilizing Ru [19–24], Ir [25–27], have been the most advanced strategy [14]. For example, Fujita et al. reported a water-soluble iridium catalyst [Cp*Ir(NH₃)₃][I]₂ for multialkylation of aqueous ammonia with primary and secondary alcohols, and selectively convert to tertiary and secondary amines, respectively. The catalyst could be recycled by a facile procedure maintaining high activity for at least 3 cycles [25]. Water-soluble iridium complex catalysts bearing N-heterocyclic carbene ligands that

enable the selective N-monoalkylation of aqueous ammonia with a variety of alcohols were developed. Meanwhile, heterogeneous catalysts using Ir [28], Ni [29–34], Ru [35–37], Au-Pd [38], and Rh-In [39] have newly emerged. Nevertheless, there are still some restrictions in the catalytic reactions such as indispensability of organic solvent, high-pressure atmosphere of hydrogen or ammonia, and high temperature. On the other hand, during previous studies by us and other researchers, a series of titania-supported iridium catalysts which showed excellent activity in the catalytic synthesis of nitrogen heterocycles from amines or diamine with alcohols under mild conditions has been developed [40–45].

In this chapter, it is reported that titania-supported iridium catalysts of high efficiency for the multialkylation of aqueous ammonia with alcohols without any additional solvent in the air or argon atmosphere. The TEM images reveal the highly dispersed iridium species of less than 2 nm in diameter. Whereas there are many reports for the heterogeneous catalytic synthesis of amines from ammonia with alcohols, the development of the catalytic synthesis procedure without organic solvent and high-pressure of H₂ (or NH₃) simultaneously at low temperature is highly desired. The catalysis smoothly proceeded on larger scales. In marked contrast to the traditional cognition, the desired product formed promptly within 6 h and gave a yield of over 99% in argon or over 85% in air, respectively.

2.2 Experiment section

2.2.1 General information

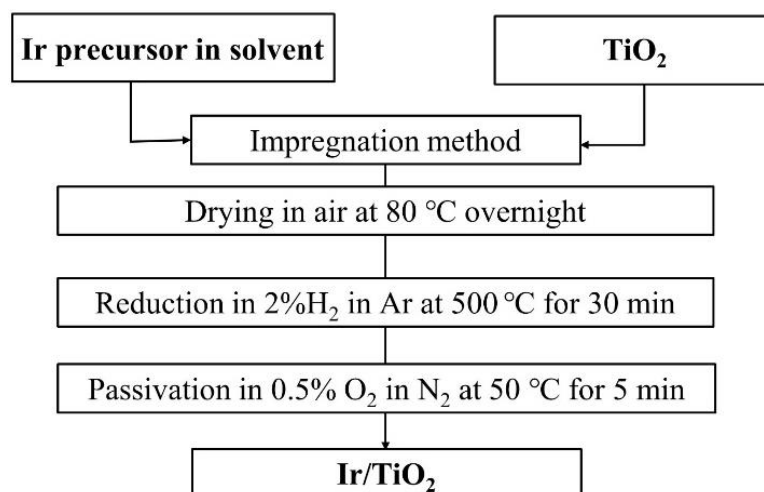
Tris(acetylacetonate)iridium(III) (Ir(acac)₃, C₁₅H₂₁O₆Ir), di- μ -chlorobis[(η -

cycloocta-1,5-diene) iridium(I)] ($[\text{Ir}(\text{cod})\text{Cl}]_2$, $\text{C}_{16}\text{H}_{24}\text{Cl}_2\text{Ir}_2$), IrO_2 , mesitylene, biphenyl, benzyl alcohol, and ammonia solution were delivered from Wako. Methanol, 1-octanol, and tetrahydrofuran (THF) were delivered from NACALAI. 4-methylbenzyl alcohol, 4-chlorobenzyl alcohol, and 4-fluorobenzyl alcohol, and 1-Phenylethanol were delivered from TCI.

JRC (Japan Reference Catalyst) titania (further designated as TIO-4, 6, and 10), silica (Cabot, Cab-O-Sil), alumina (JRC-ALO-7) and ceria were delivered by the Catalysis Society of Japan. All reagents were used as received.

2.2.2 Preparation of supported iridium catalyst

The supported catalysts were prepared by an impregnation method. Ir precursor (mainly $[\text{Ir}(\text{cod})\text{Cl}]_2$) was added in 10~15 mL of THF (or methanol for $\text{Ir}(\text{acac})_3$) under magnetic stirring at 80 °C, then 1.0 g of titania was added in air. After stirring thoroughly, the obtained powder sample was dried overnight in an oven at 80 °C. The resulting powder was reduced in a H_2 (2 vol.%) / Ar flow ($40 \text{ cm}^3 \text{ min}^{-1}$) at 500 °C (ramping rate; 10 °C/min) for 30 min by the use of a conventional flow reactor to give Ir/TiO₂ catalysts. After purged by N₂, the catalysts were passivated in O₂ (2 vol.%) / N₂ flow ($40 \text{ cm}^3 \text{ min}^{-1}$) at 50 °C for 5 min.



Scheme 1. Preparation procedure of titania-supported iridium catalysts.

2.2.3 General procedure for the catalytic runs

Catalytic reactions were performed in a glass Schlenk tube reactor (20 cm³) equipped with hot stirrer and cooling block to reflux the solution. A typical reaction procedure for the synthesis of desired product is as follows: the substrates and catalyst were added into the Schlenk tube equipped with a balloon. The reaction mixture was stirred at a desired temperature for 18 h under an air or argon atmosphere. Then the solid catalyst was removed by passing the mixture through a polytetrafluoroethylene (PTFE) filter (Millipore Millex LH, 0.45 μm), and the yield of products were quantified by a gas-liquid chromatography using biphenyl as an internal standard. The major products were isolated by silica gel column chromatography (hexane:ethyl acetate = 97:3 to 85:15).

2.2.4 Physical and analytical measurements

The organic products of catalytic runs were analyzed by GC-MS (Shimadzu GC-MS Parvum 2; Zebron ZB-1 capillary column, i.d. 0.25 mm, length 30 m, at 50–250 °C),

^1H and ^{13}C NMR (JEOL JNM-ECA 600; tetramethylsilane (TMS) was used as an internal standard) and gas-liquid chromatography (Shimadzu GC-14A; Zebtron ZB-1 capillary column, i.d. 0.25 mm, length 30 m, at 50–250 °C). The structures of titania and corresponding catalysts were investigated by using a powder X-ray diffractometer (XRD-6100, Shimadzu, Japan) with Cu K α ($\lambda = 0.15418$ nm) radiation. The inductively coupled plasma atomic emission spectroscopy (ICP/AES) was conducted on a Hitachi High-Tech Science PS7800 (sequential type ICP optical emission spectrometer). Transmission electron microscopy (TEM) observation was performed on a JEOL Model JEM-3010 system at 300 kV, and the powder sample was supported on a Cu microgrid. X-ray photoelectron spectroscopy (XPS) were collected utilizing an ULVAC-PHI 5500MT system equipped with a hemispherical energy analyzer. Samples were mounted on indium foil and then transferred to an XPS analysis chamber under Ar. The spectra were measured at room temperature using Mg K α radiation (1254 eV) generated by an X-ray tube operating at 15 kV, 400 W. The electron take-off angle was set at 45 deg. The residual gas pressure during data acquisition was less than 1×10^{-8} Torr (1 Torr; 133.3 N m^{-2}). The XP spectra of the Ir(6wt%)/TiO $_2$ catalyst and the recovered Ir/TiO $_2$ catalysts were measured using ULVAC-PHI VersaProbe 5000 using Al K α radiation (1486.6 eV) generated at 15 kV, 25 W at less than 1×10^{-7} Pa. Binding energies were referenced to the C 1s level of residual graphitic carbon. Temperature-programmed reduction of hydrogen (H_2 -TPR) was performed on a gas flow system, where hydrogen (2 vol.% in Ar; atmospheric pressure of 40 mL/min) was fed in a quartz tube containing the catalyst. The tube was heated in an electric furnace at a ramping rate of 10 °C/min and the amount of H_2 consumed was monitored with a TC detector on a Shimadzu 8AIT gas chromatograph. Temperature-programmed desorption of

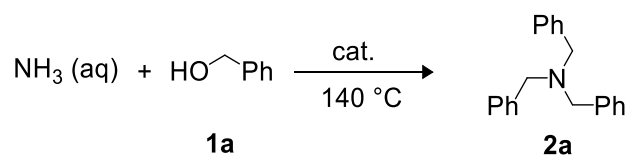
ammonia (NH₃-TPR) was performed on a Micromeritics Auto Chem 2920 apparatus. The sample (c.a. 100 mg) was pretreated for 1 h at 180 °C, and then cooled down to 40 °C to allow the adsorption of ammonia (10 % NH₃ in He, 30 mL/min) for 1 h. The desorption of NH₃ was conducted from 40 to 400 °C at a ramp rate of 10 °C/min in a helium flow (40 mL/min). In situ Fourier transform infrared (FTIR) spectra were recorded using a JASCO FT/IR-4000 spectrometer with an in situ reactor. A total of 64 scans with a resolution of 4 cm⁻¹ were performed to acquire each spectrum. First the powder samples were impregnate with benzyl alcohol and vacuum overnight to remove the physisorbed benzyl alcohol. The sample was pressed on KBr powder in the reactor. Before the measurements were initiated, the reactor was treated under dynamic vacuum at 140 °C for 0.5 h to remove surface contaminants. Subsequently, diluted ammonia gas (0.1 vol.% in He; atmospheric pressure of 20 mL/min) was fed into the reactor, and the in situ FTIR spectra of the samples were collected.

2.3 Results and discussion

The effects of various catalysts were compared in the N-alkylation of aqueous ammonia (28%) with benzyl alcohol (**1a**) to give tribenzylamine (**2a**) without additional solvents (bath temp; 140 °C, 18 h, in atmospheric pressure of air). The results are shown in Table 1. The titania-supported iridium catalysts are all effective in the reaction (entries 1-3, 7). On the other hand, the iridium catalysts supported on other metal oxides such as silica, alumina, and ceria are inactive, implying the critical effects of titania supports for the present catalysis. The titanias of anatase and rutile phases were used for the supports (Figure 1). The anatase-supported catalyst showed excellent activity (entry 1), while the catalyst supported on rutile showed lower activity (entry 2). Our

previous study reveals anatase-supported iridium catalysts show lower ability in CO uptake than that of rutile due to their strong metal-support interaction (SMSI) between iridium and anatase [41], suggesting SMSI significantly affects the present catalytic system. The possible reason is that anatase supports with the higher surface area have a higher concentration of lattice defects which facilitates the formation of TiO_x species during reduction treatment [46]. When the precursor switch from [Ir(cod)Cl]₂ to Ir(acac)₃, the catalyst shows the good activity as well (entry 7). Whereas no formation of **2a** was observed using [Ir(cod)Cl]₂ or Ir(acac)₃ as a homogeneous catalyst (entries 8 and 9). The reaction did not proceed in the presence of IrO₂. Titania supports did not show any catalytic activity for the reaction without iridium species regardless of the crystal structure. Besides, the reaction of aqueous ammonia with **1a** never occurred in the absence of the catalyst.

Table 1. N-Alkylation of aqueous ammonia with benzyl alcohol by various catalysts.^[a]



Entry	Catalysts ^[b]	Yield [%] ^[c]
1	Ir/TiO-10 (A) ^[d]	71
2	Ir/TiO-6 (R) ^[d]	26
3	Ir/TiO-4 (A/R) ^[d]	60
4	Ir/SiO ₂	trace
5	Ir/Al ₂ O ₃	0
6	Ir/CeO ₂	0

7	Ir/TIO-10 (A) ^[e]	66
8	[Ir(cod)Cl] ₂ ^[f]	0
9	Ir(acac) ₃ ^[f]	0
10	IrO ₂	0
11	TIO-10 (A)	0
12	TIO-6 (R)	0
13	TIO-4 (A/R)	0
14	No catalyst	0

[a] Reaction conditions: NH₃ (0.5 mmol, 28% aqueous solution), **1a** (2.5 mmol), catalyst (3 mol% as Ir, 6 wt%, 50 mg), 140 °C, 18 h, in air. [b] JRC (Japan Reference Catalyst) titania designated as TIO-x (x=4, 6, 10), (A): anatase, (R): rutile titanias, (A/R): mixture of anatase and rutile, the catalysts were prepared using [Ir(cod)Cl]₂ as a precursor. [c] Yields were based on the amount of nitrogen in NH₃ and determined by GC analyses. [d] The BET surface areas of TIO-4, 6, and 10 are 50, 100, and 100 m² g⁻¹, respectively. [e] The catalyst prepared using Ir(acac)₃ as a precursor. [f] [Ir(cod)Cl]₂ and Ir(acac)₃ were used as homogeneous catalysts.

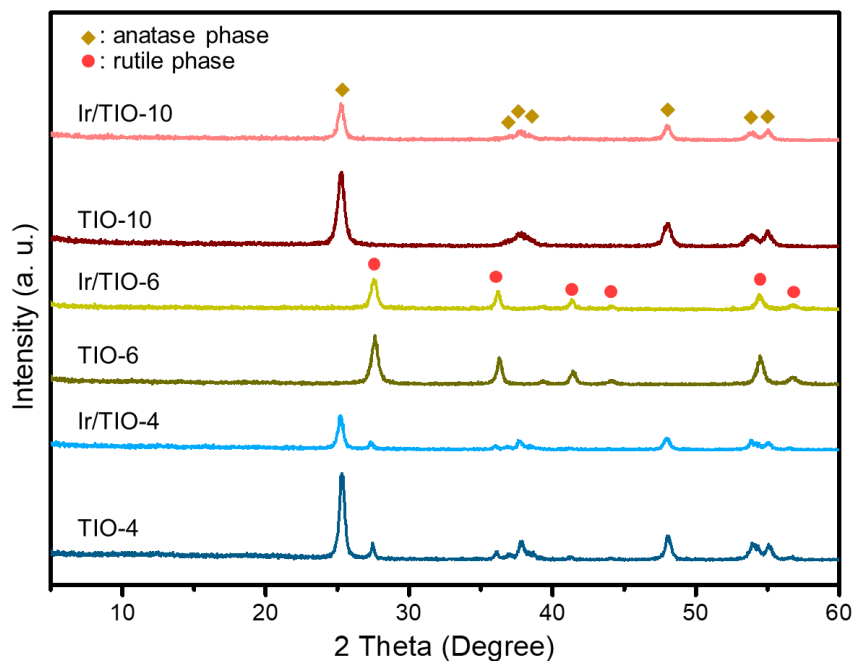
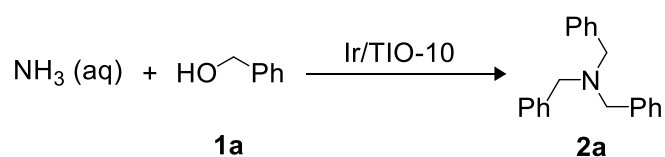


Figure 1. XRD patterns of titania and corresponding iridium catalysts.

In the next step, the effects of various reaction conditions were examined for the catalytic reaction in the presence of Ir/TiO-10 catalyst (Table 2). Entries 1-3 show the effect of the bath temperature on the catalytic reaction. The reaction carried out at 120 °C gave **2a** in high yield, while the yield of **2a** dramatically declined as the bath temperature increase to 160 °C. This result could be attributed to the high temperature accelerate the reflux of water which may impede the adsorption of ammonia onto the catalytically active sites. To our surprise, the reaction more smoothly proceeded to a 90% yield of **2a** in the 4-fold catalytic reaction (entry 4). The catalysts with 1 and 4 wt% of metal loading levels show no real distinction in the yields at the same substrates to catalyst ratio (3 mol% to N). Interestingly, the TEM images (Figure 2) reveal the particle size of iridium species mainly distribute around 1 to 2 nm regardless of the increasing loading level. This could be the reason for the similar activity for the catalyst with different loading level. The addition of organic solvent did not contribute to the

conversion of the desired product. The results shown in entries 8-11 testifies that the addition of water rather impedes the conversion of the substrates. The activity of the catalyst was further improved in an argon atmosphere as shown in entries 12-19. The substrates can be totally converted to the desired product with 2 or 3 mol% of Ir catalyst at 140 °C and an excellent yield can be achieved at lower temperatures of 120 °C and 100 °C.

Table 2 Optimization of the reaction conditions.^[a]



Entry	Amount of Ir (mol%)	Bath temp. [°C]	Solvent [mL]	Time [h]	Yield [%] ^[b]
1	3	120	/	18	66
2	3	140	/	18	71
3	3	160	/	18	38
4 ^[c]	3	140	/	18	90
5 ^[d]	3	140	/	18	71
6 ^[e]	3	140	/	18	69
7	3	140	Mesitylene [0.5]	18	64
8	3	140	/	2	28
9	3	140	H ₂ O [0.1]	2	18
10	3	140	H ₂ O [0.2]	2	24
11	3	140	H ₂ O [0.5]	2	0
12 ^[f]	3	140	/	18	99
13 ^[f]	2	140	/	18	82
14 ^[f]	2	140	/	24	99

15 ^[f]	1	140	/	18	72
16 ^[f]	1	140	/	24	72
17 ^{[f][g]}	3	140	/	24	(90)
18 ^[f]	3	120	/	24	98
19 ^[f]	3	100	/	24	78

[a] Reaction conditions: NH₃ (0.5 mmol, 28% aqueous solution), **1a** (2.5 mmol), catalyst (3 mol% as Ir, 6 wt%, 50 mg), 140 °C, 18 h, in air. [b] Yields were based on the amount of nitrogen in NH₃ and determined by GC analyses. Isolated yields are shown in the parenthesis. [c] 4-Fold reaction under the condition of NH₃ (2 mmol, 28% aqueous solution), **1a** (10 mmol), catalyst (3 mol% as Ir, 6 wt%, 200 mg). [d] Catalyst (3 mol% as Ir, 4 wt%, 75 mg). [e] Catalyst (3 mol% as Ir, 1 wt%, 300 mg). [f] The reaction was performed in argon. [g] NH₃ (1.5 mmol, 28% aqueous solution), **1a** (7.5 mmol).

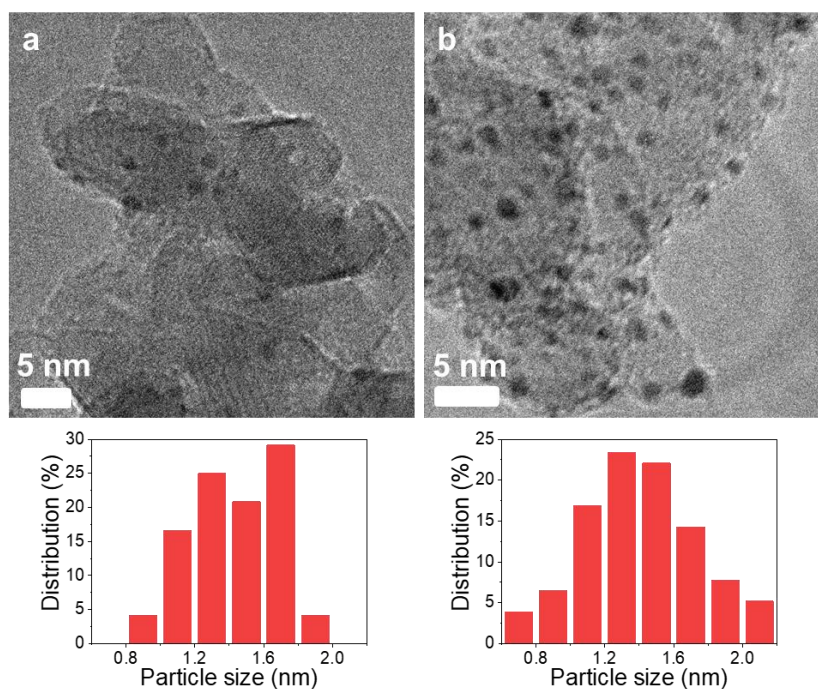


Figure 2. TEM image and corresponding particle size distribution histograms of Ir/TiO-10 with (a) 1 wt% and (b) 6 wt% loading of iridium.

The production of **2a** was completely stopped by the hot filtration of the solid catalyst using a PTFE filter (pore size 0.45 μm) after the reaction was allowed for 1 h (see Figure 3). The inductively coupled plasma atomic emission spectroscopy (ICP/AES) analysis shows that the presence of iridium in pure water and the filtrate (50 cm^3) were 0.087 and 0.110 ppm, respectively, suggesting the leaching of iridium to the solution is negligible. These results reveal that the catalysis of reaction is intrinsically based on the presence of the solid catalyst and proceeds heterogeneously. The present catalysts could be recycled by a simple method (Scheme 2). After the reaction was complete, the solid catalyst was separated from the reaction mixture by centrifugation and washed with THF, followed by calcination at 400 $^\circ\text{C}$ for 30 minutes and reduction at 500 $^\circ\text{C}$ for 30 minutes. The catalyst can stabilize the output yield of over 90% for at least 5 cycles for 18 h reactions. To evaluate reaction rates at the intermediate conversion levels, recycling tests for 2 h reactions were also performed. During the first 3 cycles, the total yields of **2a** and the intermediate amines were in the range between 64 to 67%, while the lower yields of 51 and 54% were shown in the 4th and 5th cycles.

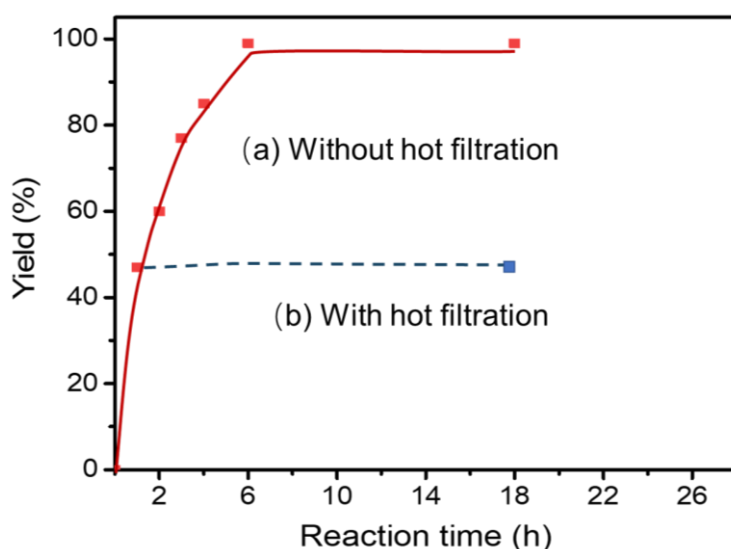
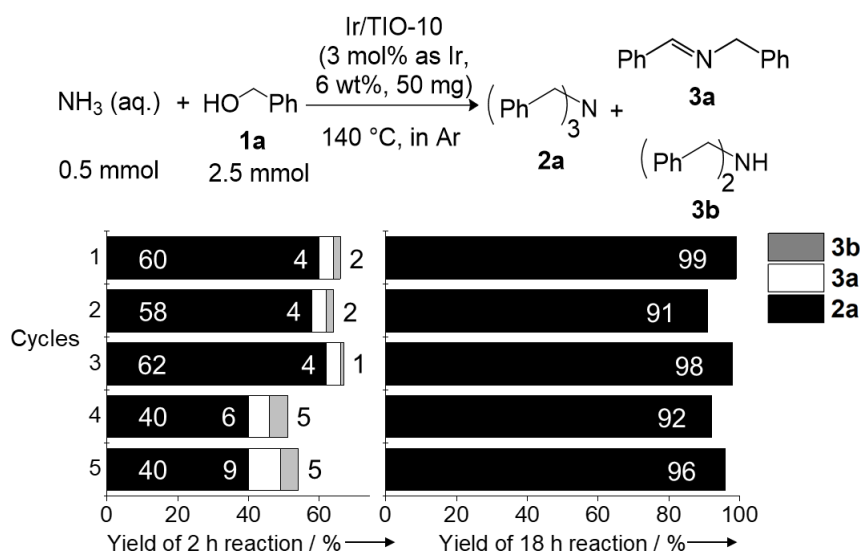


Figure 3. Hot filtration of Ir/TiO-10 (6 wt%) catalyst in the catalytic reaction.

Reaction conditions: NH₃ (0.5 mmol, 28% aqueous solution), **1a** (2.5 mmol), catalyst (3 mol% as Ir, 6 wt%, 50 mg), 140 °C, 18 h, in Ar.



Scheme 2. Recycle of Ir/TiO-10 catalyst.

The catalyst was further characterized to understand the factors responsible for the high activity. The state of iridium species on titania was investigated by XPS, and the deconvolution pattern of the Ir 4f spectrum is shown in Figure 5. The Ir 4f_{7/2} binding energies assigned for Ir³⁺ (61.5 eV) and metallic Ir⁰ (60.4 eV) are shown by vertical lines [47]. The contribution of IrO₂ (62.3 eV) was not confirmed in the fresh catalyst. The ratio of Ir³⁺ and Ir⁰ was ca. 3 to 7, suggesting that a major part of the Ir species on the titania support are fully reduced after hydrogen reduction and a part of Ir species is in an intermediate oxidation state (3+). As shown in Figure 4, Ir³⁺ species are more predominant in anatase-supported catalysts, which show higher activity for the present reaction (see Table 1). Similar results have been reported in the related catalytic systems before [43]. Note that homogeneous catalysts based in the “Ir(III)Cp*” system were reported to be effective for the N-alkylation reactions [25,26]. These results suggest

that the Ir³⁺ species could be responsible for the catalytic activity. Besides, the XP spectra of the recycled Ir/TIO-10 and Ir/TIO-6 catalysts recovered from the reaction mixture indicated that while the Ir⁰ species were predominant in both catalysts, the surface Ir³⁺ species (and Ir⁴⁺ species in the Ir/TIO-10 catalyst) were also found. This suggests a partial oxidation of iridium species during the catalytic runs (Figure 4(c), (d)). Temperature-programmed desorption (TPD) profile of ammonia was performed to evaluate the acid strength of the catalyst (Figure 5). A strong peak at around 86 °C can be attributed to the desorption of ammonia on Ti sites which are saturated by hydroxyl groups. While the peak at 327.9 °C was assigned to the desorption of ammonia on free Ti sites due to the strong interaction between a relatively strong base (ammonia) with a Lewis acid site [48]. These results evidence that the catalyst possesses weak acid sites on the surface and the weak adsorption of ammonia could facilitate the conversion of the N-alkylation of benzylic alcohols.

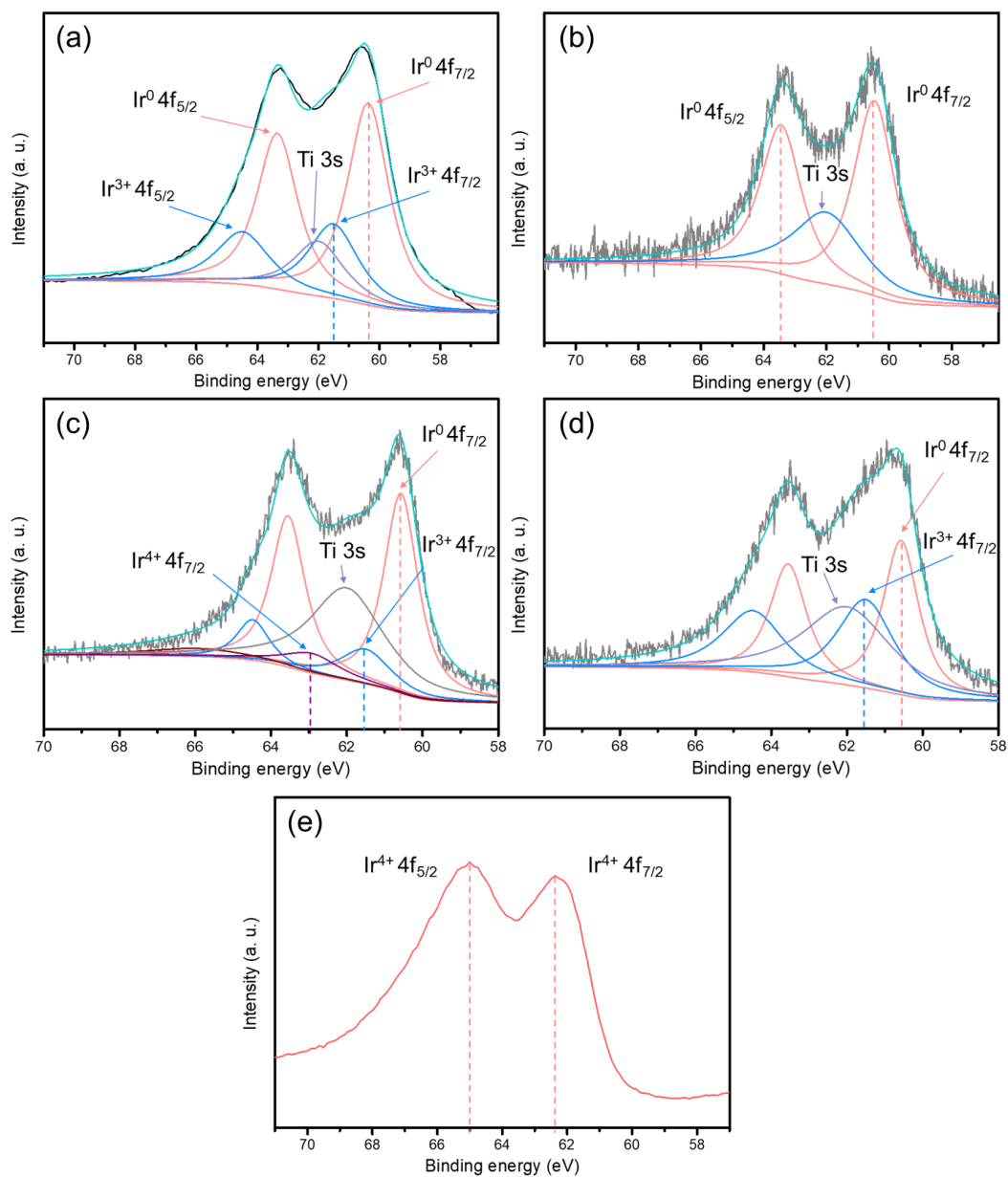


Figure 4. XP spectra (Ir 4f) of (a) Ir/TIO-10 (6 wt%, Ir⁰ 70%, Ir³⁺ 30%), (b) Ir/TIO-6 (6 wt%, Ir⁰ 100%), (c) recycled Ir/TIO-10 (6 wt%, Ir⁰ 71%, Ir³⁺ 18%, Ir⁴⁺ 11%), (d) recycled Ir/TIO-6 (6 wt%, Ir⁰ 53%, Ir³⁺ 47%), and (e) IrO₂ (Wako). The recycled catalysts were recovered after the reactions under the following conditions: NH₃ (0.5 mmol, 28% aqueous solution), **1a** (2.5 mmol), catalyst (3 mol% as Ir), 140 °C, 18 h, in Ar.

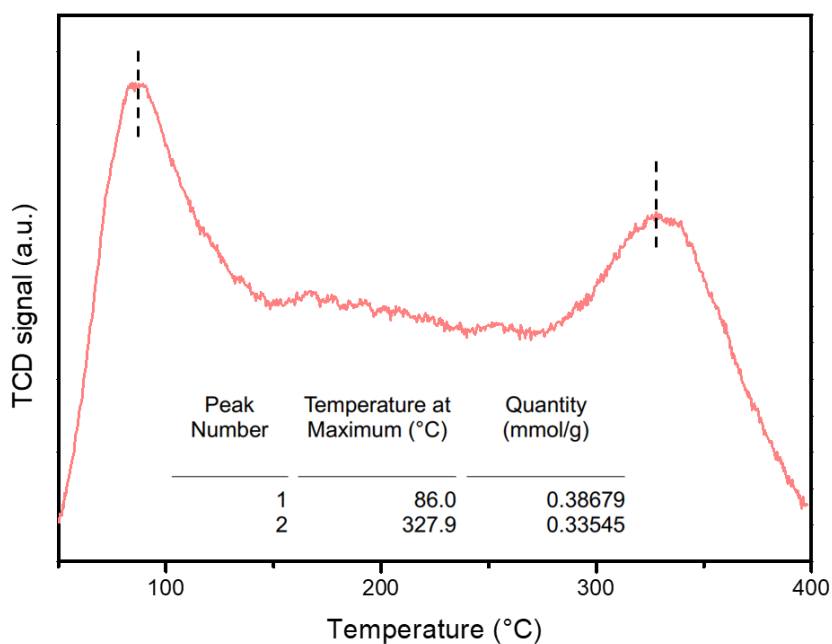


Figure 5. NH₃-TPR profiles of Ir/TiO-10 (6 wt%).

The interactions between the surface of catalyst and substrate were further observed by in situ FTIR (Figure 6). CH₂ stretching (2948 cm⁻¹) and aromatic CH stretching (3100-3000 cm⁻¹) suggest benzyl alcohol strongly chemisorbs on the surface of the catalyst after heating at 140 °C for 30 min with evacuation. As ammonia gas (0.1 vol.% in He) was being insufflated, NH₃ symmetric bending (930 and 965 cm⁻¹) [49] and symmetric stretch of NH in proton-acceptor ammonia (3333 cm⁻¹) [50] can be observed distinctly and increase cumulatively. The decreasing of O-H bending in benzyl alcohol (1209 cm⁻¹) [51,52] shows the conversion of benzyl alcohol. Meanwhile, the formation of benzylamine was evidenced by the C-N stretching vibration cluster around 1180-1020 cm⁻¹ [52] and N-H stretching vibration (3393 cm⁻¹) of primary amine [53]. Remarkably, the whole procedure performed as soon as the ammonia gas passed through.

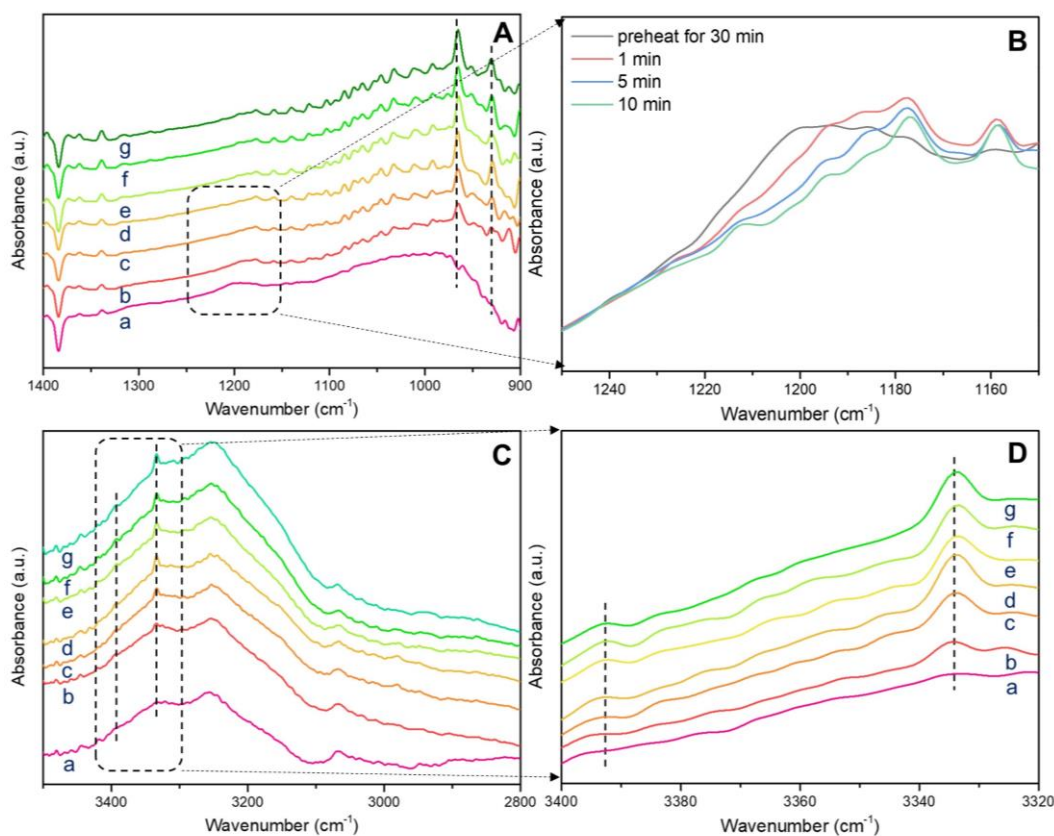
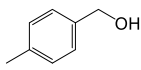
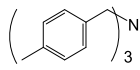
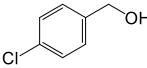
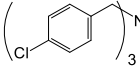
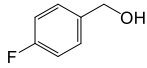
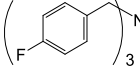
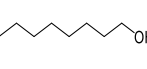
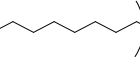
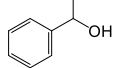
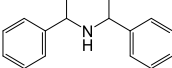


Figure 6. In situ FTIR of NH_3 adsorption on the Ir/TiO-10 (6 wt%) impregnated with benzyl alcohol. The powder sample was evacuated overnight to remove the physisorbed benzyl alcohol in advance (see experiment section): (a) preheat at 140 °C for 30 min with evacuating, adsorption of NH_3 for (b) 1 min, (c) 5 min, (d) 10 min, (e) 30 min, (f) 60 min, and (g) evacuating for 30 min.

As shown in Table 3, the effect of the present Ir/TiO-10 catalyst in large-scale reactions with representative benzylic alcohols was examined. This catalytic system possessed good tolerance to air and argon as well. Both primary benzylic alcohols containing electron-donating substituents and electron-withdrawing substituents undergo efficient conversion to corresponding benzylic tertiary amines in high yields. The reaction of ammonia with 1-octanol gave trioctylamine, but the yields were

insufficient (entry 4). Moreover, the selective formation of secondary amines from secondary benzylic alcohol was also achieved (entry 5). The high yield of secondary amine even though using excess amounts of alcohol probably due to the steric hindrance [25,54].

Table 3. Synthesis of tertiary and secondary amines from aqueous ammonia and benzylic alcohols by Ir/TIO-10 (6 wt%).^[a]

Entry	Alcohol	Product	Yield [%] ^[b]	
			In air ^[c]	In Ar ^[d]
1			73	85 (80)
2			84	91 (85)
3			79	85 (74)
4			24	23
5			95	>99 (82) ^[e]

[a] Reaction conditions: NH₃ (1.5 mmol, 28% aqueous solution), alcohols (7.5 mmol), Ir/TIO-10 (6 wt%, 0.060 mmol as Ir), 140 °C. [b] The products were determined by GC-MS and NMR, the yields were based on the amount of nitrogen in NH₃ and determined by GC analyses. [c] Reactions run for 20 h. [d] Reactions run for 24 h. Isolated yields are shown in the parenthesis. [e] A mixture of diastereomers (meso/dl ca. 50:50 by NMR) was formed.

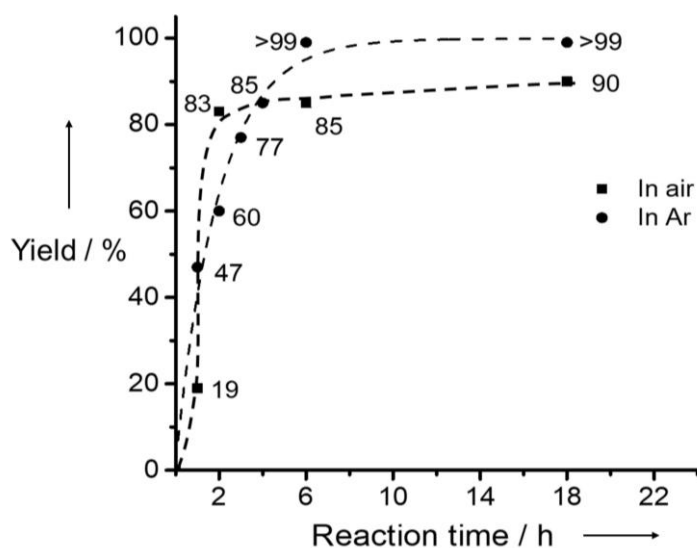
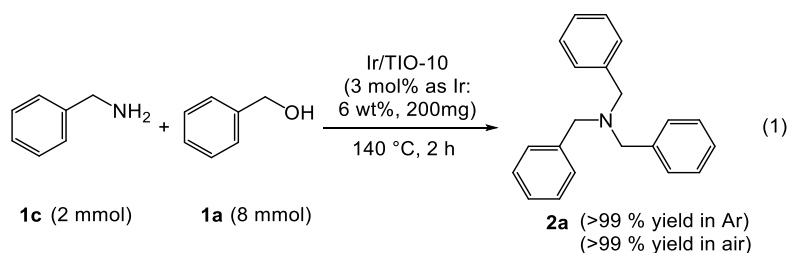


Figure 7. Time-course profiles of the yields (%) of **2a** from aqueous ammonia with **1a** over Ir/TIO-10 catalyst at 140 °C. The conditions of in air reactions: NH₃ (2 mmol, 28% aqueous solution), **1a** (10 mmol), catalyst (3 mol% as Ir, 6 wt%, 200 mg); The conditions of in argon reactions: NH₃ (0.5 mmol, 28% aqueous solution), **1a** (2.5 mmol), catalyst (3 mol% as Ir, 6 wt%, 50 mg).

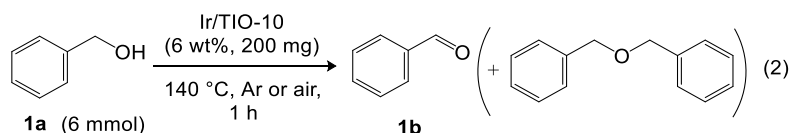


The time course profiles for the yield over Ir/TIO-10 catalyzed alkylation of ammonia with **1a** in both air and argon atmosphere are shown in Figure 7. The catalysis behaviors in air and argon are slightly different. When the reaction performed in air, the reaction proceeded slightly faster and gave the desired product in 19% yield in the initial hour. As the reaction proceeded, the yield of the product dramatically increased to 83% within 2 hours and then levelled off with further increases in the reaction time. In the following time, there was no substantial increase in production and finally

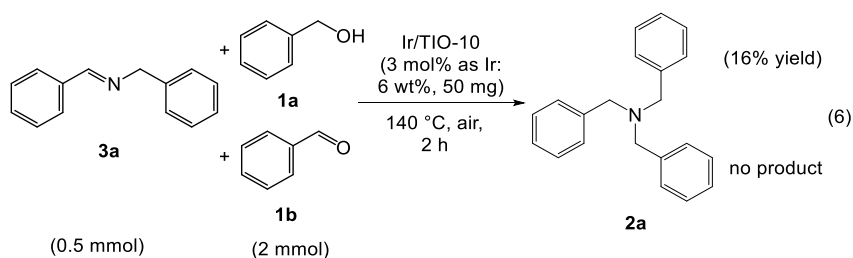
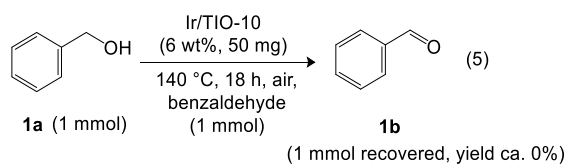
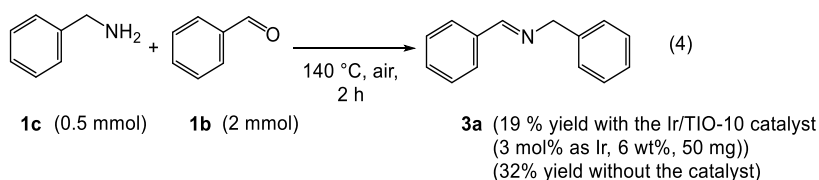
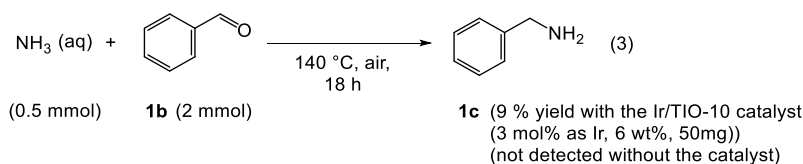
achieved a 90% yield after 18 hours. As for the reaction in argon, the catalytic reaction gave the product in a yield of 47% in the initial hour. Then, the reaction proceeded smoothly and completed the conversion of all substrates within 6 hours. A separate experiment reveals that the formation of tribenzylamine from benzylamine and benzyl alcohol was rapidly finished in 2 hours both in air or argon atmosphere [Eq. (1)], suggesting the reaction rate hinges on the formation of benzylamine from benzyl alcohol and ammonia. As one possible reason for the different time course profiles in air or argon, the oxidation of benzyl alcohol to benzaldehyde by air and subsequent conversion to imines might accelerate the reaction at the early stage [51,55,56]. The further detailed study on the different behaviors in the reactions in air and argon is ongoing. Consequently, the presence of air is proved not to significantly hamper the reaction.

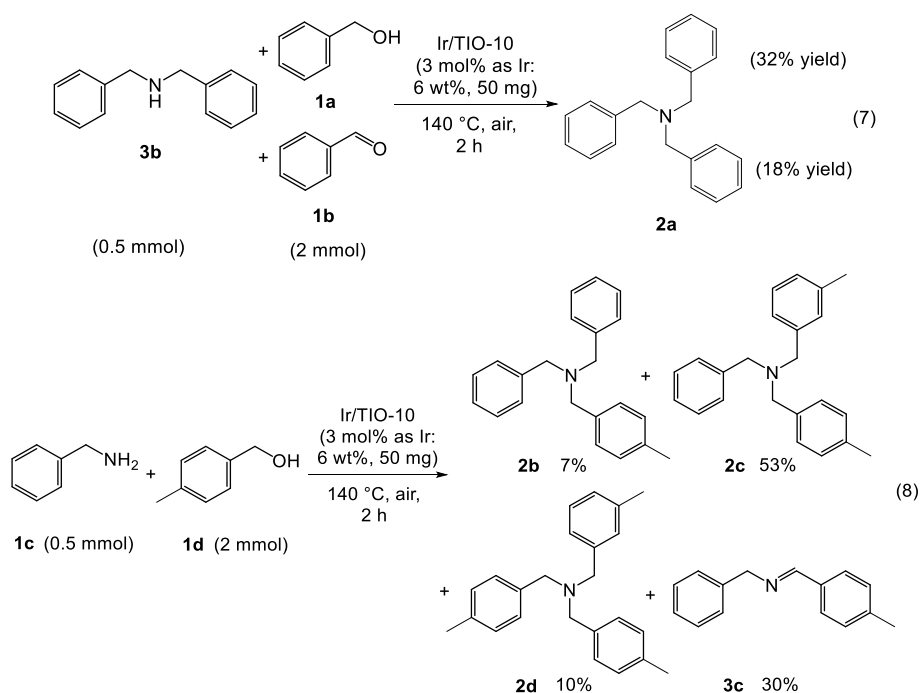
To understand the reaction mechanisms, a serial of separate experiments was performed. Since Ir/TiO₂ is well known for its high performance in the aerobic oxidation of **1a** [51,55,56], we first investigated the conversion of **1a** in the presence of the catalyst for one hour in argon or air [Eq. (2)]. The result shows that 36% or 27% of **1a** was converted to benzaldehyde and its dimers in argon or air, respectively. On the other hand, the alkylation of aqueous ammonia with free benzaldehyde was slow in the presence of the iridium catalyst [Eq. (3)], probably because of the poisoning by benzaldehyde (see below). Without the catalyst the formation of **1c** as well as the corresponding imines were not detected under the present conditions, suggesting the present catalyst have a promotional role for this step. It is generally accepted that the hydrogen transfer pathway over heterogeneous [29,35] or homogeneous [24,25,57] catalyst proceeds via the oxidation of alcohol and the following amination of aldehyde. Also, the reaction of benzylamine **1c** and benzaldehyde **1b** gave N-benzylidenebenzylamine **3a** in low yield (19%), while the reaction in the absence of the catalyst smoothly proceeded [Eq. (4)]. This suggests that the catalyst retarded the transformation from aldehyde to imine, probably due to the strong adsorption of

benzaldehyde **1b** on the surface of the catalysts (see below). Note that the dehydrogenation of benzyl alcohol to benzaldehyde over titania-supported iridium catalyst was completely suppressed in the presence of an equimolar amount of benzaldehyde [Eq. (5)] as previously reported by us in a similar catalytic system (see Fig S5 of [40]). This suggests that benzaldehyde poisons the active sites on the surface of the present catalyst. In the reactions shown in Eq. (2) to Eq. (5), the presence of a significant amount of benzaldehyde **1b** will hamper the reaction. In the present alkylation of ammonia by benzylic alcohols, the rapid transformation of aldehydes to imine would prevent the poisoning of the catalyst.



Conversion of **1a**: 36% (in Ar), 27% (in air)

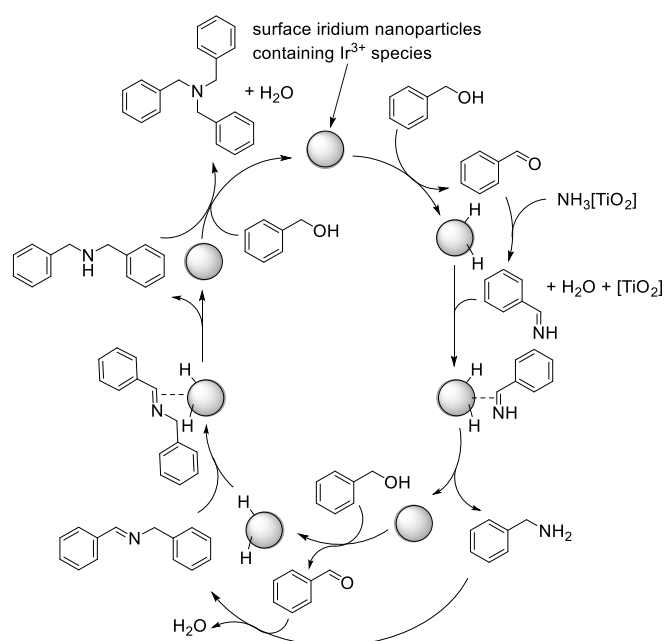




Scheme 3. Separate experiments for the reaction mechanism.

In addition, we further examined the reactivity of the possible intermediate, **3a** and **3b**. The reaction of **3a** or **3b** with benzyl alcohol **1a** produced a small amount of the desired product **2a** [Eq. (6) and (7)], while over 99% of product **2a** was rapidly achieved in 2-hours from **1c** and **1a** [Eq. (1)]. Again, the reaction of **3a** or **3b** with **1b** gave **2a** in low yields. These results suggest that the multi-alkylation proceeds via **3a** and **3b** kept in the coordination sphere of the surface iridium species rather than “free” **3a** or **3b**. The catalytic reaction of **1c** and **1d** smoothly proceeded to give corresponding tertiary amines **2b**, **2c**, and **2d** together with imine **3c** in a 2-hour reaction, and the formation of **3a** was not observed [Eq. (8)]. This indicates the predominance of the dialkylation rather than the self-condensation of **1c** [58]. Therefore, the present catalytic transformation would proceed through hydrogen auto-transfer pathways as demonstrated in Scheme 4, which is based on that previously proposed for homogeneous catalysis [25]. The first N-alkylation proceeds via the rate-determining

dehydrogenation of benzylic alcohols to aldehydes and hydride species on the surface of the iridium nanoparticles. The thus formed aldehyde would immediately react with ammonia, probably adsorbed on the weak acidic sites of the titania surface, to form an imine. The hydrogenation of imine by the surface hydride species would produce a corresponding primary amine. Subsequently, the hydrogen auto-transfer of an obtained primary amine with benzylic alcohol would proceed on the iridium sites through similar sequential processes to give a corresponding tertiary amine. The whole reaction process can be completed rapidly within 2 hours under the condition of adequate benzylic alcohol. The formation of small nanoparticles is generally preferable to achieve the excellent activity since it can maximize the area of the catalytically active surface of metallic species [45]. As evidenced by TEM study, the formation of iridium nanoparticles of less than 2 nm in diameter would be one reason for the excellent catalytic activity.



Scheme 4. A possible mechanism for the N-alkylation of aqueous ammonia with benzyl alcohol.

2.4 Conclusion

In conclusion, titania-supported iridium catalysts with simple reaction conditions and excellent activity for the synthesis of organic amines from aqueous ammonia have been developed. The catalytic system possesses a high tolerance in the reaction condition. No additional solvent is required, and the reaction can be performed readily in an air or argon atmosphere. The crystal structure of titania supports for iridium catalysts markedly affected their activities. The detailed characterization revealed that highly-dispersed partially-reduced iridium nanoparticles of less than 2 nm in diameter would be responsible for the excellent catalytic activity. Over Ir/TIO-10 catalyst, tertiary and secondary amines were synthesized by the multialkylation of aqueous ammonia with primary and secondary benzylic alcohols, respectively. The formation of the product smoothly proceeded in large-scale reactions. This catalytic system elucidates a green and simple method with high efficiency for the synthesis of organic amines.

2.5 References

- [1] U.S. Geological Survey, Nitrogen (Fixed) — Ammonia, PDF Format: (2021), (2021).
- [2] J.L. Klinkenberg, J.F. Hartwig, Catalytic organometallic reactions of ammonia, *Angew. Chemie - Int. Ed.* 50 (2011) 86–95.
- [3] S. Giddey, S.P.S. Badwal, A. Kulkarni, Review of electrochemical ammonia production technologies and materials, *Int. J. Hydrogen Energy.* 38 (2013) 14576–14594.
- [4] J. Kim, H.J. Kim, S. Chang, Synthetic uses of ammonia in transition-metal catalysis, *European J. Org. Chem.* (2013) 3201–3213.
- [5] Q. Shen, J.F. Hartwig, Palladium-catalyzed coupling of ammonia and lithium amide with aryl halides, *J. Am. Chem. Soc.* 128 (2006) 10028–10029.
- [6] N. Xia, M. Taillefer, A very simple copper-catalyzed synthesis of anilines by employing aqueous ammonia, *Angew. Chemie - Int. Ed.* 48 (2009) 337–339.

- [7] G.D. Vo, J.F. Hartwig, Palladium-catalyzed coupling of ammonia with aryl chlorides, bromides, iodides, and sulfonates: A general method for the preparation of primary arylamines, *J. Am. Chem. Soc.* 131 (2009) 11049–11061.
- [8] X.F. Wu, C. Darcel, Ligand-free iron/copper-cocatalyzed amination of aryl iodides, *European J. Org. Chem.* 3 (2009) 4753–4756.
- [9] X.F. Wu, H. Neumann, M. Beller, Selective palladium-catalyzed aminocarbonylation of aryl halides with CO and ammonia, *Chem. - A Eur. J.* 16 (2010) 9750–9753.
- [10] P. Anastas, N. Eghbali, Green chemistry: principles and practice, *Chem. Soc. Rev.* 39 (2010) 301–312.
- [11] M. Poliakoff, P. Licence, Green chemistry, *Nature.* 450 (2007) 810–812.
- [12] C. Anastas, T., Warner, Green chemistry: theory and practice, Oxford University Press Inc., New York, 1998.
- [13] D.M. Roundhill, Transition Metal and Enzyme Catalyzed Reactions involving Reactions with Ammonia and Amines, *Chem. Rev.* 92 (1992) 1–27.
- [14] S. Bähn, S. Imm, L. Neubert, M. Zhang, H. Neumann, M. Beller, The catalytic amination of alcohols, *ChemCatChem.* 3 (2011) 1853–1864.
- [15] G. Guillena, D.J. Ramón, M. Yus, Hydrogen autotransfer in the N-alkylation of amines and related compounds using alcohols and amines as electrophiles, *Chem. Rev.* 110 (2010) 1611–1641.
- [16] C. Gunanathan, D. Milstein, Applications of acceptorless dehydrogenation and related transformations in chemical synthesis, *Science (80-.).* 341 (2013) 1229712.
- [17] X. Ma, C. Su, Q. Xu, N-Alkylation by Hydrogen Autotransfer Reactions, *Top. Curr. Chem.* 374 (2016) 27.
- [18] T. Irrgang, R. Kempe, 3d-Metal Catalyzed N- and C-Alkylation Reactions via Borrowing Hydrogen or Hydrogen Autotransfer, *Chem. Rev.* 119 (2019) 2524–2549.
- [19] E. Balaraman, D. Srimani, Y. Diskin-Posner, D. Milstein, Direct Synthesis of Secondary Amines From Alcohols and Ammonia Catalyzed by a Ruthenium Pincer Complex, *Catal. Letters.* 145 (2015) 139–144.
- [20] P. Daw, Y. Ben-David, D. Milstein, Acceptorless Dehydrogenative Coupling Using Ammonia: Direct Synthesis of N-Heteroaromatics from Diols Catalyzed by Ruthenium, *J. Am. Chem. Soc.* 140 (2018) 11931–11934.
- [21] X. Ye, P.N. Plessow, M.K. Brinks, M. Schelwies, T. Schaub, F. Rominger, R. Paciello, M. Limbach, P. Hofmann, Alcohol amination with ammonia catalyzed by an acridine-based ruthenium pincer complex: A mechanistic study, *J. Am. Chem. Soc.* 136 (2014) 5923–5929.
- [22] D. Pinggen, C. Müller, D. Vogt, Direct amination of secondary alcohols using ammonia, *Angew. Chemie - Int. Ed.* 49 (2010) 8130–8133.
- [23] S. Imm, L. Neubert, H. Neumann, M. Beller, An efficient and general synthesis

- of primary amines by ruthenium-catalyzed amination of secondary alcohols with ammonia, *Angew. Chemie - Int. Ed.* 49 (2010) 8126–8129.
- [24] C. Gunanathan, D. Milstein, Selective synthesis of primary amines directly from alcohols and ammonia, *Angew. Chemie - Int. Ed.* 47 (2008) 8661–8664.
- [25] R. Kawahara, K.I. Fujita, R. Yamaguchi, Multialkylation of aqueous ammonia with alcohols catalyzed by water-soluble Cp*Ir-amine complexes, *J. Am. Chem. Soc.* 132 (2010) 15108–15111.
- [26] K.I. Fujita, S. Furukawa, N. Morishima, M. Shimizu, R. Yamaguchi, N-Alkylation of Aqueous Ammonia with Alcohols Leading to Primary Amines Catalyzed by Water-Soluble N-Heterocyclic Carbene Complexes of Iridium, *ChemCatChem*. 10 (2018) 1993–1997.
- [27] C. Segarra, E. Mas-Marzá, J.A. Mata, E. Peris, Shvo's catalyst and [IrCp*Cl₂(amidine)] effectively catalyze the formation of tertiary amines from the reaction of primary alcohols and ammonium salts, *Adv. Synth. Catal.* 353 (2011) 2078–2084.
- [28] H. Ohta, Y. Yuyama, Y. Uozumi, Y.M.A. Yamada, In-water dehydrative alkylation of ammonia and amines with alcohols by a polymeric bimetallic catalyst, *Org. Lett.* 13 (2011) 3892–3895.
- [29] K.I. Shimizu, K. Kon, W. Onodera, H. Yamazaki, J.N. Kondo, Heterogeneous Ni catalyst for direct synthesis of primary amines from alcohols and ammonia, *ACS Catal.* 3 (2013) 112–117.
- [30] K.I. Shimizu, S. Kanno, K. Kon, S.M.A. Hakim Siddiki, H. Tanaka, Y. Sakata, N-alkylation of ammonia and amines with alcohols catalyzed by Ni-loaded CaSiO₃, *Catal. Today*. 232 (2014) 134–138.
- [31] A. Tomer, Z. Yan, A. Ponchel, M. Pera-Titus, Mixed oxides supported low-nickel formulations for the direct amination of aliphatic alcohols with ammonia, *J. Catal.* 356 (2017) 133–146.
- [32] A.Y.K. Leung, K. Hellgardt, K.K.M. Hii, Catalysis in Flow: Nickel-Catalyzed Synthesis of Primary Amines from Alcohols and NH₃, *ACS Sustain. Chem. Eng.* 6 (2018) 5479–5484.
- [33] Y. Liu, A. Afanasenko, S. Elangovan, Z. Sun, K. Barta, Primary Benzylamines by Efficient N-Alkylation of Benzyl Alcohols Using Commercial Ni Catalysts and Easy-to-Handle Ammonia Sources, *ACS Sustain. Chem. Eng.* 7 (2019) 11267–11274.
- [34] X. Cui, X. Dai, Y. Deng, F. Shi, Development of a general non-noble metal catalyst for the benign amination of alcohols with amines and ammonia, *Chem. - A Eur. J.* 19 (2013) 3665–3675.
- [35] K. Yamaguchi, J. He, T. Oishi, N. Mizuno, The “borrowing hydrogen strategy” by supported ruthenium hydroxide catalysts: Synthetic scope of symmetrically and unsymmetrically substituted amines, *Chem. - A Eur. J.* 16 (2010) 7199–7207.
- [36] D. Ruiz, A. Aho, T. Saloranta, K. Eränen, J. Wärnå, R. Leino, D.Y. Murzin,

- Direct amination of dodecanol with NH₃ over heterogeneous catalysts. Catalyst screening and kinetic modelling, *Chem. Eng. J.* 307 (2017) 739–749.
- [37] L. Fang, Z. Yan, J. Wu, A. Bugaev, C. Lamberti, M. Pera-Titus, Highly selective Ru/HBEA catalyst for the direct amination of fatty alcohols with ammonia, *Appl. Catal. B Environ.* 286 (2021) 119942.
- [38] M.R. Ball, T.S. Wesley, K.R. Rivera-Dones, G.W. Huber, J.A. Dumesic, Amination of 1-hexanol on bimetallic AuPd/TiO₂ catalysts, *Green Chem.* 20 (2018) 4695–4709.
- [39] T. Takanashi, Y. Nakagawa, K. Tomishige, Amination of alcohols with ammonia in water over Rh catalyst, *Chem. Lett.* 43 (2014) 822–824.
- [40] T. Fukutake, K. Wada, H. Yu, S. Hosokawa, Q. Feng, Development of titania-supported iridium catalysts with excellent low-temperature activities for the synthesis of benzimidazoles via hydrogen transfer, *Mol. Catal.* 477 (2019) 110550.
- [41] T. Fukutake, K. Wada, G.C. Liu, S. Hosokawa, Q. Feng, Striking effects of a titania support on the low-temperature activities of Ir catalysts for the dehydrogenative synthesis of benzimidazole and indole, *Catal. Today.* 303 (2018) 235–240.
- [42] K. Wada, H. Yu, Q. Feng, Titania-supported iridium catalysts for dehydrogenative synthesis of benzimidazoles, *Chinese Chem. Lett.* 31 (2020) 605–608.
- [43] K. Tateyama, K. Wada, H. Miura, S. Hosokawa, R. Abe, M. Inoue, Dehydrogenative synthesis of benzimidazoles under mild conditions with supported iridium catalysts, *Catal. Sci. Technol.* 6 (2016) 1677–1684.
- [44] H. Yu, K. Wada, T. Fukutake, Q. Feng, S. Uemura, K. Isoda, T. Hirai, S. Iwamoto, Effect of phosphorus-modification of titania supports on the iridium-catalyzed synthesis of benzimidazoles, *Catal. Today.* 375 (2021) 410–417.
- [45] L. He, J.Q. Wang, Y. Gong, Y.M. Liu, Y. Cao, H.Y. He, K.N. Fan, Titania-supported iridium subnanoclusters as an efficient heterogeneous catalyst for direct synthesis of quinolines from nitroarenes and aliphatic alcohols, *Angew. Chemie - Int. Ed.* 50 (2011) 10216–10220.
- [46] T.W. van Deelen, C. Hernández Mejía, K.P. de Jong, Control of metal-support interactions in heterogeneous catalysts to enhance activity and selectivity, *Nat. Catal.* 2 (2019) 955–970.
- [47] K.D.M. J.F., S. W.F., S. P.E., Bomben, *Handbook of X-ray Photoelectron Spectroscopy*, 1992.
- [48] A. Markovits, J. Ahdjoudj, C. Minot, A theoretical analysis of NH₃ adsorption on TiO₂, *Surf. Sci.* 365 (1996) 649–661.
- [49] G. Laroche, J. Vallade, R. Bazinette, P. Van Nijnatten, E. Hernandez, G. Hernandez, F. Massines, Fourier transform infrared absorption spectroscopy characterization of gaseous atmospheric pressure plasmas with 2 mm spatial resolution, *Rev. Sci. Instrum.* 83 (2012) 103508.

- [50] B. Zhang, S. Yang, Q.-R. Huang, S. Jiang, R. Chen, X. Yang, D.H. Zhang, Z. Zhang, J.-L. Kuo, L. Jiang, Deconstructing Vibrational Motions on the Potential Energy Surfaces of Hydrogen-Bonded Complexes, *CCS Chem.* 3 (2021) 829–835.
- [51] S. Ito, X. Wang, A. Waheed, G. Li, N. Maeda, D.M. Meier, S. Naito, A. Baiker, Support effects in iridium-catalyzed aerobic oxidation of benzyl alcohol studied by modulation-excitation attenuated total reflection IR spectroscopy, *J. Catal.* 393 (2021) 42–50.
- [52] S. Carmona-Télez, G. Alarcón-Flores, E. Zaleta-Alejandre, Z. Rivera-Alvarez, A.N. Meza-Rocha, R. Martínez-Martínez, H.S. Murrieta, M. Aguilar-Frutis, C. Falcony, Luminescent polystyrene films, a novel way to reduce styrofoam residues, *Rev. Mex. Fis.* 61 (2015) 323–329.
- [53] M. Asandulesa, I. Topala, Y.M. Legrand, S. Roualdes, V. Rouessac, V. Harabagiu, Chemical investigation on various aromatic compounds polymerization in low pressure helium plasma, *Plasma Chem. Plasma Process.* 34 (2014) 1219–1232.
- [54] R. Yamaguchi, S. Kawagoe, C. Asai, K.I. Fujita, Selective synthesis of secondary and tertiary amines by Cp*iridium-catalyzed multialkylation of ammonium salts with alcohols, *Org. Lett.* 10 (2008) 181–184.
- [55] A. Yoshida, Y. Mori, T. Ikeda, K. Azemoto, S. Naito, Enhancement of catalytic activity of Ir/TiO₂ by partially reduced titanium oxide in aerobic oxidation of alcohols, *Catal. Today.* 203 (2013) 153–157.
- [56] A. Yoshida, Y. Takahashi, T. Ikeda, K. Azemoto, S. Naito, Catalytic oxidation of aromatic alcohols and alkylarenes with molecular oxygen over Ir/TiO₂, *Catal. Today.* 164 (2011) 332–335.
- [57] D. Balcells, A. Nova, E. Clot, D. Gnanamgari, R.H. Crabtree, O. Eisenstein, Mechanism of homogeneous iridium-catalyzed alkylation of amines with alcohols from a DFT study, *Organometallics.* 27 (2008) 2529–2535.
- [58] S.I. Murahashi, Synthetic Aspects of Metal-Catalyzed Oxidations of Amines and Related Reactions, *Angew. Chemie - Int. Ed.* 34 (1995) 2443–2465.

Chapter III Effect of Phosphorus-Modification of Titania Supports on the Iridium-Catalyzed Synthesis of Benzimidazoles

3.1 Introduction

Benzimidazoles are important building blocks in pharmaceutical and agricultural industries because of excellent biological, physiological, and/or therapeutic activities of themselves or their derivatives. A series of benzimidazole derivatives have been developed and applied in the antiviral, anti-cancer, anti-inflammatory, anti-hypertension treatments, and so on [1–6]. Recently the heterogeneous catalysis for synthesis of benzimidazole derivatives has attracted great attention as one of the most promising approaches because of their advantages in reusability, scalability, and environmental friendliness [7], which is different from the traditional routes using homogeneous catalysts [8–17]. Supported gold, palladium, platinum and iridium catalysts have been reported to be effective for the synthesis of benzimidazoles via dehydrogenative or hydrogen transfer pathways [18–24] [25–31], in which titania supported iridium (Ir/TiO₂) catalysts are most attractive due to their reusabilities, high selectivities, and high yield under significantly mild conditions [32,33].

Furthermore, the optimization of supports has been reported to improve the performance of the supported catalyst. Remarkably, the dehydrogenative synthesis of benzimidazoles from 1,2-phenylenediamine and primary alcohols was significantly promoted in the presence of the iridium catalysts supported on rutile titania, namely JRC-TIO-6 (JRC: Japan Reference Catalyst) [34]. On the other hand, anatase titania

enclosed by {010} and {101} facets was found to be an excellent support for the iridium-catalyzed synthesis of benzimidazoles from 2-nitroaniline and primary alcohols via hydrogen transfer [35]. Meanwhile, the enhanced catalytic activities of iridium catalysts by adding other elements have been reported [36–39]. For example, Tomishige et al. reported that supported rhenium-modified iridium catalysts show excellent activities for various reactions including hydrogenolysis of glycerol [36] and cyclic ethers [37,39], and transformation of hemicellulose [38].

In this chapter, a significant promotional effect of the modification of titania supports by phosphorus species on the activities of iridium catalysts is reported. The phosphorus-modified titania supports significantly improved the activities of the iridium catalysts. Roles of the phosphorus species are discussed on the bases of the characterization of the catalysts using nitrogen adsorption, transmission electron microscopy (TEM), H₂ temperature-programmed reduction (H₂-TPR), Fourier-transform infrared spectroscopy (FTIR), and X-ray photoelectron spectroscopy (XPS).

3.2 Experiment section

3.2.1 General information

All reactions were carried out under an argon atmosphere in Schlenk tubes. Tris(acetylacetonate)iridium(III) (Ir(acac)₃, C₁₅H₂₁O₆Ir), mesitylene, methanol, tetrahydrofuran (THF), biphenyl, and benzyl alcohol were delivered from Wako and used as received. Phosphoric acid, 2-nitroaniline, and butan-1-ol were delivered from TCI Cooperation and used as received. JRC (Japan Reference Catalyst) titanias (JRC-TIO-7 and 10, further designated as TIO-7 and -10, respectively) were delivered by the Catalysis Society of Japan.

3.2.2 Preparation of phosphorus-doped rutile titania by a hydrothermal method

The phosphorus-doped rutile titanias (TiO_2 , designated as Rutile (HT)) were prepared by a hydrothermal process as described in a previous report by one of the present authors [40]. A white precipitate was obtained by adding titanium tetraisopropoxide (TTIP; 24.2 g) to 450 mL of deionized water. The white precipitate collected by filtration was added to 340 mL of 0.5 M hydrochloric acid aqueous solution, stirred at room temperature for 4 h to obtain a transparent solution. After aging at 40 °C for 48 h in an incubator, the solution was centrifuged and washed repeatedly with deionized water, and then dried at 100 °C for 12 h. Subsequently, 3.0 g of the obtained powder was added to 10 mL of deionized water, and a desired amount of phosphoric acid (P/Ti molar ratio, 0 to 0.06) was added to the suspension. The mixture was hydrothermally treated at 220 °C for 4 h, and the product was centrifuged and washed with deionized water, and then dried at 100 °C for 12 h. The products thus-obtained are designated as P(x)-Rutile (HT), where x is the P/Ti changed molar ratio.

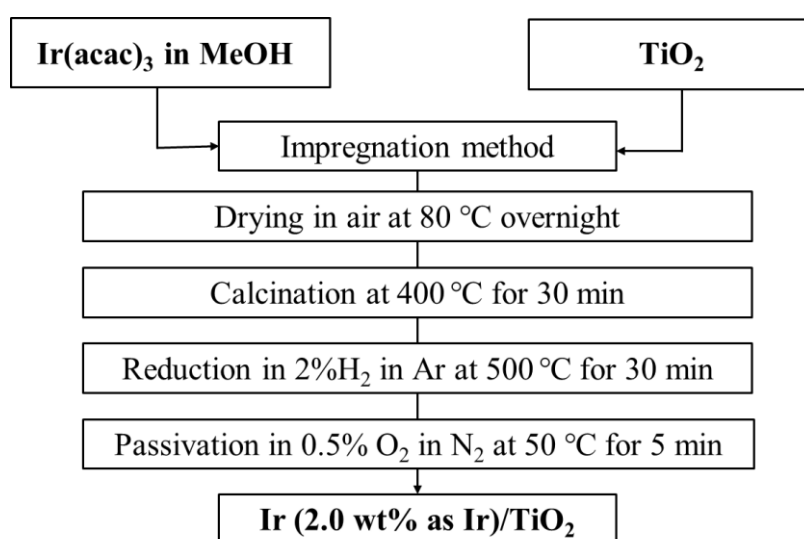
3.2.3 Preparation of phosphorus-modified TiO_2 by an impregnation method

The phosphorus-modified TiO_2 was prepared using an impregnation method. One gram of TiO_2 was put in a glass evaporation dish, and a desired amount of phosphoric acid (P/Ti molar ratio, 0 to 0.06) aqueous solution was added. The mixture was dried on a hot plate at 70 °C under stirring conditions. The obtained powder was dried at 80 °C for 3 h.

3.2.4 Preparation of supported iridium catalyst

TiO_2 -supported iridium catalysts were prepared by an impregnation method as

shown in Scheme 1. Ir(acac)₃ (0.10 mmol as Ir) was dissolved in 10 mL of methanol under stirring, then 1.0 g of titania was added in air at 80 °C. Subsequently, the obtained sample was dried overnight in air at 80 °C. The resulting powder was calcined in air at 400 °C for 30 min in a box furnace (rising rate; 10 °C/min), and then reduced in a H₂(2 vol.)/Ar flow (40 mL/min) at 500 °C (rising rate; 10 °C /min) for 30 min by using a conventional flow reactor to give Ir/TiO₂ catalysts. After purged by N₂, the catalysts were passivated in O₂(0.5 vol.)/N₂ flow (40 mL/min) at 50 °C for 5 min.



Scheme 1. Preparation procedure of titania-supported iridium catalysts.

3.2.5 General procedure for the catalytic runs

Catalytic reactions were performed in a glass Schlenk tube reactor (20 mL) equipped with hot stirrer and cooling block to reflux the solution. A typical reaction procedure for the synthesis of 2-phenylbenzimidazole is as follows: 2-nitroaniline, benzyl alcohol and mesitylene solvent were added to the Schlenk tube containing the Ir/TiO₂ catalyst. The reaction mixture was stirred at a desired temperature for 18 h under an argon atmosphere. Then the solid catalyst was removed by passing the mixture through a polytetrafluoroethylene (PTFE) filter (Millipore Millex LH, 0.45 μm), and

the yield of products were quantified by a gas-liquid chromatography using biphenyl as an internal standard.

3.2.6 Hot filtration tests

The Schlenk tube (20 mL) was charged with 2-nitroaniline (2.0 mmol), benzyl alcohol (8.0 mmol), and Ir/TiO₂ catalyst (0.010 mmol as Ir) in mesitylene (2 mL) solvent together with an internal standard (hexadecane, 0.1 mL) under an argon atmosphere. After the reaction was allowed to proceed at 120 °C for 6 h, the mixture was filtered through the PTFE filter into another preheated Schlenk tube reactor and then was heated at 120 °C for 24 h under stirring conditions.

3.2.7 Physical and analytical measurements

The resulting organic products of the catalytic reactions were analyzed by a gas-liquid chromatography (Shimadzu GC-14A; Zebron ZB-1 capillary column, i.d. 0.25 mm, length 30 m, at 50–250 °C). Solid catalysts were analyzed by the X-ray photoelectron spectroscopy (ULVAC-PHI 5500MT) equipped with Mg K α radiation (1254 eV) generated by an X-ray tube operating at 15 kV, 400 W. Binding energies were referenced to the C 1s level of residual graphitic carbon [41]. The structures of samples were investigated by using a powder X-ray diffractometer (XRD-6100, Shimadzu, Japan) with Cu K α ($\lambda = 0.15418$ nm) radiation. Transmission electron microscopy (TEM) observation was performed on a JEOL Model JEM-3010 system at 300 kV, and the powder sample was supported on a Cu microgrid. Brunauer-Emmett-Teller (BET) surface areas were determined by a computer-controlled automatic gas sorption system (Quantachrome NOVA 4200e), and samples were degassed at 300 °C

for 2 h just before the measurements. Temperature-programmed reduction (TPR) was performed with a gas flow system, where hydrogen (2 vol.% in Ar; atmospheric pressure of 40 mL/min) was fed in a quartz tube containing the catalyst. The tube was heated in an electric furnace at rising rate of 10 °C/min and the amount of H₂ consumed was monitored with a TC detector on a Shimadzu 8AIT gas chromatograph. Zeta potential was measured by a Zeta-potential & particle size analyzer (Photal ELSZ-2KG) in distilled water at pH 6.8.

3.3 Results and discussion

3.3.1 Effects of phosphorus-doped rutile prepared by the hydrothermal method

One of the present authors has reported the hydrothermal preparation of nanocrystalline rutile titanium dioxides having larger surface areas by the addition of small amounts of phosphoric acid to the precursor solution [40]. Therefore, in the present study the P-doping effects of hydrothermally-prepared rutile (see Figure 1) as a support of the iridium catalysts on the activity were examined. The reactions (1) and (2) were performed at 120 °C for 18 h using 25 mg of the catalysts unless otherwise noted. As shown in entries 1 to 3 of Table 1, the yields of 2-phenylbenzimidazole (**3aa**) from 2-nitroaniline (**1a**) and benzyl alcohol (**2a**) (eq. 1) gradually increased with an increase in the amount of phosphorus dopant. This trend was also true for the solvent-free synthesis of 2-propylbenzimidazole (**3ab**) using a large excess of butan-1-ol (**2b**) by eq. 2. The desired product **3aa** was obtained in the highest yield up to 93% in the presence of 100 mg of the iridium catalyst supported on Rutile (HT) with P/Ti molar ratio of 0.06 (Table 1, entry 7), while the iridium catalyst supported on undoped JRC-TIO-4 that contains 80% anatase and 20% rutile of TiO₂ phases similar to P25 showed

a significantly lower activity (Table 1, entry 8). These results demonstrate the promotional effect of phosphorus-doping on rutile TiO₂ (HT).

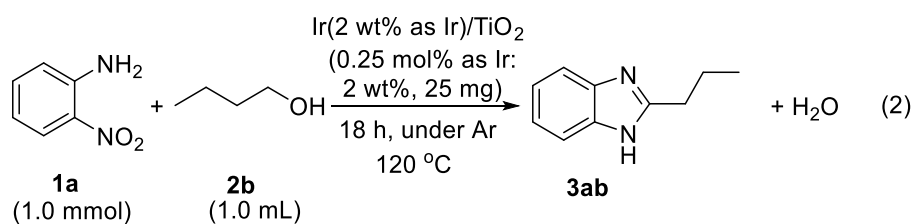
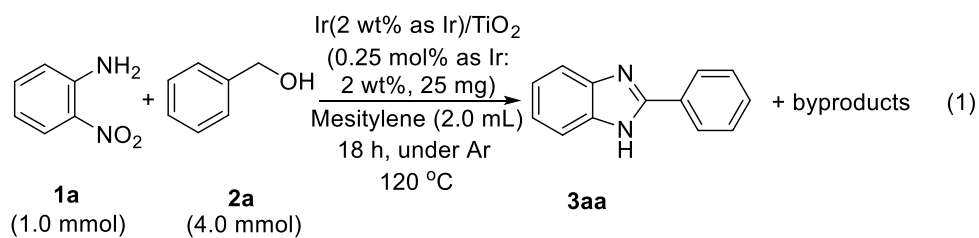


Table 1. P-doping effects of rutile (HT) as a support on the iridium-catalyzed synthesis of benzimidazoles

Entry	Alcohol	TiO ₂ support	BET S.A. (m ² /g)	Yield of 3 (%)
1	2a	P ₀ -Rutile (HT)	32	6
2	2a	P _{0.02} -Rutile (HT)	82	9
3	2a	P _{0.06} -Rutile (HT)	94	29
4	2b	P ₀ -Rutile (HT)	32	6
5	2b	P _{0.02} -Rutile (HT)	82	11
6	2b	P _{0.06} -Rutile (HT)	94	28
7 ^a	2a	P _{0.06} -Rutile (HT)	94	93
8 ^a	2a	JRC-TIO-4	51	15

Reaction conditions; at 120 °C for 18 h, Ir loading level 2.0 wt%.

For other conditions, see eqs. (1) and (2).

^aCatalysts amounts are 100 mg for Ir 2.0 wt% loading.

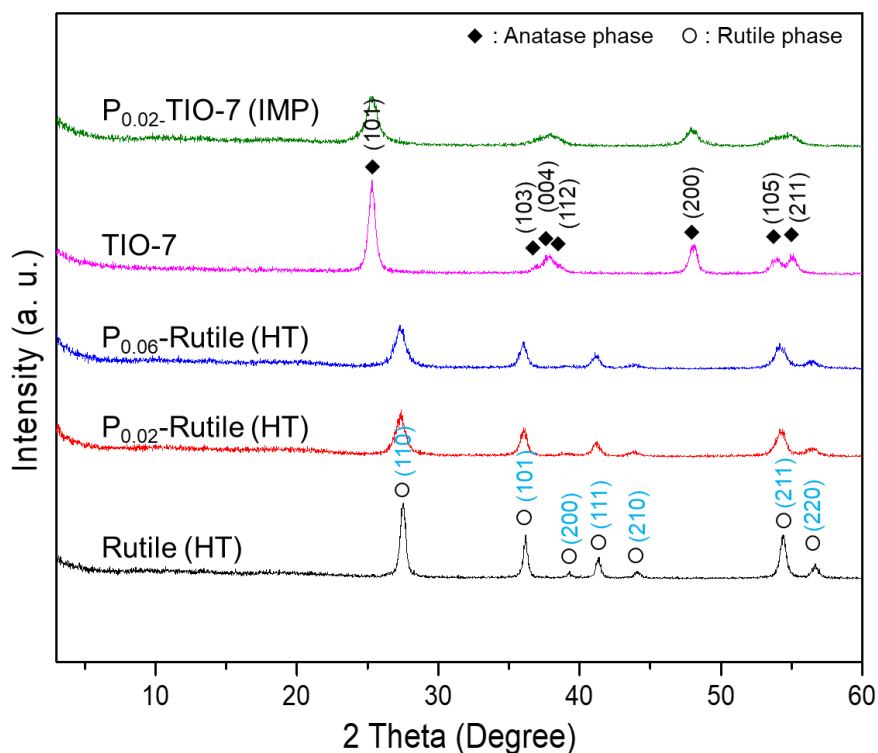


Figure 1. XRD pattern of sample rutile (HT), P modified rutile (HT), JRC-TIO-7, and P modified JRC-TIO-7.

The removal of the solid catalyst by the hot filtration using a PTFE filter (pore size 0.45 μm) after the reaction for 6 h completely stopped further progress of the formation of **3aa** by reaction (1) as shown in Figure 2. This result substantiates that the catalysis of reaction (1) is essentially dependent on the presence of the solid catalyst and proceeds heterogeneously [42,43].

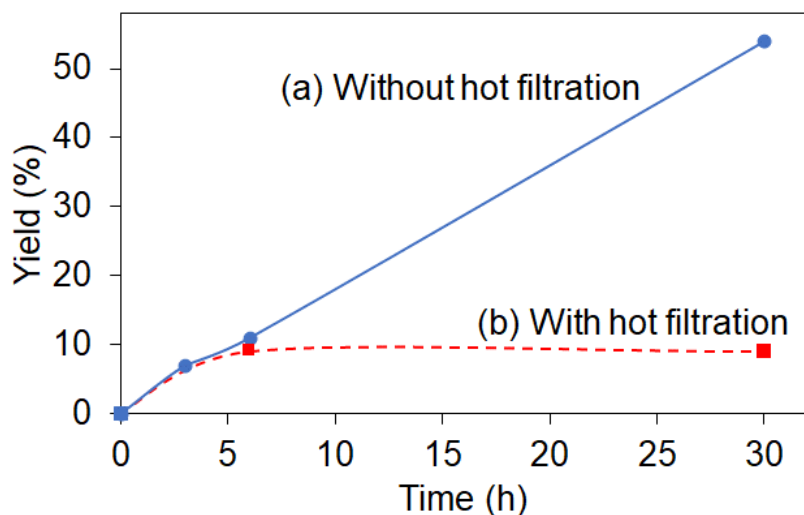


Figure 2. Time-course of the yield of **3aa** over Ir/P_{0.06}-Rutile (HT) (a) without and (b) with the removal of the catalyst by hot filtration after 6 h. Reaction conditions are shown in the Experimental section.

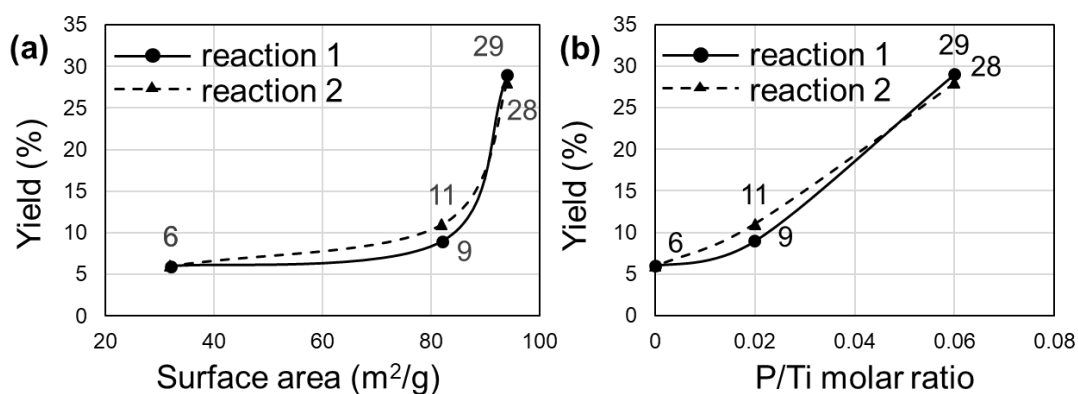


Figure 3. The dependences of the yields of the products on (a) surface area of the supported catalysts and (b) P/Ti molar ratio and the yield of the product. Numbers in the graphs show the yields of corresponding benzimidazoles.

As reported previously, P-doping on to Rutile (HT) significantly increases its surface area [40]. To examine the reason of the promotional effects of P-doping, the dependences of the yield of the desired products on the surface area and P/Ti molar ratio were plotted as shown in Figure 3(a) and (b), respectively. The results show that

there is a non-linear increasing relationship between the surface area of supports and the yield of products, suggesting that although the surface area affects catalytic activities, it is not the dominant factor of the catalytic activities. Meanwhile, a near linear increasing relationship between the amount of doped phosphorus atoms and the yield of products was found. This result suggests that the presence of phosphorus species is responsible for the enhanced activities.

Effect of loading level of iridium of the Ir/P_{0.06}-Rutile catalysts (25 mg) was examined, and the results are shown in Figure 4 in the Supporting Information. The yield of the desired products increased in proportion to the iridium loading level. This result implies that the activity per iridium atom is not greatly affected by the iridium loading level from 0.5 to 4%.

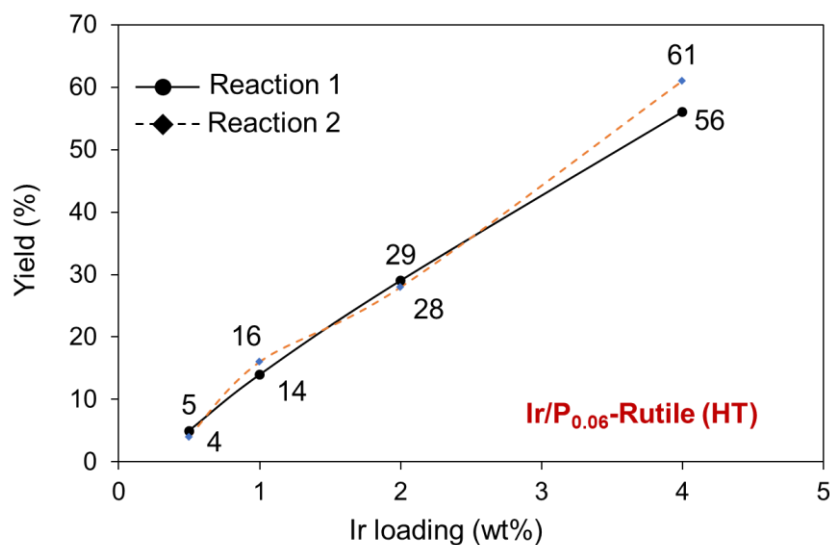


Figure 4. The correlation between Ir loading level on P_{0.06}-Rutile (HT) and the product yield. Numbers in the graph show the yields of corresponding benzimidazoles.

Figure 5 shows HR-TEM images of Rutile (HT)-supported iridium catalysts with different loading levels. Regardless of the iridium loading level, nanoparticles

located on the surface of supports have a uniform particle size in a range of 1.0 to 2.4 nm. This result is consistent with the result that the activity of the catalyst is just dependent on the amount of iridium species on supports surface (see Figure 4). The similarity of the lattice parameter of IrO₂ and rutile titania would be one reason: The close Ir–O (0.1976 and 0.1978 nm) and Ti–O (0.1962 and 0.1963 nm) bond lengths and crystalline structure would restrict the growth of Ir particles [44]. Besides, from these TEM photographs, changes of the particle morphology and size distribution of iridium nanoparticles on supports surface by the P-doping could not be confirmed.

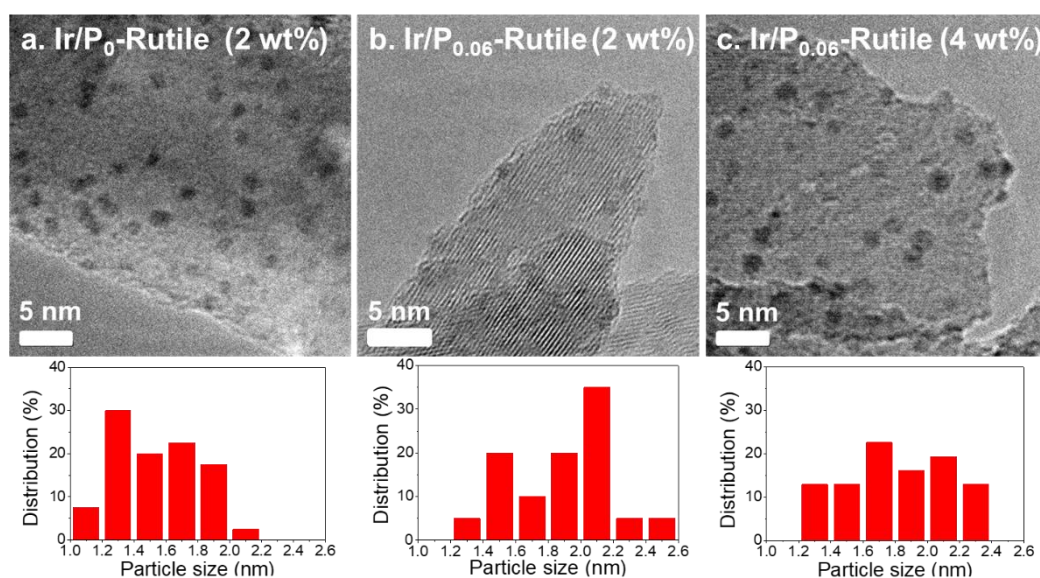


Figure 5. HR-TEM images and the particle size distribution histograms of (a) Ir(2 wt%)/P₀-Rutile (HT), (b) Ir(2 wt%)/P_{0.06}-Rutile (HT), and (c) Ir(4 wt%)/P_{0.06}-Rutile (HT).

The XPS depth profile (Table 2) clearly shows uneven distribution of phosphorus atoms. For example, the surface compositional ratio of phosphorus atom was 1.86% on the surface of P_{0.02}-Rutile (HT), and decreased dramatically to 0.72% after ion sputtering for 1 min. As the sputtering carried on for 15 minutes, there was only 0.18%

of phosphorus atom left. These results reveal that the phosphorus species mainly present on the surface layer of the P-doped rutile particles.

Table 2. XPS analysis of P_x-Rutile (HT) supports^a

Entry	Ion sputtering time (min)	C (atom%)	O (atom%)	Ti (atom%)	P (atom%)
P ₀ -Rutile (HT)	0	7.49	65.71	26.80	0.00
P _{0.02} -Rutile (HT)	0	4.81	68.37	24.96	1.86
	1	0.71	69.42	29.16	0.72
	5	0.62	68.14	30.57	0.67
	15	0.97	67.52	31.33	0.18
P _{0.06} -Rutile (HT)	0	2.10	70.38	23.99	3.53
	1	0.35	69.73	27.99	1.93
	5	0.17	69.02	29.51	1.29
	15	0.42	68.79	29.98	0.80

^a The surface was sputtered by Xe⁺ ion beam (3.0 kV).

3.3.2 Effects of phosphorus-modification of titania by the impregnation method

Following the results using the Ir/P_x-Rutile (HT) catalysts shown above, in which phosphorus species located on the surface layer play a significant promotional role, the effect of phosphorus-modification by an impregnation method was examined. Note that the modification of titania surface by phosphoric acid (H₃PO₄) has been reported to enhance the adsorption capacity for organic compounds and accelerate the photocatalytic degradation of these adsorbed organic species [45]. Our preliminary

experiments evidenced that the adsorption capacity of Ir/TIO-7 catalyst towards methylene blue in water increased by the phosphorus-modification (data not shown). On the other hand, phosphorus-modification only slightly changed its surface Zeta potential under neutral conditions (see Table 3).

Table 3. Zeta potential of supported iridium catalysts^a

Entry	Sample	Zeta potential (mV)
1	JRC-TIO-7	-9.81
2	Ir/TIO-7	-0.10
3	Ir/P _{0.02} -TIO-7 (IMP)	-0.08

^a Sample was dispersed in distilled water.

In the present study, an anatase titania sample with a high surface area, namely JRC-TIO-7, was impregnated in dilute phosphoric acid (H₃PO₄) solution, followed by drying. The iridium catalysts were prepared using the thus-prepared P-impregnated JRC-TIO-7 (further designated as P_x-TIO-7 (IMP)) (see Figure 1). Figure 6 shows the effect of the atomic ratio of phosphorus to titanium on the solvent-free synthesis of 2-propylbenzimidazole (**3ab**) from 2-nitroaniline (**1a**) and butan-1-ol (**2b**) (eq. 2). While unmodified JRC-TIO-7 gave **3ab** in the yield of 25%, the highest yield of 69% was achieved in the presence of Ir/P_{0.02}-TIO-7 (IMP), as shown in Figure 6. As the molar ratio of phosphorus further increased, the yield decreased correspondingly.

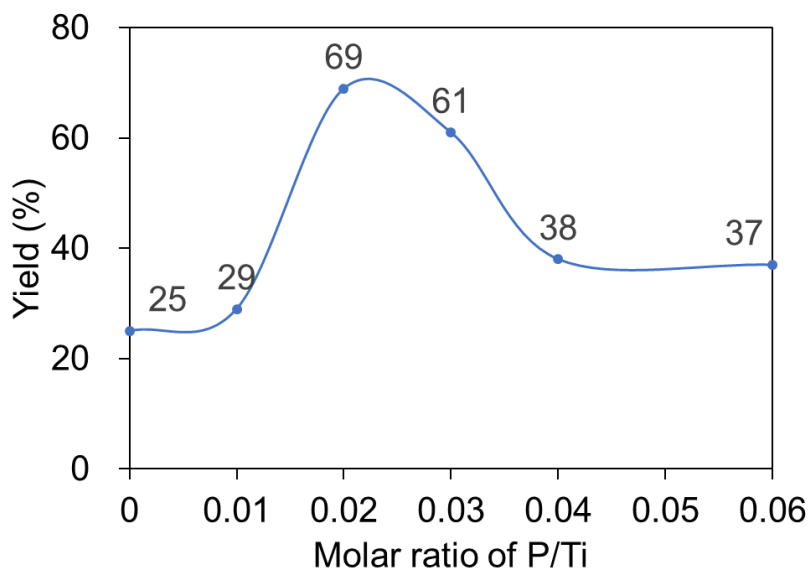


Figure 6. Effect of P/Ti molar ratio (x) of the Ir/P_x-TiO-7 (IMP) catalyst on the yield of **3ab**. Reaction conditions are shown in eq. 2.

To examine whether the Ir/P_{0.02}-TiO-7 (IMP) catalyst was still active or not after the reaction for 18 h, we added another 1.0 mmol of 2-nitroaniline through a syringe and allowed the reaction for another 24 h. The amount of **3ab** formed was increased from 0.69 mmol (69%) to 0.96 mmol, indicating that the phosphorus-modified catalysts kept their activity after the initial run for 18 h. On the other hand, when the used catalyst was recovered from the mixture by centrifugation in an air atmosphere followed by the calcination at 400 °C and the reduction at 500 °C for 30 min, the thus-recovered catalyst showed poor activities: the yield of **3ab** was only 11%. The reasons of the lower activity of used catalysts are discussed below.

Meanwhile, the titanium phosphate (TiP₂O₇, see Figure 7) prepared by a liquid-assisted synthesis method [46] was also utilized to compare the effect of phosphorus on the catalytic activity. As shown in Table 4, the use of TiP₂O₇ resulted in poor catalytic activity.

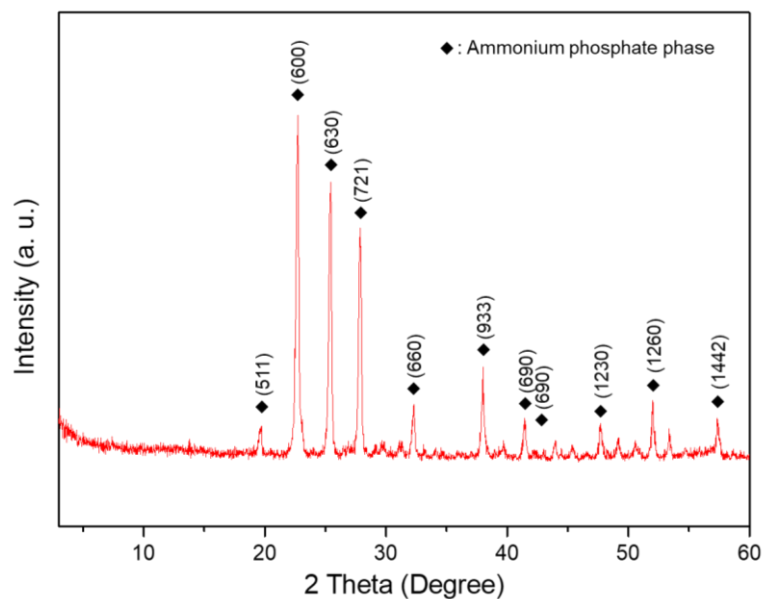


Figure 7. XRD pattern of titanium phosphate sample obtained by the mixture of $\text{NH}_4\text{H}_2\text{PO}_4$ and TiO_2 heated at $900\text{ }^\circ\text{C}$ for 6 h.

Table 4. Effect of $\text{Ir}/\text{TiP}_2\text{O}_7$ catalyst

Entry	Substrate	Alcohol	Amount of catalyst (mg)	Reaction temperature ($^\circ\text{C}$)	Yield of product (%)
1	2-Nitroaniline	1-Butanol	25	120	5
2	2-Phenylenediamine	Benzyl alcohol	100	80	0
3	2-Aminophenol	Benzyl alcohol	100	160	4
4	Ammonium carbonate	Benzyl alcohol	100	160	8

As can be seen in Figure 8, the HR-TEM image shows that small iridium particles are irregularly distributed on $\text{P}_{0.02}\text{-TiO}_7$ (IMP). Particle size statistics suggest that most of the iridium particles are smaller than 1 nm. These small particles would be responsible for the high catalytic activity, as discussed in our previous report [35]. The

fast Fourier transform (FFT) pattern evidence the dark small particles dispersed in the lattice fringe are metallic iridium phase. Again, changes of the morphology and size of surface iridium particles by the phosphorus-modification could not be confirmed, since TEM images of Ir/TIO-7 were very similar to Ir/P_{0.02}-TIO-7 (IMP) (mean diameter of iridium nanoparticles; 0.7 nm [34,35]). Whereas the isolated iridium atoms formed on the support along with nanoparticles were often reported [47], it cannot be identified in the lattice fringe probably due to that the small particles are an amorphous phase.

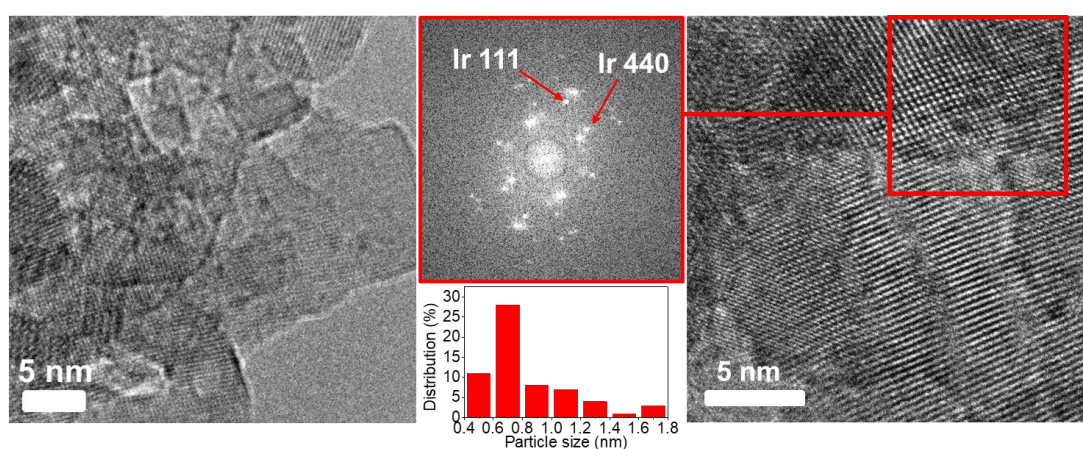


Figure 8. HR-TEM images, corresponding FFT pattern, and particle size distribution histograms of Ir/P_{0.02}-TIO-7 (IMP) catalyst.

Changes of surface functional groups by phosphorus-modification on JRC-TIO-7 and the Ir/P_x-TIO-7 (IMP) catalysts were examined by DRIFT (diffuse-reflectance infrared Fourier transform) spectra, as shown in Figure 9. For all the samples, a broad band at around 3400 cm⁻¹ as well as a narrow peak at around 1634 cm⁻¹ due to the stretching and bending vibrations of the surface hydroxyl group, respectively, were observed [48,49]. Note that the phosphorus-modification significantly enhanced the intensity of band due to the O-H stretching vibrations, suggesting an increase of surface

hydroxyl groups as discussed in the following XPS study, which would be one reason of the enhanced adsorption capacity towards organic substrates of phosphorus-modified catalysts (see above). An intense peak present at 750 cm^{-1} is assignable to the Ti-OTi stretching vibration octahedral coordination [50]. The peaks of Ir/P_{0.02}-TiO-7 (IMP) after impregnation with Ir(acac)₃ around $1205\text{--}1558\text{ cm}^{-1}$ would be responsible for organic ligands of Ir(acac)₃ [51]. Two shoulders at around 1120 cm^{-1} and 1020 cm^{-1} were observed on the P-modified samples, which are assigned to the stretching vibration of P–O bonds of bidentate adsorbed phosphorus species [52]. These peaks were observable even after the reduction of the catalyst. However, the stretching vibration of P=O bond of phosphoric acid cannot be observed around $1200\text{--}1250\text{ cm}^{-1}$ probably due to the coordination of the phosphoryl oxygens to surface Lewis acidic sites [53]. Since earlier studies reported that the phosphorus was located in the coordinatively unsaturated site of Ti⁴⁺ cations [52], it is believed that the phosphorus exists as bidentate phosphoric acid and anchoring on the surface of TiO₂ through Ti–O–P bonds [54].

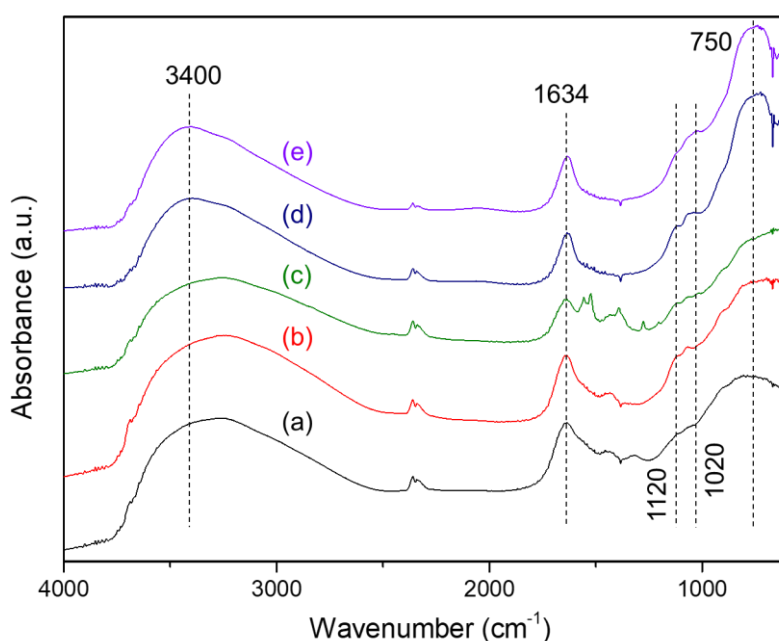


Figure 9. FT-IR spectra of titania (a) JRC-TIO-7, (b) P_{0.02}-TIO-7 (IMP), and supported iridium catalysts (c) Ir/P_{0.02}-TIO-7 (IMP) just after impregnation with Ir(acac)₃, (d) Ir/P_{0.02}-TIO-7 (IMP) after calcination at 400 °C for 30 min, (e) Ir/P_{0.02}-TIO-7 (IMP) after reduction in an H₂ flow at 500 °C for 30 min.

The catalysts were characterized by XPS. Figure 10(a) shows the P 2p XP spectra of Ir/P_{0.02}-TIO-7 (IMP), Ir/P_{0.02}-Rutile (HT), and Ir/P_{0.06}-Rutile (HT). For those catalysts, the P 2p binding energy appeared at around 133.3 eV, suggesting that the phosphorus species on the catalyst were in the pentavalent oxidation (P⁵⁺) state even after the hydrogen reduction. This is consistent with the FTIR results, which suggests the formation of bidentate surface phosphoric species (see above). A peak at around 129 eV, characteristic for P-Ti species was not observed [55]. Figure 10(b-d) shows the O 1s XP spectra on the surface of phosphorus-modified and unmodified titania-supported iridium catalysts. The O 1s spectra of phosphorus-modified catalysts were significantly different from that of unmodified one: There were additional bands at higher binding energies. These new bands were assignable to oxygen atoms of phosphorus species and/or those of surface OH groups [56]. As discussed above, FTIR study revealed that the use of phosphorus-modified titania promotes the formation of surface OH groups, which is consistent with the present XPS results. On the other hand, Ir 4f bands of phosphorus-modified catalysts were almost identical to those of unmodified catalysts as shown in Figure 11. Note that bands at 60.7 eV and 62.0 eV have been assigned to Ir⁰ and Ir^{IV} species, respectively [35], while a band due to Ti 3s was overlapped with Ir 4f bands.

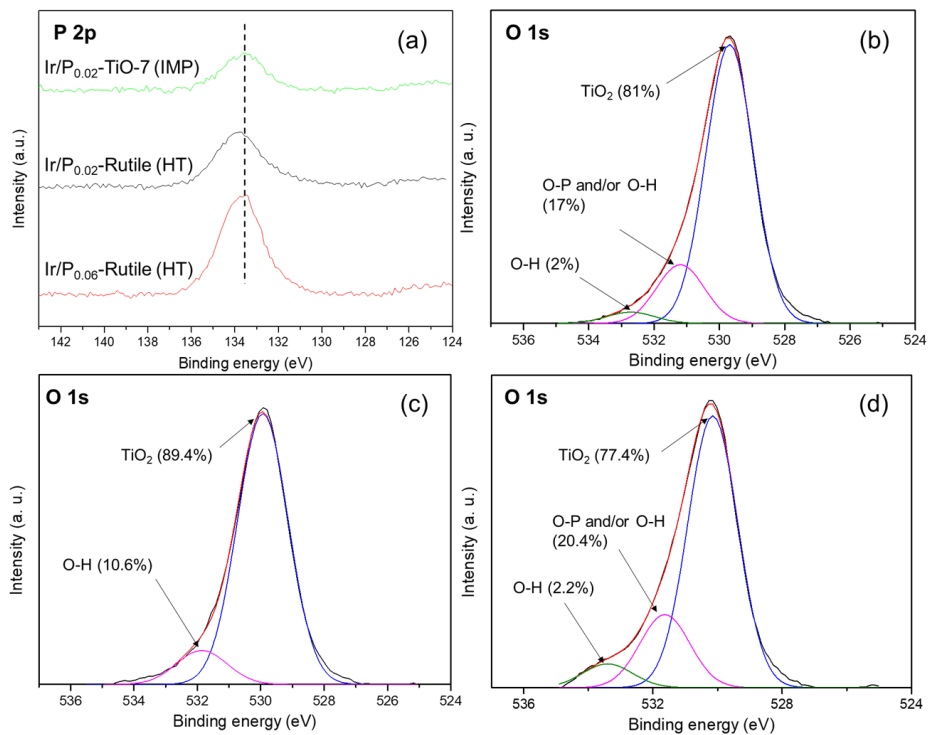


Figure 10. XPS spectra of (a) P 2p of Ir/P_{0.02}-TiO₂-7 (IMP), Ir/P_{0.02}-Rutile (HT) and Ir/P_{0.06}-Rutile (HT), (b) O 1s of Ir/P_{0.02}-TiO₂-7 (IMP), (c) Ir/P₀-Rutile (HT), and (d) Ir/P_{0.06}-Rutile (HT).

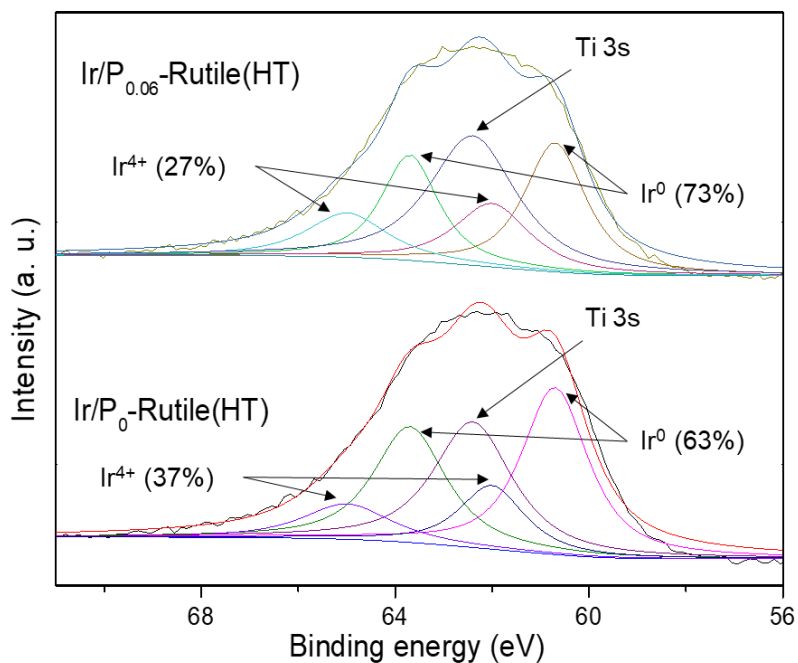


Figure 11. Ir 4f XPS spectra of Ir/P₀-Rutile (HT) and Ir/P_{0.06}-Rutile (HT).

The H₂ temperature-programmed reduction (TPR) study demonstrates the effect of phosphorus modification on the reducibility of iridium catalysts as shown in Figure 12. The profile of P_{0.02}-TiO₂ (IMP) exhibited a hydrogen consumption peak at around 500 °C which can be ascribed to the reduction of surface titanium species [57,58], and there are no significant reduction peaks at below 400 °C. The Ir/TIO-7 catalyst leads to three reduction peaks at 153 °C and 372 °C together with a weak peak at 220 °C. A significant shift of the TiO₂ reduction temperature to 372 °C would be due to the spillover effects by supported iridium species [59]. For the Ir/P_{0.02}-TIO-7 (IMP) catalyst, the reduction peaks of surface Ti⁴⁺ species shifted to a lower temperature, 345 °C, while the peak at around 220 °C increased significantly. The intensity of the peak at 220 °C further increased with Ir/P_{0.06}- TIO-7 (IMP). The first peak at around 150 °C could be assigned to the reduction of iridium particles around 0.5 nm in diameter or above. The iridium oxide species reduced around 220 °C have been identified as those having strong interaction with the support, namely well-dispersed iridium species smaller than 0.5 nm [57,58]. While the formation of such small iridium species could not be confirmed by the TEM photographs in the present study, the iridium species adjacent to phosphorus species would further decrease the reduction temperature of titania surface to ca. 340 °C. On the other hand, the Ir/P_{0.06}-Rutile (HT) catalysts do not show a significant reduction peak at 220 °C. Instead, it showed broad peaks at lower temperatures, which indicates that iridium oxide species on Rutile (HT) are more easily reducible than those on anatase titania and suggests that the interaction between iridium species and phosphorus species of P_{0.06}-Rutile (HT) is weak.

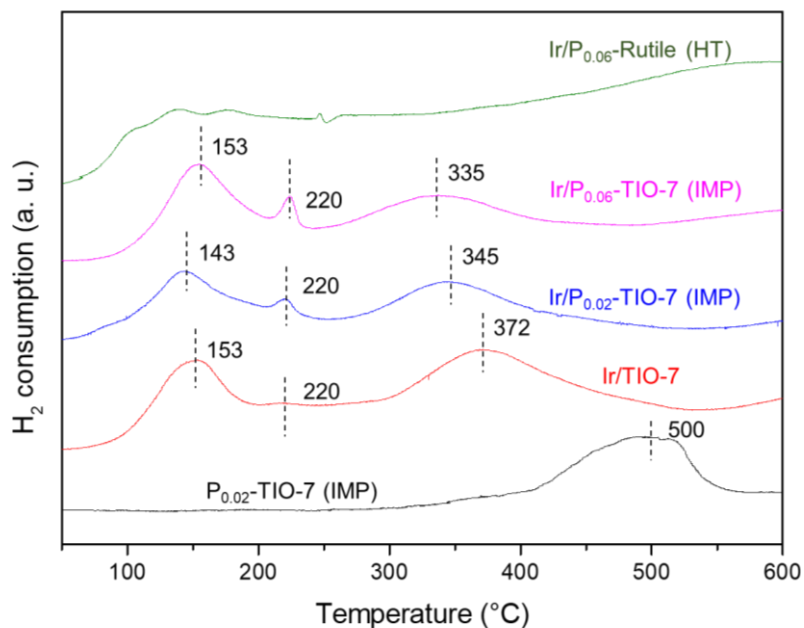


Figure 12. H₂-TPR profiles of phosphorus-modified titania and the iridium catalysts.

As noted above, the recovered Ir/P_{0.02}-TiO-7 (IMP) catalyst showed low activity. The BET surface area of the used catalyst (157 m² g⁻¹) is slightly smaller than the fresh catalyst (173 m² g⁻¹). The TEM image of the used catalyst (see Figure 13) indicates the absence of large iridium particles. On the other hand, the H₂-TPR (see Figure 14) profile shows a more significant reduction peak at around 220 °C, suggesting the presence of more strong interaction between titania surface and iridium species. Such a very strong interaction would be one reason for the lower activity of the used catalyst. Moreover, the XP spectrum (see Figure 15) reveals the adsorption of nitrogen species on the surface of the used catalyst. These results indicate that the recovery procedure of the used catalyst needs further improvement.

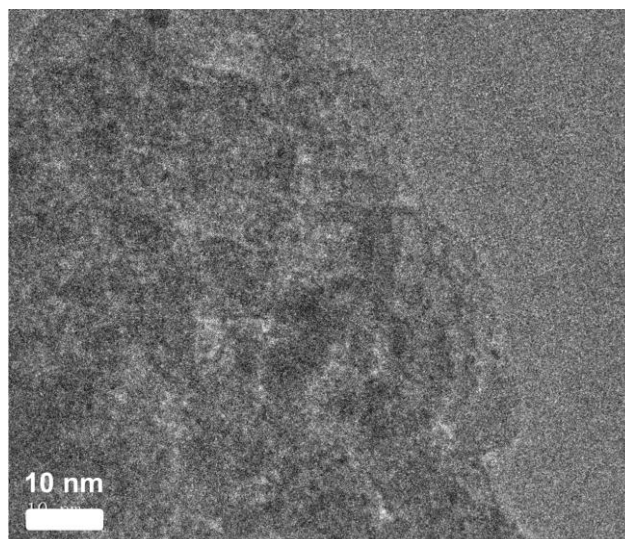


Figure 13. TEM image of used Ir/P_{0.02}-TiO-7 (IMP) catalyst.

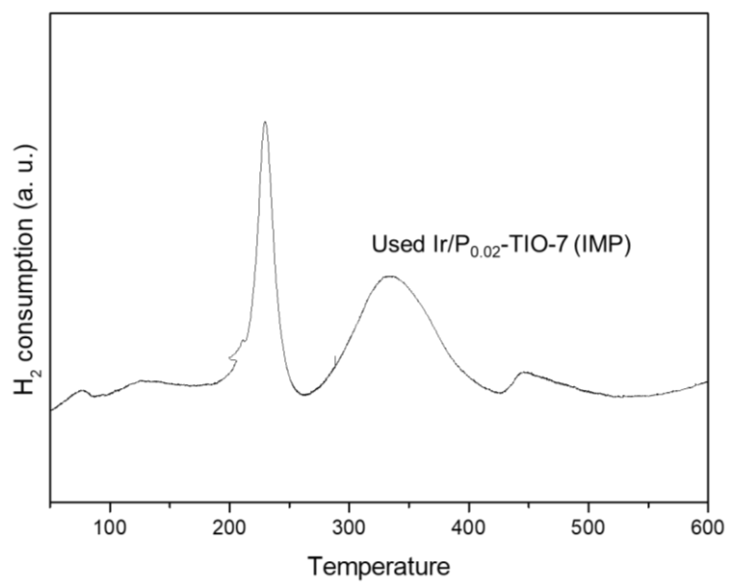


Figure 14. H₂-TPR profiles of used Ir/P_{0.02}-TiO-7 (IMP) catalyst.

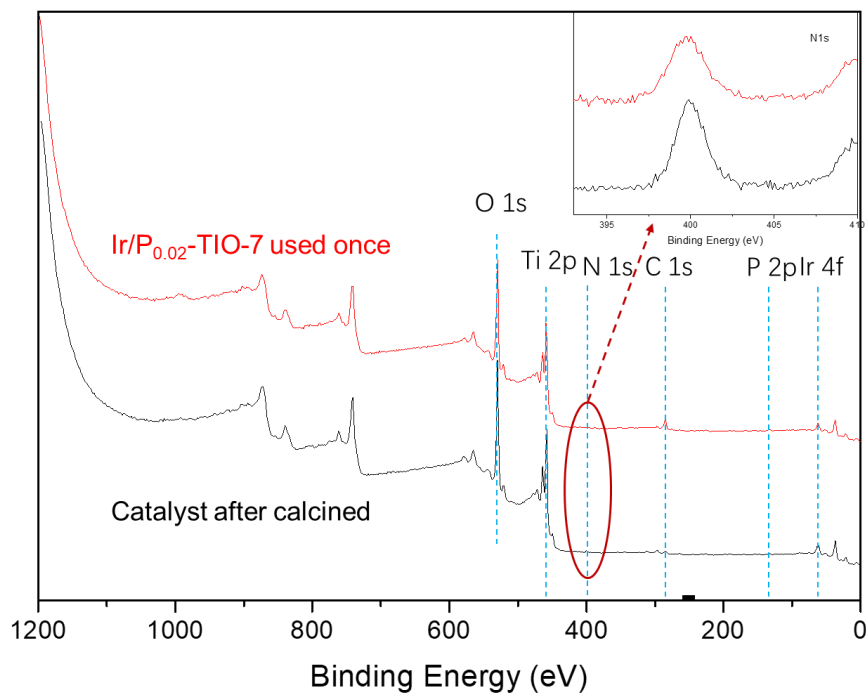


Figure 15. XPS Survey spectrum of used Ir/P_{0.02}-TiO-7 (IMP) catalyst.

As discussed above, the phosphorus-modification of titania support changed the redox properties of the surface iridium species, whereas the size and morphology were not significantly affected. The processes of the formation of iridium nanoparticles on the surface of (IMP)-titania are discussed based on the above results. Initially, bidentate phosphorus species would be formed on the surface by the impregnation of titania with phosphoric acid as supported by the FTIR study. The bidentate structure would be most stable because of its highest adsorption energies of 257–286 kJ/mol [60]. During the subsequent impregnation with Ir(acac)₃ in methanol, interaction of surface phosphorus species and an iridium complex could be expected. In the course of the calcination and reduction procedure at a high temperature, these surface iridium complexes would be converted to small iridium nanoparticles. Meanwhile, the iridium species adjacent to phosphorus species would play an important role in the

enhancement of the catalytic activity. Our previous study revealed that relatively high-valent iridium species would be responsible for the synthesis of benzimidazole via hydrogen transfer [35]. Transition metal species were often reduced to be zero-valent in the presence of alcohols even under aerobic conditions [61]. The interaction by phosphorus-modified surface would stabilize the relatively high-valent state of iridium species during the course of the reactions. Further characterization of phosphorus-modified catalysts are ongoing.

3.4 Conclusion

Phosphorus-modified titania supports were prepared in two different ways, namely by the hydrothermal and wet impregnation methods. In both cases, the iridium catalysts supported on phosphorus-modified titanias showed the enhanced activity for the synthesis of benzimidazoles from 2-nitroaniline and primary alcohols via hydrogen transfer. The hydrothermal P-doping resulted in ca. 5 times promotion of the catalytic activity. The modification by the wet impregnation of titania with a high surface area such as JRC-TIO-7 with phosphoric acid also increased the activity of supported iridium catalysts. The P-modification of both anatase and rutile has a positive effect on the promotion of the catalytic activity. Especially the catalysts supported on P-modified anatase with high surface area showed excellent activity. The hot filtration study indicates that the catalysis proceeded heterogeneously. These modified catalysts kept their activity even after the additional supply of the substrate, indicating their fair durability. On the other hand, the lower activity of the recovered catalysts points out the need for further improvement of the recovery procedure. The detailed characterization of the catalysts such as the H₂-TPR study revealed that phosphorus-

modification facilitated the formation of iridium species reduced at higher temperature, and would stabilize the state of iridium species suitable for the present catalysis. Further application of the present catalysts to a wider range of reactions via hydrogen transfer, as well as the detailed investigation on the effects of phosphorus and various promoters, are now in progress.

3.5 References

- [1] J. Cheng, J. Xie, X. Luo, Synthesis and antiviral activity against Cocksackie virus B3 of some novel benzimidazole derivatives, *Bioorg. Med. Chem. Lett.* 15 (2005) 267–269.
- [2] K.C.S. Achar, K.M. Hosamani, H.R. Seetharamareddy, In-vivo analgesic and anti-inflammatory activities of newly synthesized benzimidazole derivatives, *Eur. J. Med. Chem.* 45 (2010) 2048–2054.
- [3] B. Narasimhan, D. Sharma, P. Kumar, Benzimidazole: A medicinally important heterocyclic moiety, *Med. Chem. Res.* 21 (2012) 269–283.
- [4] Y. Bansal, O. Silakari, The therapeutic journey of benzimidazoles: A review, *Bioorg. Med. Chem.* 20 (2012) 6208–6236.
- [5] Salahuddin, M. Shaharyar, A. Mazumder, Benzimidazoles: A biologically active compounds, *Arab. J. Chem.* 10 (2017) S157–S173.
- [6] I. Shimomura, A. Yokoi, I. Kohama, M. Kumazaki, Y. Tada, K. Tatsumi, T. Ochiya, Y. Yamamoto, Drug library screen reveals benzimidazole derivatives as selective cytotoxic agents for KRAS-mutant lung cancer, *Cancer Lett.* 451 (2019) 11–22.
- [7] K. Wada, H. Yu, Q. Feng, Titania-supported iridium catalysts for dehydrogenative synthesis of benzimidazoles, *Chinese Chem. Lett.* 31 (2020) 605–608.
- [8] Z.H. Zhang, L. Yin, Y.M. Wang, An expeditious synthesis of benzimidazole derivatives catalyzed by Lewis acids, *Catal. Commun.* 8 (2007) 1126–1131.
- [9] A.R. Katritzky, X. Lan, J.Z. Yang, O. V. Denisko, Properties and synthetic utility of N-substituted benzotriazoles, *Chem. Rev.* 98 (1998) 409–548.
- [10] R. Gedye, F. Smith, K. Westaway, H. Ali, L. Baldisera, L. Laberge, J. Rousell, The use of microwave ovens for rapid organic synthesis, *Tetrahedron Lett.* 27 (1986) 279–282.
- [11] P.N. Preston, Synthesis, Reactions, and Spectroscopic Properties of Benzimidazoles, *Chem. Rev.* 74 (1974) 279–314.
- [12] J.B. wright, The chemistry of the benzimidazoles, *Chem. Rev.* 48 (1951) 397–541.

- [13] T. Kondo, S. Yang, K.-T. Huh, M. Kobayashi, S. Kotachi, Y. Watanabe, Ruthenium Complex-Catalyzed Facile Synthesis of 2-Substituted Benzoxazoles, *Chem. Lett.* 20 (1991) 1275–1278.
- [14] M. Bala, P.K. Verma, U. Sharma, N. Kumar, B. Singh, Iron phthalocyanine as an efficient and versatile catalyst for N-alkylation of heterocyclic amines with alcohols: One-pot synthesis of 2-substituted benzimidazoles, benzothiazoles and benzoxazoles, *Green Chem.* 15 (2013) 1687–1693.
- [15] G. Li, J. Wang, B. Yuan, D. Zhang, Z. Lin, P. Li, H. Huang, Iron-catalyzed one-pot synthesis of benzimidazoles from 2-nitroanilines and benzylic alcohols, *Tetrahedron Lett.* 54 (2013) 6934–6936.
- [16] T. Hille, T. Irrgang, R. Kempe, The synthesis of benzimidazoles and quinoxalines from aromatic diamines and alcohols by iridium-catalyzed acceptorless dehydrogenative alkylation, *Chem. - A Eur. J.* 20 (2014) 5569–5572.
- [17] R. Ramachandran, G. Prakash, S. Selvamurugan, P. Viswanathamurthi, J.G. Malecki, V. Ramkumar, Efficient and versatile catalysis of N-alkylation of heterocyclic amines with alcohols and one-pot synthesis of 2-aryl substituted benzazoles with newly designed ruthenium(ii) complexes of PNS thiosemicarbazones, *Dalt. Trans.* 43 (2014) 7889–7902.
- [18] J.W. Kim, J. He, K. Yamaguchi, N. Mizuno, Heterogeneously catalyzed one-pot synthesis of aldimines from primary alcohols and amines by supported ruthenium hydroxides, *Chem. Lett.* 38 (2009) 920–921.
- [19] Y. Shiraishi, Y. Sugano, S. Tanaka, T. Hirai, One-pot synthesis of benzimidazoles by simultaneous photocatalytic and catalytic reactions on Pt@TiO₂ nanoparticles, *Angew. Chemie - Int. Ed.* 49 (2010) 1656–1660.
- [20] H. Wang, J. Zhang, Y.M. Cui, K.F. Yang, Z.J. Zheng, L.W. Xu, Dehydrogenation and oxidative coupling of alcohol and amines catalyzed by organosilicon-supported TiO₂@PMHSIPN, *RSC Adv.* 4 (2014) 34681–34686.
- [21] L. Tang, X. Guo, Y. Yang, Z. Zha, Z. Wang, Gold nanoparticles supported on titanium dioxide: An efficient catalyst for highly selective synthesis of benzoxazoles and benzimidazoles, *Chem. Commun.* 50 (2014) 6145–6148.
- [22] J. Chen, S. Huang, J. Lin, W. Su, Recyclable palladium catalyst for facile synthesis of imines from benzylic alcohols and nitroarenes, *Appl. Catal. A Gen.* 470 (2014) 1–7.
- [23] C. Chaudhari, S.M.A.H. Siddiki, K.I. Shimizu, Acceptorless dehydrogenative synthesis of benzothiazoles and benzimidazoles from alcohols or aldehydes by heterogeneous Pt catalysts under neutral conditions, *Tetrahedron Lett.* 56 (2015) 4885–4888.
- [24] P.L. Reddy, R. Arundhathi, M. Tripathi, P. Chauhan, N. Yan, D.S. Rawat, Solvent-Free Oxidative Synthesis of 2-Substituted Benzimidazoles by Immobilized Cobalt Oxide Nanoparticles on Alumina/Silica Support, *ChemistrySelect.* 2 (2017) 3889–3895.

- [25] S.M.A. Hakim Siddiki, T. Toyao, K.I. Shimizu, Acceptorless dehydrogenative coupling reactions with alcohols over heterogeneous catalysts, *Green Chem.* 20 (2018) 2933–2952.
- [26] J. Mokhtari, A. Hasani Bozcheloei, One-pot synthesis of benzoazoles via dehydrogenative coupling of aromatic 1,2-diamines/2-aminothiophenol and alcohols using Pd/Cu-MOF as a recyclable heterogeneous catalyst, *Inorganica Chim. Acta.* 482 (2018) 726–731.
- [27] B. Guo, H.X. Li, S.Q. Zhang, D.J. Young, J.P. Lang, C-N Bond Formation Catalyzed by Ruthenium Nanoparticles Supported on N-Doped Carbon via Acceptorless Dehydrogenation to Secondary Amines, Imines, Benzimidazoles and Quinoxalines, *ChemCatChem.* 10 (2018) 5627–5636.
- [28] F. Feng, Y. Deng, Z. Cheng, X. Xu, Q. Zhang, C. Lu, L. Ma, X. Li, Heterogeneous Catalytic Synthesis of 2-Methylbenzimidazole from 2-Nitroaniline and Ethanol Over Mg Modified Cu-Pd/ γ -Al₂O₃, *Catal.* 2019, Vol. 9, Page 8. 9 (2018) 8.
- [29] C. Bäumler, R. Kempe, The Direct Synthesis of Imines, Benzimidazoles and Quinoxalines from Nitroarenes and Carbonyl Compounds by Selective Nitroarene Hydrogenation Employing a Reusable Iron Catalyst, *Chem. - A Eur. J.* 24 (2018) 8989–8993.
- [30] Q. Guan, Q. Sun, L. Wen, Z. Zha, Y. Yang, Z. Wang, The synthesis of benzimidazoles via a recycled palladium catalysed hydrogen transfer under mild conditions, *Org. Biomol. Chem.* 16 (2018) 2088–2096.
- [31] S. Sharma, A. Sharma, Yamini, P. Das, Supported Rhodium (Rh@PS) Catalyzed Benzimidazoles Synthesis Using Ethanol/Methanol as C₂H₃/CH Source, *Adv. Synth. Catal.* 361 (2019) 67–72.
- [32] K. Tateyama, K. Wada, H. Miura, S. Hosokawa, R. Abe, M. Inoue, Dehydrogenative synthesis of benzimidazoles under mild conditions with supported iridium catalysts, *Catal. Sci. Technol.* 6 (2016) 1677–1684.
- [33] K. Tateyama, K. Wada, H. Miura, S. Hosokawa, R. Abe, M. Inoue, Dehydrogenative synthesis of benzimidazoles under mild conditions with supported iridium catalysts, *Catal. Sci. Technol.* 6 (2016) 1677–1684.
- [34] T. Fukutake, K. Wada, G.C. Liu, S. Hosokawa, Q. Feng, Striking effects of a titania support on the low-temperature activities of Ir catalysts for the dehydrogenative synthesis of benzimidazole and indole, *Catal. Today.* 303 (2018) 235–240.
- [35] T. Fukutake, K. Wada, H. Yu, S. Hosokawa, Q. Feng, Development of titania-supported iridium catalysts with excellent low-temperature activities for the synthesis of benzimidazoles via hydrogen transfer, *Mol. Catal.* 477 (2019) 110550.
- [36] Y. Nakagawa, Y. Shinmi, S. Koso, K. Tomishige, Direct hydrogenolysis of glycerol into 1,3-propanediol over rhenium-modified iridium catalyst, *J. Catal.* 272 (2010) 191–194.

- [37] K. Chen, D.G. Feng, P.R. Su, Y.J. Zhang, Black-box testing based on colorful taint analysis, *Sci. China Inf. Sci.* 55 (2012) 171–183.
- [38] S. Liu, Y. Okuyama, M. Tamura, Y. Nakagawa, A. Imai, K. Tomishige, Selective transformation of hemicellulose (xylan) into n-pentane, pentanols or xylitol over a rhenium-modified iridium catalyst combined with acids, *Green Chem.* 18 (2015) 165–175.
- [39] L. Liu, S. Kawakami, Y. Nakagawa, M. Tamura, K. Tomishige, Highly active iridium–rhenium catalyst condensed on silica support for hydrogenolysis of glycerol to 1,3-propanediol, *Appl. Catal. B Environ.* 256 (2019).
- [40] Y. Hayashi, S. Nakamura, M. Takagishi, S. Iwamoto, Synthesis of thermally stable nanocrystalline phosphorus-modified titanium(IV) dioxides with rutile structure, *Chem. Lett.* 46 (2017) 307–309.
- [41] C. J., R.C.K. Jr, *Handbook of X-ray Photoelectron Spectroscopy*, Perkin-Elmer Corp. 40 (1992) 242.
- [42] N.T.S. Phan, M. Van Der Sluys, C.W. Jones, On the nature of the active species in palladium catalyzed Mizoroki-Heck and Suzuki-Miyaura couplings - Homogeneous or heterogeneous catalysis, a critical review, *Adv. Synth. Catal.* 348 (2006) 609–679.
- [43] M. Weck, C.W. Jones, Mizoroki-Heck coupling using immobilized molecular precatalysts: Leaching active species from Pd pincers, entrapped Pd salts, and Pd NHC complexes, *Inorg. Chem.* 46 (2007) 1865–1875.
- [44] X. Bokhimi, R. Zanella, C. Angeles-Chavez, Rutile-supported Ir, Au, and Ir-Au catalysts for CO oxidation, *J. Phys. Chem. C.* 114 (2010) 14101–14109.
- [45] A. Zaleska, Doped-TiO₂: A Review, *Recent Patents Eng.* 2 (2008) 157–164.
- [46] Y. Hao, C. Wu, Y. Cui, K. Xu, Z. Yuan, Q. Zhuang, Preparation and electrochemical performances of submicro-TiP₂O₇ cathode for lithium ion batteries, *Ionics (Kiel)*. 20 (2014) 1079–1085.
- [47] O. Hernández-Cristóbal, J. Arenas-Alatorre, G. Díaz, D. Bahena, M. J. Yacamán, High resolution HAADF characterization of Ir/TiO₂ catalyst reduced at 500 °c: Intensity profile analysis, *J. Phys. Chem. C.* 119 (2015) 11672–11678.
- [48] A. Markovits, J. Ahdjoudj, C. Minot, A theoretical analysis of NH₃ adsorption on TiO₂, *Surf. Sci.* 365 (1996) 649–661.
- [49] Y. Lv, L. Yu, H. Huang, H. Liu, Y. Feng, Preparation, characterization of P-doped TiO₂ nanoparticles and their excellent photocatalytic properties under the solar light irradiation, *J. Alloys Compd.* 488 (2009) 314–319.
- [50] D. Zhao, C. Chen, Y. Wang, H. Ji, W. Ma, L. Zang, J. Zhao, Surface modification of TiO₂ by phosphate: Effect on photocatalytic activity and mechanism implication, *J. Phys. Chem. C.* 112 (2008) 5993–6001.
- [51] G. Xu, J. Hu, Y.T. Wang, The effects of sodium bicarbonate concentration on the synthesis of Tris-acetylacetonate-iridium(III), *Adv. Mater. Res.* 1058 (2014) 213–216.

- [52] K. HADJIIVANOV, Study of phosphate-modified TiO₂ (anatase), *J. Catal.* 116 (1989) 498–505.
- [53] G. Guerrero, P.H. Mutin, A. Vioux, Anchoring of phosphonate and phosphinate coupling molecules on titania particles, *Chem. Mater.* 13 (2001) 4367–4373.
- [54] A.R. Ramadan, N. Yacoub, H. Amin, J. Ragai, The effect of phosphate anions on surface and acidic properties of TiO₂ hydrolyzed from titanium ethoxide, *Colloids Surfaces A Physicochem. Eng. Asp.* 352 (2009) 118–125.
- [55] Q. Shi, D. Yang, Z. Jiang, J. Li, Visible-light photocatalytic regeneration of NADH using P-doped TiO₂ nanoparticles, *J. Mol. Catal. B Enzym.* 43 (2006) 44–48.
- [56] J.C. Yu, L. Zhang, Z. Zheng, J. Zhao, Synthesis and characterization of phosphated mesoporous titanium dioxide with high photocatalytic activity, *Chem. Mater.* 15 (2003) 2280–2286.
- [57] J. Lin, A. Wang, B. Qiao, X. Liu, X. Yang, X. Wang, J. Liang, J. Li, J. Liu, T. Zhang, Remarkable performance of Ir¹/FeO_x single-atom catalyst in water gas shift reaction, *J. Am. Chem. Soc.* 135 (2013) 15314–15317.
- [58] O. Hernández-Cristóbal, G. Díaz, A. Gómez-Cortés, Effect of the reduction temperature on the activity and selectivity of titania-supported iridium nanoparticles for methylcyclopentane reaction, *Ind. Eng. Chem. Res.* 53 (2014) 10097–10104.
- [59] S. Hosokawa, Y. Hayashi, S. Imamura, K. Wada, M. Inoue, Effect of the preparation conditions of Ru/CeO₂ catalysts for the liquid phase oxidation of benzyl alcohol, *Catal. Letters.* 129 (2009) 394–399.
- [60] R. Lushtinetz, J. Frenzel, T. Milek, G. Seifert, Adsorption of phosphonic acid at the tio₂ anatase (101) and rutile (110) surfaces, *J. Phys. Chem. C.* 113 (2009) 5730–5740.
- [61] B.A. Steinhoff, S.S. Stahl, Ligand-modulated palladium oxidation catalysis: Mechanistic insights into aerobic alcohol oxidation with the Pd(OAc)₂/pyridine catalyst system, *Org. Lett.* 4 (2002) 4179–4181.

Chapter IV Development of Titania-Supported Iridium Catalysts for the Acceptor-Less Dehydrogenative Synthesis of Benzoxazoles

4.1 Introduction

Benzoxazoles, aromatic heterocyclic nitrogen-containing compounds, commonly occur in natural products and have various biological activities, so are important intermediates in pharmaceutical, agrochemical, and chemical industries [1,2]. The most common routes for the synthesis of benzoxazoles [3,4] include condensation of 2-aminophenols with carboxylic acid derivatives [5], oxidation with aldehydes [6,7] or oxidative coupling with amines [8]. The transition metal complex-catalyzed conversion of alcohols to benzoxazoles via the dehydrogenative pathway [9,10] is supposed to provide a more environmentally benign alternative to classical synthetic reactions [11]. For example, several ruthenium or iridium complex-catalyzed syntheses of 2-substituted benzoxazoles with or without hydrogen acceptors have been reported [9,10,12]. In addition, reactions are known via aerobic oxidation of alcohols [13–15], electrochemical oxidation of alcohol [16], and transition metal-catalyzed 2-arylbenzoxazole formation from *o*-nitrophenols and benzylic alcohols using hydrogen transfer [17,18].

Heterogeneous catalysis has advantages from both practical and environmental viewpoints, such as easy recovery and reuse of the catalysts, prevention of contamination of the products by heavy metallic species, and other factors [19–28]. The present authors previously developed heterogeneous supported ruthenium [25,26] and rhodium [29] catalysts which enable various highly atom-efficient organic transformations. In particular, titania-supported iridium catalysts are effective for the synthesis of benzimidazoles via acceptor-less dehydrogenative or hydrogen transfer routes [30–33], which are dependent on the high activity of iridium in hydrogen

activation [34] and coordinatively unsaturated titanium sites on the TiO₂ surface as adsorption and/or activation sites of alcohols [35]. Pt/Al₂O₃ catalysts have also been developed for the acceptor-less dehydrogenative synthesis of benzothiazoles and benzimidazoles [36]. Titania-supported gold catalysts achieved benzoxazole formation from 2-nitrophenols and primary alcohols under mild conditions via hydrogen transfer [18]. However, very few examples of effective heterogeneous catalysis through the acceptor-less dehydrogenative synthesis of benzoxazoles are known. Immobilized ruthenium complex catalyst [12], as well as palladium oxide nanoparticles on mesoporous silica together with a large amount of strong base additive have been reported [37]. Therefore, development of solid, recyclable catalysts not requiring additives for this reaction would be very valuable.

This chapter extended the application of the simple, recyclable titania-supported iridium catalysts to the acceptor-less dehydrogenative synthesis of benzoxazoles. The titania supports had important effects on the activity of the iridium catalysts, and various primary alcohols could be reacted to give the corresponding 2-substituted benzoxazoles in moderate to excellent yields. The present recyclable catalysts are advantageous from both environmental and practical perspectives.

4.2 Experiment section

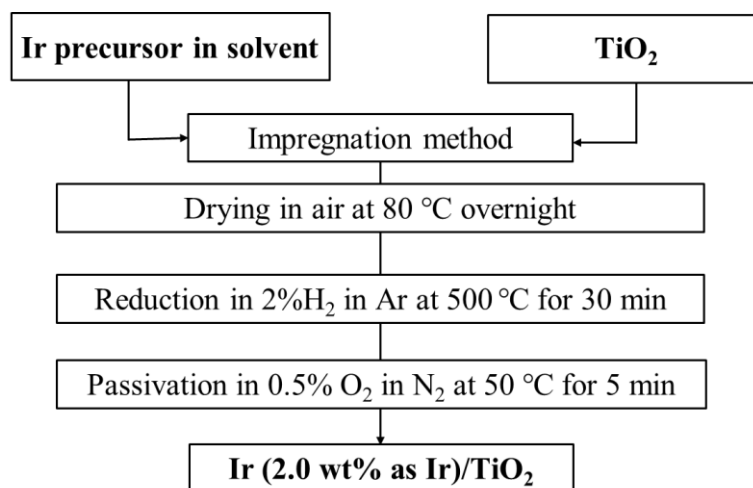
4.2.1 General information

Tris(acetylacetonate)iridium(III) (Ir(acac)₃, C₁₅H₂₁O₆Ir), di- μ -chlorobis[(η -cycloocta-1,5-diene)iridium(I)] ([Ir(cod)Cl]₂, C₁₆H₂₄Cl₂Ir₂), mesitylene, biphenyl and benzyl alcohol were obtained from Wako. Methanol, 1-octanol, tetrahydrofuran (THF), and phosphoric acid were obtained from Nacalai. 2-Aminophenol, 4-methylbenzyl alcohol, 4-methoxybenzyl alcohol, 4-chlorobenzyl alcohol, and 4-fluorobenzyl alcohol

were obtained from TCI. JRC (Japan Reference Catalyst) titania powders (here designated as TIO-4, 6, 7, 8, 9, 10 and 11) were obtained from the Catalysis Society of Japan. All reagents were used as received, and reactions were carried out under an argon atmosphere in Schlenk tubes.

4.2.2 Preparation of supported iridium catalyst

The supported catalysts were prepared by an impregnation method as shown in Scheme 1. Iridium precursor was dissolved in 10 mL of methanol for Ir(acac)₃ or THF for [Ir(cod)Cl]₂ under stirring, then 1.0 g of titania was added in air at 80 °C. Subsequently, the obtained sample was dried overnight in air at 80 °C. The resulting powder was reduced in an H₂ (2 vol.%)/Ar flow (40 cm³ min⁻¹) at 500 °C (ramping rate of 10 °C min⁻¹) for 30 min in a conventional flow reactor to give the Ir/TiO₂ catalysts. After N₂ purging, the catalysts were passivated in an O₂ (2 vol.%)/N₂ flow (40 cm³ min⁻¹) at 50 °C for 5 min for safety reasons.



Scheme 1. Preparation procedure of titania-supported iridium catalysts.

4.2.3 General procedure for catalytic runs

Catalytic reactions were performed in a glass Schlenk tube reactor (20 cm³) equipped with a hot stirrer and cooling block to reflux the reaction solution. A typical reaction procedure for the synthesis of the desired product is as follows: the substrates and solvent were added into the Schlenk tube containing the Ir/TiO₂ catalyst. The reaction mixture was stirred at the desired temperature for 18 h under an argon atmosphere. Then the solid catalyst was removed by passing the mixture through a polytetrafluoroethylene (PTFE) filter (Millipore Millex LH, 0.45 μm), and the yield of products was quantified by gas-liquid chromatography using biphenyl as an internal standard.

4.2.4 Physical and analytical measurements

The organic products of catalytic runs were analyzed by GC–MS (Shimadzu GC–MS Parvum 2; Zebron ZB-1 capillary column, i.d. 0.25 mm, length 30 m, at 50–250 °C) and gas-liquid chromatography (Shimadzu GC-14A; Zebron ZB-1 capillary column, i.d. 0.25 mm, length 30 m, at 50–250 °C). The amount of hydrogen gas formed during the reaction was monitored with a Shimadzu 8AIT gas chromatograph (Molecular Sieves 5A column, i.d. 3 mm, length 2 m, at 50 °C) with a TC detector.

Powder XRD patterns were recorded using Cu Kα radiation (40 kV, 40 mA) and a carbon monochromator (Shimadzu XRD-6100). Scanning electron microscopy (SEM) (JEOL, JSM-5500S) was performed to measure the size and morphology of the crystalline samples. Transmission electron microscopy (TEM) was performed on a JEOL Model JEM-3010 system at 300 kV, and the powder sample was supported on a Cu microgrid. Temperature-programmed reduction (TPR) was performed with a gas

flow system, using hydrogen (2 vol.% in Ar; atmospheric pressure of 40 cm³ min⁻¹) fed into a quartz tube containing the catalyst. The tube was heated in an electric furnace at a heating rate of 10 °C min⁻¹ and the amount of H₂ consumed was monitored with a TC detector. XP spectra of the catalysts were recorded using a ULVAC-PHI 5500MT system equipped with a hemispherical energy analyzer. Reduced catalysts without passivation were mounted on indium foil in a glovebox (Korea Kiyon, O₂ < 0.5 ppm) and then transferred to an XPS analysis chamber without any contact with air. The spectra were measured at room temperature using Mg K α radiation (1254 eV) generated by an X-ray tube operating at 15 kV, 400 W. The electron take-off angle was set at 45 deg. The residual gas pressure during data acquisition was less than 1 \times 10⁻⁸ Torr (1 Torr; 133.3 N m⁻²). Binding energies were referenced to the C 1s level of residual graphitic carbon [38]. Inductively coupled plasma atomic emission spectroscopy (ICP/AES) used a Hitachi High-Tech Science PS7800 (sequential type ICP optical emission spectrometer).

4.3 Results and discussion

4.3.1 Effects of titania support on the dehydrogenative synthesis of 2-phenyl benzoxazole

The activities of various titania-supported iridium catalysts for the reaction of 2-aminophenol (1 mmol) with benzyl alcohol (0.41 mL) were examined at 80 to 170 °C for 18 h in the presence of mesitylene (2 cm³) as a solvent (Eq. 1 in Table 1). Table 1 shows the results of the reactions in the presence of 1.0 mol% Ir titania-supported iridium catalysts prepared using Ir(acac)₃ as the iridium source. All catalysts were used after calcination at 400 °C in air followed by reduction at 500 °C in a hydrogen stream.

Anatase and rutile are denoted as (A) and (R) in Table 1, respectively. XRD revealed that the titania supports in the catalysts had both anatase and rutile structures (Fig. 1) [39]. The diffraction peak of the iridium phase was not observed in the XRD patterns due to the low loading weight. FE-SEM images of the catalysts (Fig. 2) showed that Ir/TIO-7, 9, and 10 consisted of small aggregated particles of the supported catalysts, whereas Ir/TIO-6, 8, and 11 formed larger aggregates.

Table 1. Effects of various titania supports on the activity of the iridium catalysts

prepared from Ir(acac)₃.

Reaction scheme: 1a (1.0 mmol) + 2a (4.0 mmol) $\xrightarrow[\text{Mesitylene (2 cm}^3\text{)}]{\text{Ir/TiO}_2 \text{ (from Ir(acac)}_3\text{) (2.0 wt\%, 1.0 mol\% as Ir), 18 h, under Ar}}$ 3aa + 2H₂ + H₂O (1)

Reaction	Support ^a	Crystal structure	S _{BET} of support (m ² g ⁻¹)	Temp. (°C)	3aa Yield (%)
1	TIO-4	A/R	50	170	9
2	TIO-6	R	100	170	48
3	TIO-7	A	270	80	5
4				100	5
5				120	13
6				130	15
7				150	35
8				170	58
9	P _{0.02} -TIO-	A	/	130	16
10	7 ^b			150	22
11				170	29
12	TIO-8	A	338	130	13

13				150	20
14				170	68
15	TIO-9	A	300	130	11
16				150	25
17				170	58
18	TIO-10	A	100	130	16
19				150	36
20				170	74
21	TIO-11	A/R	97	130	6
22				150	6
23				170	7
24	PA-135-	A	66	130	17
25	3.5 ^c			150	6
26				170	8
27	SiO ₂		130	170	trace
28	Al ₂ O ₃		180	170	trace
29	CeO ₂		92	170	trace

^a A: Anatase, R: rutile, A/R and R/A: mixtures, predominantly anatase and predominantly rutile, respectively. ^b P_{0.02}-TIO-7 is phosphorus-modified TIO-7 with phosphoric acid (P/Ti molar ratio of 0.02) [33]. ^c PA-135-3.5 is {010}/{101}-faceted anatase developed by our group [40–43].

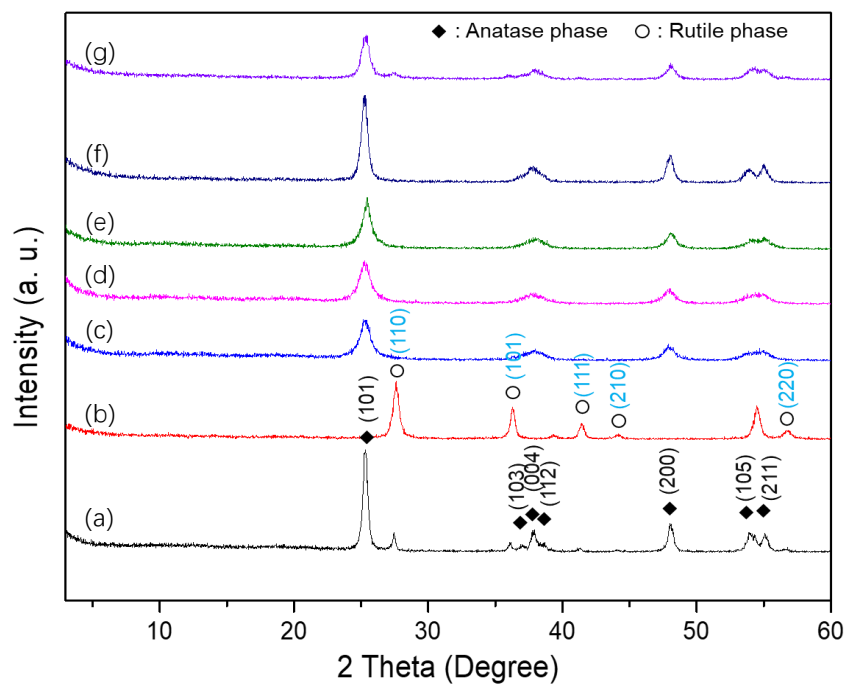


Fig. 1 XRD patterns of the iridium catalysts supported on (a) JRC-TIO-4, (b) JRC-TIO-6, (c) JRC-TIO-7, (d) JRC-TIO-8, (e) JRC-TIO-9, (f) JRC-TIO-10, (g) JRC-TIO-11.

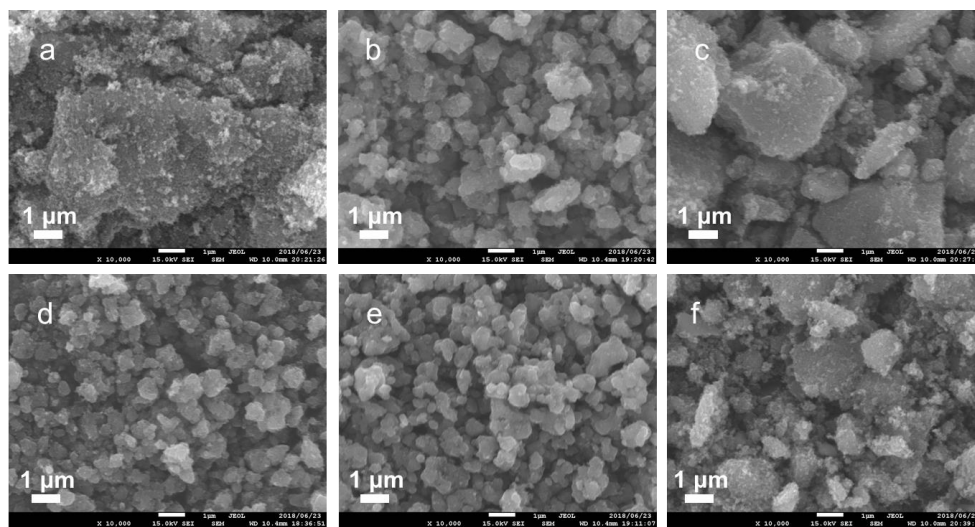


Fig. 2 FE-SEM images of the catalyst samples (2.0 wt% as Ir), (a) Ir/JRC-TIO-6, (b) Ir/JRC-TIO-7, (c) Ir/JRC-TIO-8, (d) Ir/JRC-TIO-9, (e) Ir/JRC-TIO-10, (f) Ir/JRC-TIO-11. Iridium catalysts were prepared from Ir(acac)₃.

The results of reactions 3 to 8 indicate that reaction of 2-aminophenol requires a relatively high temperature of 170 °C, markedly different to the dehydrogenative synthesis of benzimidazoles which smoothly proceeds at 100 to 120 °C [27,30,31]. JRC-TiO titania catalysts supported on anatase (TIO-7, 8, 9, 10) showed higher activities than those on TIO-4 (P-25 equivalent) and 11 which contained mixtures of anatase and rutile. Ir/TIO-10 catalyst achieved almost 100% conversion of 2-aminophenol (**1a**) at 170 °C. Our previous study of the dehydrogenative synthesis of benzimidazole [31] showed that the iridium species were not homogeneously loaded on TIO-4, and formation of relatively large iridium nanoparticles was considered to be responsible for the low activity of these catalysts. The catalyst supported on rutile TIO-6 showed significant activity (reaction 2): This is in accordance with our previous study, which shows excellent activity of rutile-supported catalysts for the dehydrogenative reactions [31]. However, the BET surface area obviously made a minor contribution to catalyst activity. Reactions 9-11 suggested surface modification of titania by phosphoric acid was not effective, but has a positive effect for the hydrogen transfer synthesis of benzimidazole [33]. The {010}/{101}-faceted anatase was developed by our group [40–43] and acts as an effective catalyst support for the synthesis of benzimidazole via hydrogen transfer [32]. However, this anatase was not effective on the present reaction as shown in reactions 24-26. In addition, the iridium catalysts supported on other metal oxides such as silica, alumina, and ceria were inactive (reactions 27-29), implying the titania supports had critical effects for the present catalysis. Conversions of **1a** in the presence of the Ir/SiO₂, Ir/Al₂O₃, and Ir/CeO₂ catalysts at 170 °C were 31%, 36% and 34%, respectively. Conversion of benzyl alcohol **2a** was negligible for the Ir/SiO₂ and Ir/CeO₂-catalyzed reactions, while only 15% with Ir/Al₂O₃ and the formation of a small

amount of 2-(benzylideneamino)phenol was detected by GC-MS. No benzaldehyde was detected with these three catalysts.

To investigate the catalytic efficiency of iridium species for the dehydrogenative reactions, the activities of TIO-10-supported catalysts with different iridium loadings were compared at 130, 150 and 170 °C, respectively. Here, the weight of the catalysts was fixed at 100 mg, so the substrate to catalyst (S/C) ratio decreased with higher loading. Fig. 3 shows the yield of the desired product, **3aa**, linearly increased with higher loading at 130 °C and 150 °C. The yield markedly increased up to 1.0 wt% (0.50 mol% as Ir) at 170 °C, but increased less significantly over 1.0 wt%, indicating that the activity per unit amount of iridium species was highest at around 1.0 wt% or lower.

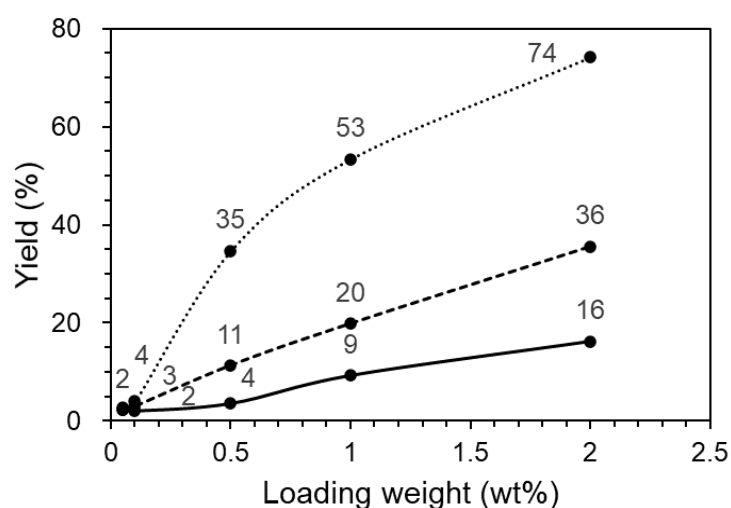


Fig. 3 Correlation between the iridium loading on TIO-10 and yield of product **3aa** from 2-aminophenol (**1a**, 1.0 mmol) with benzyl alcohol (**2a**, 4.0 mmol). Numbers in the figure show the yields of **3aa**. Ir/TIO-10 catalysts were prepared using Ir(acac)₃ as an iridium source. Reactions were performed in the presence of the iridium catalyst (100 mg) in mesitylene 2 cm³, 18 h, in Ar.

4.3.2 Effect of [Ir(cod)Cl]₂ as an Ir precursor on the catalytic activity

To further optimize the activity of the catalyst, [Ir(cod)Cl]₂ was used as the iridium source in the catalyst preparation (Eq. 2 in Table 2). Table 2 shows the activities of these Ir/TiO-10 catalysts with different iridium loadings for the dehydrogenative synthesis of 2-phenylbenzoxazole. The weight of the catalysts was fixed at 100 mg. The yield of **3aa** monotonically increased with higher iridium loading at 170 °C, and the highest yield of **3aa**, 81%, was achieved with Ir (2.0 wt%)/TiO-10 catalyst (1.0 mol% as Ir). However, 1.0 wt%-loaded catalysts showed higher activity than 2.0 wt%-loaded catalysts at the same amount of Ir species (0.50 mol% Ir) as shown in reactions 9 and 10 of Table 2.

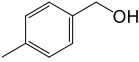
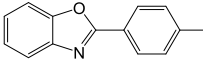
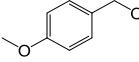
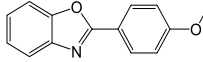
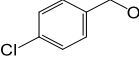
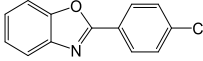
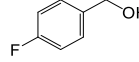
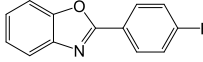
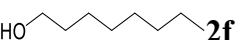
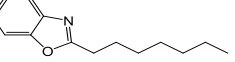
Table 2. Activities of the Ir/TiO-10 catalysts prepared using [Ir(cod)Cl]₂ for the synthesis of 2-phenylbenzoxazole.

Reaction scheme showing the synthesis of 2-phenylbenzoxazole (**3aa**) from 2-aminophenol (**1a**) and benzyl alcohol (**2a**). The reaction is catalyzed by Ir/TiO₂ (from [Ir(cod)Cl]₂, 100 mg) in mesitylene (2 cm³) for 18 h under Ar. The products are 2-phenylbenzoxazole (**3aa**), 2H₂, and H₂O (2).

Reaction	Ir loading (wt%, mol% as Ir in the parenthesis)	Temperature (°C)	Yield of 3aa (%)
1	0.10 (0.050)	150	7
2		160	8
3		170	6
4	0.20 (0.10)	160	10
5		170	17
6	0.4 (0.20)	160	16

high yields using 2.0 wt% catalyst. Simple aliphatic alcohol, octan-1-ol, was also applicable and the desired product was formed in moderate yield. Unfortunately, reaction of **1a** with methanol at 100 °C (bath temp.) did not produce any benzoxazole.

Table 3. Activities of Ir/TIO-10 for the synthesis of 2-substituted benzoxazole.

Reaction	Substrate	Product	Yield (%)
1	 2b	 3ab	68
2	 2c	 3ac	99
3	 2d	 3ad	90
4	 2e	 3ae	99
5	 2f	 3af	40

Reaction conditions: 2-Aminophenol (**1a**, 1.0 mmol), alcohols (1.5 mmol), mesitylene (1 cm³), Ir/TIO-10 (prepared using [Ir(cod)Cl]₂ as an iridium source, 2.0 wt%, Ir: 1.0 mol%, 100 mg), 20 h, at 170 °C, in Ar.

Fig. 4 shows the effect of hot filtration on the time-course of the reaction of **1a** and **2a** to form **3aa** over the Ir/TIO-10 catalyst at 170 °C. The catalytic reaction proceeded smoothly, and the yield of the product increased linearly with time increasing without hot filtration. The yield of the product showed almost no substantial increase after reaction for 18 hours. This result suggests that the Ir/TIO-10 catalyst has high and steady activity. To examine whether the catalysis occurs on the surface of the solid catalysts, the effects of removal of the solid catalysts by hot filtration through a PTFE filter (pore size 0.45 μm) were examined after the reaction was continued for 1 h.

Formation of **3aa** was completely stopped by the hot filtration. In addition, inductively coupled plasma atomic emission spectroscopy (ICP/AES) analysis indicated that leaching of iridium into the solution was negligible. These results suggest the heterogeneous nature of the present catalysis.

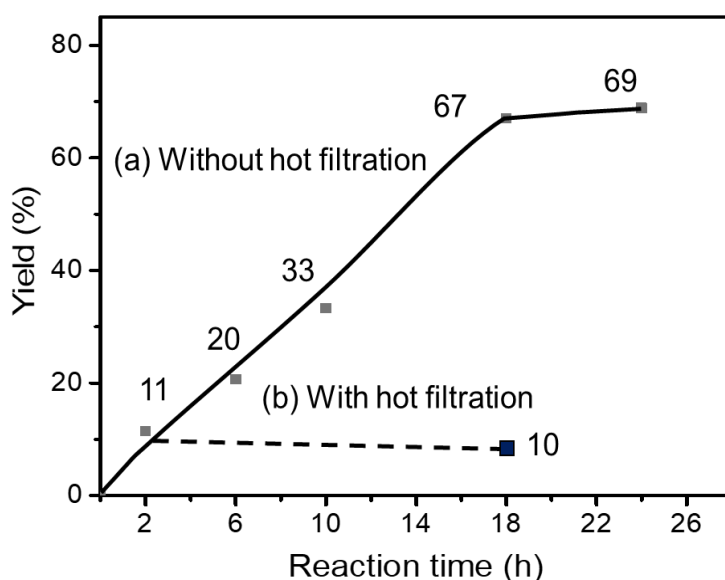
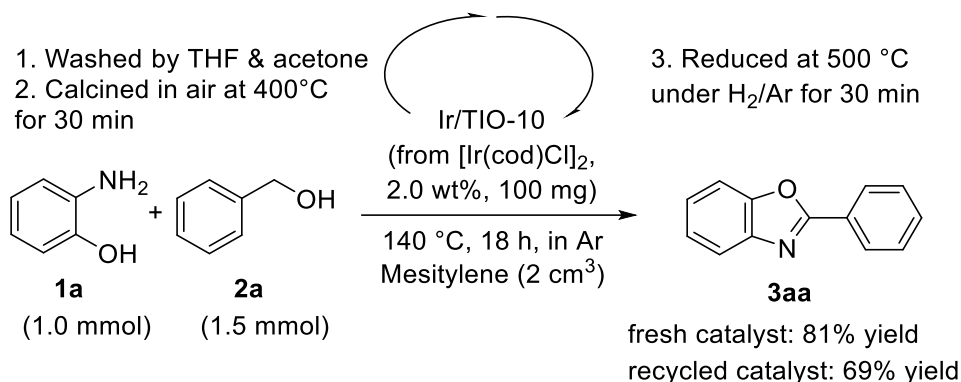


Fig. 4 The effect of hot filtration on the yield of **3aa** over Ir/TIO-10.

Reaction conditions: 2-Aminophenol (**1a**, 1.0 mmol), benzyl alcohol (**2a**, 1.5 mmol), mesitylene (1 cm³), Ir/TIO-10 (prepared using [Ir(cod)Cl]₂, 1.0 wt%, 0.50 mol% as Ir, 100 mg), at 170 °C, in Ar.

To investigate the reusability of the catalyst, the used Ir/TIO-10 catalyst (prepared using [Ir(cod)Cl]₂, 2.0 wt%, 1.0 mol% as Ir) was simply separated from the reaction solution by centrifugation and washed with THF after reaction at 170 °C for 18 h (**3aa** yield; 81%). The resulting powder was reduced in a stream of 2% H₂/Ar gas at 500 °C for 30 min and passivated at 50 °C for 5 min as usual. The treated catalyst gave **3aa** in 69% yield, indicating the catalyst is basically recyclable (Scheme 2). Further optimization of the recovery procedure is ongoing.



Scheme 2. Recycle test of the catalyst.

Fig. 5 shows TEM images of TIO-10-supported iridium catalysts prepared from Ir(acac)₂ and [Ir(cod)Cl]₂, respectively, after reduction at 500 °C for 30 min. Most TIO-10 secondary particles were in the range of 300-400 nm diameter as shown in Fig. 5(a), and consisted of many smaller particles with 10-20 nm diameter. Fig. 5(b) and (c) and the iridium particle distribution histograms indicate the formation of iridium nanoparticles of less than 2 nm diameter on the surfaces of both Ir/TIO-10 catalysts, which may explain the high activity of the Ir/TIO-10 catalyst. Note that much smaller iridium nanoparticles were formed on the surface of TIO-7 than on TIO-10 (see Fig. 6), as previously reported [32]. The size effect of metal nanoparticles is well known in catalysis [44]. The activity of the catalyst is significantly promoted by decreasing the size of metal nanoparticles, probably because the smaller nanoparticles have higher surface area, more exposed surface atoms, and more surface defects, or affect the surface atomic structure, electronic structure, and quantum size effect [45]. However, iridium nanoparticles show different contradictory effects in specific catalytic reactions [46], as this catalyst does not comply with the expected association of smaller size and greater activity, because the iridium sub-nano cluster has stronger CO adsorption than iridium single atoms, thus favoring the oxidation of CO with higher TOF [31].

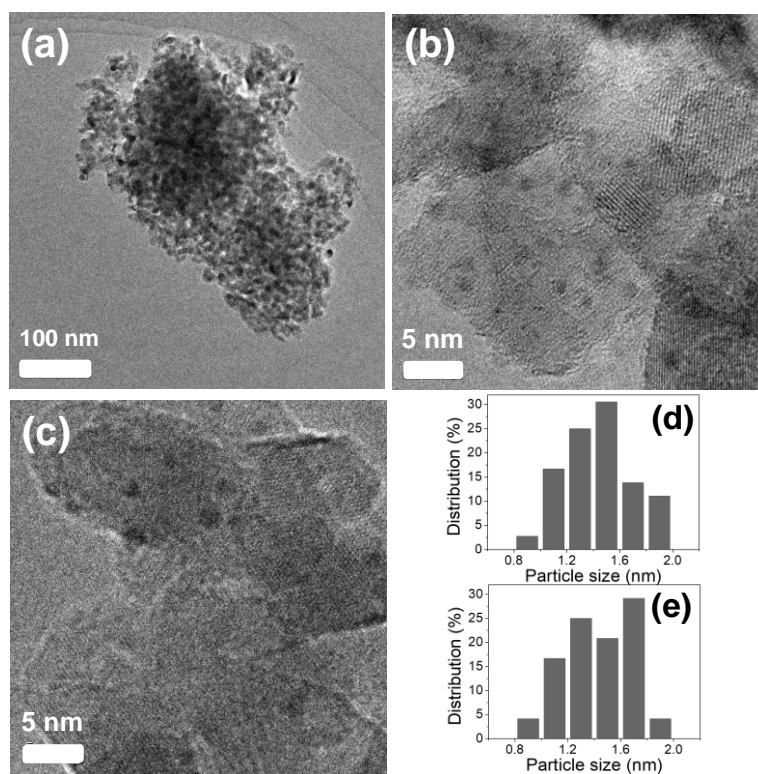


Fig. 5 (a), (b) TEM images and (d) Ir particle size distribution of Ir/TiO-10 (2.0 wt%) prepared using Ir(acac)₃ and (c), (e) for Ir/TiO-10 (1.0 wt%) prepared using [Ir(cod)Cl]₂.

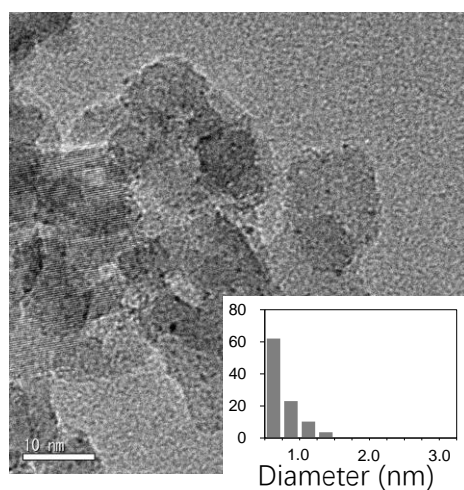


Fig. 6 TEM image of Ir/TiO-7 (2.0 wt%). Iridium catalyst was prepared from Ir(acac)₃. Inset shows the iridium particle distribution histogram [32].

The reduction characteristics of the catalysts were studied by hydrogen

temperature-programmed reduction (H_2 -TPR). Fig. 7 shows the H_2 -TPR profiles of the present Ir/TiO₂ catalysts. The TPR profile of 2 wt% Ir/TIO-10 catalyst prepared using [Ir(cod)Cl]₂ showed a clear-defined peak at 123 °C, which was identified as reduction of the iridium species, and a broad peak around 250 °C to 500 °C which was associated with reduction of the surface Ti⁴⁺ species to Ti³⁺. Significant shift of the peak towards high temperature (ca. 140 °C) for the Ir/TIO-7 catalyst suggested stronger interaction between the iridium species and TIO-7 surface. The lower reducibility of iridium species on TIO-7 is consistent with the lower CO adsorption, as discussed above [31]. Two reduction peaks appeared at around 200 °C for Ir/TIO-10 prepared using Ir(acac)₃, but no peaks in this region for the catalyst prepared from [Ir(cod)Cl]₂. Formation of such less reducible iridium species on the surface may account for the lower activities of Ir/TIO-10 catalysts prepared from Ir(acac)₃ as well as the Ir/TIO-7 catalyst (see Tables 1 and 2).

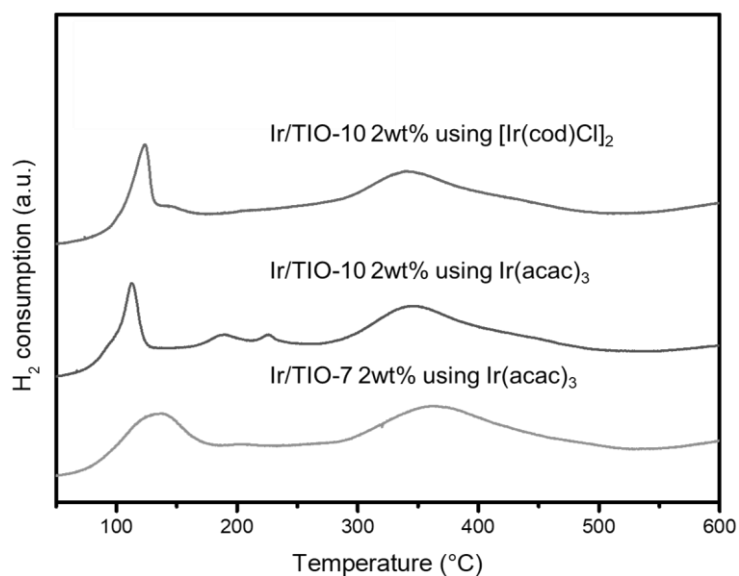


Fig. 7 Effects of supports and iridium sources on the H_2 -TPR profiles.

The Ir 4f XP spectrum of the fully reduced Ir/TIO-10 catalyst (prepared from

[Ir(cod)Cl]₂, 1.0 wt%) is shown in Fig. 8. Considering the severe overlapping of the Ti 3s band, the Ir 4f spectrum consists of bands at 60.3 eV and 61.8 eV, which were assigned to metallic Ir⁰ (60.3 eV) and intermediate oxidation state Ir³⁺ (61.8 eV), respectively, indicating iridium on titania is partially reduced. The ratio of Ir⁰ to Ir³⁺ was ca. 0.7 to 0.3, which compares well to the reduced Ir/TIO-7 catalysts in which partially oxidized iridium species are more predominant [31]. This result suggests the reduced iridium species Ir⁰ is responsible for the catalytic activity.

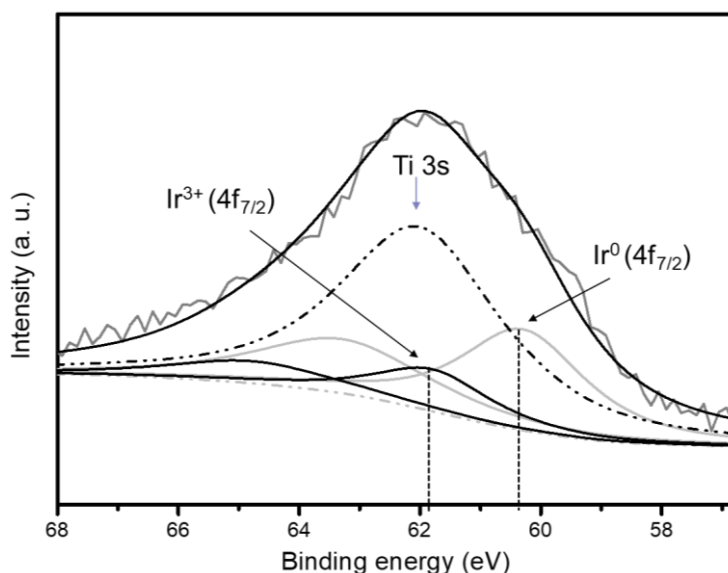
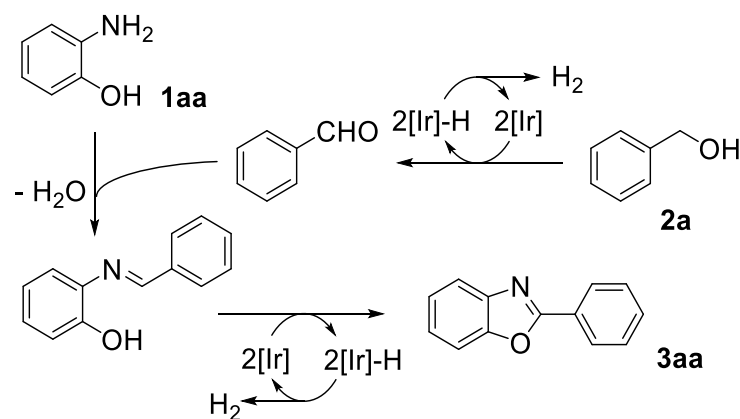


Fig. 8 XP spectra of Ir 4f of Ir/TIO-10 (prepared from [Ir(cod)Cl]₂, 1.0 wt%)

Previous investigations of acceptor-less dehydrogenative synthesis of benzimidazoles revealed that fully-reduced, well-dispersed small iridium nanoparticles are responsible for the excellent catalytic activity [30,31,33]. The iridium nanoparticles were smaller and better dispersed on titania than on other oxides such as silica or alumina [30]. In addition, the crystalline structure of titania affected both the size and reducibility of surface iridium species [31]. The present study showed suitable interaction between iridium species and the TIO-10 surface would enable the formation

of very small, well-dispersed, highly-reduced iridium nanoparticles, so further detailed study is intended.

Scheme 3 shows a possible reaction mechanism for the dehydrogenative synthesis of benzoxazole, as previously proposed [12]. The reaction is initiated by the abstraction of hydrogen from alcohol to form a corresponding aldehyde, and successive reaction of this aldehyde with 2-aminophenol proceeds to give an imine intermediate, followed by dehydrogenative cyclization to form benzoxazole. Our GC measurement showed that two equivalents of molecular hydrogen were formed after the reaction finished. Dehydrogenative synthesis of benzimidazoles proceeds via a similar mechanism at a significantly lower temperature around 100 °C [31]. The previous computational study on the iridium complex-catalyzed N-alkylation of amines by alcohols revealed that dissociation of the product from the metal, required to regenerate the catalyst, is difficult, so this step may account for the high temperature required [47]. Similarly, dissociation of the products from the catalytically active sites may be responsible for the high temperature required in the present system. Further detailed kinetic study on the reaction mechanism is ongoing.



Scheme 3. Proposed reaction mechanism.

4.4 Conclusion

The present study developed titania-supported iridium catalysts with excellent activity for the dehydrogenative synthesis of benzoxazoles from 2-aminophenol and primary alcohols. The titania supports had marked effects on the activity of iridium catalysts, with catalysts supported on TIO-10 showing the highest activity. The use of $[\text{Ir}(\text{cod})\text{Cl}]_2$ as an iridium precursor instead of $\text{Ir}(\text{acac})_3$ further promoted catalytic activity. The present catalysts could be recycled without significant loss of activity. The hot filtration test and ICP results clearly indicated the heterogeneous nature of the present catalysis process. The catalysts reacted various benzylic alcohols with both electron-withdrawing and donating substituents as well as a simple aliphatic primary alcohol. Detailed characterization of the catalysts revealed that highly-dispersed, well-reducible iridium particles in the range of 1-2 nm predominantly formed on the surface of the Ir/TIO-10 catalysts were responsible for the high activity.

4.5 References

- [1] T. Hisano, M. Ichikawa, K. Tsumoto, M. Tasaki, Synthesis of Benzoxazoles, Benzothiazoles and Benzimidazoles and Evaluation of Their Antifungal, Insecticidal and Herbicidal Activities, *Chem. Pharm. Bull.* 30 (1982) 2996–3004.
- [2] C.S. Demmer, L. Bunch, Benzoxazoles and oxazolopyridines in medicinal chemistry studies, *Eur. J. Med. Chem.* 97 (2015) 778–785.
- [3] N. Aggarwal, A. Kaur, K. Anand, H. Kumar, S. Wakode, Biologically active Benzoxazole: A comprehensive review, *Int. J. Pharm. Sci. Res.* 2 (2017) 2455–4685.
- [4] R.V. Kumar, Synthetic strategies towards benzoxazole ring systems: A review, *Asian J. Chem.* 16 (2004) 1241–1260.
- [5] Y. Wang, K. Sarris, D.R. Sauer, S.W. Djuric, A simple and efficient one step synthesis of benzoxazoles and benzimidazoles from carboxylic acids, *Tetrahedron Lett.* 47 (2006) 4823–4826.
- [6] S.M. Inamdar, V.K. More, S.K. Mandal, CuO nano-particles supported on

- silica, a new catalyst for facile synthesis of benzimidazoles, benzothiazoles and benzoxazoles, *Tetrahedron Lett.* 54 (2013) 579–583.
- [7] P.B. Gorepatil, Y.D. Mane, V.S. Ingle, Samarium(III) triflate as an efficient and reusable catalyst for facile synthesis of benzoxazoles and benzothiazoles in aqueous medium, *Synlett.* 24 (2013) 2241–2244.
- [8] Y. Endo, J.E. Bäckvall, Biomimetic oxidative coupling of benzylamines and 2-aminophenols: Synthesis of benzoxazoles, *Chem. - A Eur. J.* 18 (2012) 13609–13613.
- [9] T. Kondo, S. Yang, K.-T. Huh, M. Kobayashi, S. Kotachi, Y. Watanabe, Ruthenium Complex-Catalyzed Facile Synthesis of 2-Substituted Benzoxazoles, *Chem. Lett.* 20 (1991) 1275–1278.
- [10] A.J. Blacker, M.M. Farah, M.I. Hall, S.P. Marsden, O. Saidi, J.M.J.J. Williams, Synthesis of benzazoles by hydrogen-transfer catalysis, *Org. Lett.* 11 (2009) 2039–2042.
- [11] A.H.M. Elwahy, M.R. Shaaban, Synthesis of heterocycles and fused heterocycles catalyzed by nanomaterials, *RSC Adv.* 5 (2015) 75659–75710.
- [12] A. Khalafi-Nezhad, F. Panahi, Ruthenium-catalyzed synthesis of benzoxazoles using acceptorless dehydrogenative coupling reaction of primary alcohols with 2-aminophenol under heterogeneous conditions, *ACS Catal.* 4 (2014) 1686–1692.
- [13] J. Tang, Y. Cao, F. Ruan, F. Li, Y. Jin, M.N. Ha, X. Han, Q. Ke, New Approach for Controllable Synthesis of N-MnOx Microflowers and Their Superior Catalytic Performance for Benzoxazole Synthesis, *Ind. Eng. Chem. Res.* 59 (2020) 9408–9413.
- [14] D. Khalili, A.R. Banazadeh, Graphene oxide as a heterogeneous reagent promoted synthesis of 2-substituted 1,3-benzazoles in water, *Bull. Chem. Soc. Jpn.* 88 (2015) 1693–1706.
- [15] F. Ferlin, M.K. Van Der Hulst, S. Santoro, D. Lanari, L. Vaccaro, Continuous flow/waste-minimized synthesis of benzoxazoles catalysed by heterogeneous manganese systems, *Green Chem.* 21 (2019) 5298–5305.
- [16] Y.L. Lai, J.S. Ye, J.M. Huang, Electrochemical Synthesis of Benzazoles from Alcohols and o-Substituted Anilines with a Catalytic Amount of CoII Salt, *Chem. - A Eur. J.* 22 (2016) 5425–5429.
- [17] M. Wu, X. Hu, J. Liu, Y. Liao, G.J. Deng, Iron-catalyzed 2-arylbenzoxazole formation from o-nitrophenols and benzylic alcohols, *Org. Lett.* 14 (2012) 2722–2725.
- [18] L. Tang, X. Guo, Y. Yang, Z. Zha, Z. Wang, Gold nanoparticles supported on titanium dioxide: An efficient catalyst for highly selective synthesis of benzoxazoles and benzimidazoles, *Chem. Commun.* 50 (2014) 6145–6148.
- [19] P. Laszlo, Catalysis of Organic Reactions by Inorganic Solids, *Acc. Chem. Res.* 19 (1986) 121–127.
- [20] Y. Izumi, M. Onaka, Organic Syntheses Using Aluminosilicates, *Adv. Catal.*

- 38 (1992) 245–282.
- [21] K. Kaneda, Cation-exchanged montmorillonites as solid acid catalysts for organic synthesis, *Synlett.* (2007) 999–1015.
- [22] M. Tada, Y. Iwasawa, Advanced design of catalytically active reaction space at surfaces for selective catalysis, *Coord. Chem. Rev.* 251 (2007) 2702–2716.
- [23] L. Yin, J. Liebscher, Carbon-carbon coupling reactions catalyzed by heterogeneous palladium catalysts, *Chem. Rev.* 107 (2007) 133–173.
- [24] A. Corma, H. Garci, Supported gold nanoparticles as catalysts for organic reactions, *Chem. Soc. Rev.* 37 (2008) 2096–2126.
- [25] K. Wada, S. Hosokawa, M. Inoue, Development of Ceria-Supported Ruthenium Catalysts Effective for Various Synthetic Reactions, *Catal. Surv. from Asia.* 15 (2011) 1–11.
- [26] K. Wada, H. Miura, S. Hosokawa, M. Inoue, Development of ceria-supported ruthenium catalysts for green organic transformation processes, *J. Japan Pet. Inst.* 56 (2013) 69–79.
- [27] K. Wada, H. Yu, Q. Feng, Titania-supported iridium catalysts for dehydrogenative synthesis of benzimidazoles, *Chinese Chem. Lett.* 31 (2020) 605–608.
- [28] S.M.A. Hakim Siddiki, T. Toyao, K.I. Shimizu, Acceptorless dehydrogenative coupling reactions with alcohols over heterogeneous catalysts, *Green Chem.* 20 (2018) 2933–2952.
- [29] S. Tsukada, K. Wada, H. Miura, S. Hosokawa, R. Abe, M. Inoue, Phosphine-stabilized, oxide-supported rhodium catalysts for highly efficient silylative coupling reactions, *Res. Chem. Intermed.* 41 (2015) 9575–9586.
- [30] K. Tateyama, K. Wada, H. Miura, S. Hosokawa, R. Abe, M. Inoue, Dehydrogenative synthesis of benzimidazoles under mild conditions with supported iridium catalysts, *Catal. Sci. Technol.* 6 (2016) 1677–1684.
- [31] T. Fukutake, K. Wada, G.C. Liu, S. Hosokawa, Q. Feng, Striking effects of a titania support on the low-temperature activities of Ir catalysts for the dehydrogenative synthesis of benzimidazole and indole, *Catal. Today.* 303 (2018) 235–240.
- [32] T. Fukutake, K. Wada, H. Yu, S. Hosokawa, Q. Feng, Development of titania-supported iridium catalysts with excellent low-temperature activities for the synthesis of benzimidazoles via hydrogen transfer, *Mol. Catal.* 477 (2019) 110550.
- [33] H. Yu, K. Wada, T. Fukutake, Q. Feng, S. Uemura, K. Isoda, T. Hirai, S. Iwamoto, Effect of phosphorus-modification of titania supports on the iridium-catalyzed synthesis of benzimidazoles, *Catal. Today.* 375 (2021) 410–417.
- [34] J. Lu, C. Aydin, N.D. Browning, B.C. Gates, Hydrogen activation and metal hydride formation trigger cluster formation from supported iridium complexes, *J. Am. Chem. Soc.* 134 (2012) 5022–5025.
- [35] A. Yoshida, Y. Mori, T. Ikeda, K. Azemoto, S. Naito, Enhancement of catalytic

- activity of Ir/TiO₂ by partially reduced titanium oxide in aerobic oxidation of alcohols, *Catal. Today*. 203 (2013) 153–157.
- [36] C. Chaudhari, S.M.A.H. Siddiki, K.I. Shimizu, Acceptorless dehydrogenative synthesis of benzothiazoles and benzimidazoles from alcohols or aldehydes by heterogeneous Pt catalysts under neutral conditions, *Tetrahedron Lett.* 56 (2015) 4885–4888.
- [37] P.K. Samanta, S. Ray, T. Das, S.H. Gage, M. Nandi, R.M. Richards, P. Biswas, Palladium oxide nanoparticles intercalated mesoporous silica for solvent free acceptorless dehydrogenation reactions of alcohols, *Microporous Mesoporous Mater.* 284 (2019) 186–197.
- [38] K.D.M. J.F., S. W.F., S. P.E., Bomben, *Handbook of X-ray Photoelectron Spectroscopy*, 1992.
- [39] N. Murakami, O.O.P. Mahaney, R. Abe, T. Torimoto, B. Ohtani, Double-beam photoacoustic spectroscopic studies on transient absorption of titanium(IV) oxide photocatalyst powders, *J. Phys. Chem. C*. 111 (2007) 11927–11935.
- [40] P. Wen, H. Itoh, Q. Feng, Preparation of nanoleaf-like single crystals of anatase-type TiO₂ by exfoliation and hydrothermal reactions, *Chem. Lett.* 35 (2006) 1226–1227.
- [41] P. Wen, H. Itoh, W. Tang, Q. Feng, Single nanocrystals of anatase-type TiO₂ prepared from layered titanate nanosheets: Formation mechanism and characterization of surface properties, *Langmuir*. 23 (2007) 11782–11790.
- [42] C. Chen, G.A. Sewvandi, T. Kusunose, Y. Tanaka, S. Nakanishi, Q. Feng, Synthesis of {010}-faceted anatase TiO₂ nanoparticles from layered titanate for dye-sensitized solar cells, *CrystEngComm*. 16 (2014) 8885–8895.
- [43] C. Chen, Y. Ikeuchi, L. Xu, G.A. Sewvandi, T. Kusunose, Y. Tanaka, S. Nakanishi, P. Wen, Q. Feng, Synthesis of [111]- and {010}-faceted anatase TiO₂ nanocrystals from tri-titanate nanosheets and their photocatalytic and DSSC performances, *Nanoscale*. 7 (2015) 7980–7991.
- [44] F. Yang, D. Deng, X. Pan, Q. Fu, X. Bao, Understanding nano effects in catalysis, *Natl. Sci. Rev.* 2 (2015) 183–201.
- [45] C. Zhu, S. Fu, Q. Shi, D. Du, Y. Lin, Single-Atom Electrocatalysts, *Angew. Chemie - Int. Ed.* 56 (2017) 13944–13960.
- [46] J. Lin, Y. Chen, Y. Zhou, L. Li, B. Qiao, A. Wang, J. Liu, X. Wang, T. Zhang, More active Ir subnanometer clusters than single-atoms for catalytic oxidation of CO at low temperature, *AIChE J.* 63 (2017) 4003–4012.
- [47] D. Balcells, A. Nova, E. Clot, D. Gnanamgari, R.H. Crabtree, O. Eisenstein, Mechanism of homogeneous iridium-catalyzed alkylation of amines with alcohols from a DFT study, *Organometallics*. 27 (2008) 2529–2535.

Chapter V Summary

The synthesis protocol of nitrogen-containing chemicals from amines or ammonia and alcohols has attracted extensive attention from academic and industrial viewpoints. Various transition metal catalysts, especially homogeneous iridium complex catalysts, had been reported to catalyze the synthesis of a wide range of nitrogen-containing compounds via dehydrogenative or transfer hydrogenation (borrowing hydrogen) mechanisms. On the other hand, reports on the heterogeneous catalysts for these reactions were limited. Since our lab successfully developed titania-supported iridium catalysts effective for the synthesis of benzimidazoles via both dehydrogenative and hydrogen-transfer routes, application of these catalysts to other reactions was expected as well as the further improvement of the catalytic activities.

In the present study, titania supported iridium catalysts were prepared by a facile impregnation method. The catalysts are well applied to synthesize three valuable nitrogen-containing compounds: tertiary amines, benzimidazoles, and benzoxazoles from ammonia/amines and alcohols. The catalytic reactions proceeded efficiently under mild conditions via hydrogen transfer or dehydrogenation route and produced only water (and hydrogen) as byproducts, which are in accord with the green chemistry principles. These results reveal that the titania-supported iridium catalyst has extraordinary potential in heterogeneous catalysis. The main results of this study are summarized as follows:

In chapter I, the general background and progress concerning the present study were reviewed. The conception and evolution of green chemistry and its practices were elucidated. The features and application of transition metals iridium catalysts, and

titania support in catalytic organic synthesis, were introduced. The developments and recent advances in the synthesis of our target product catalyzed by various catalyst systems were described. Based on these studies, we proposed the purposes of the present study.

Chapter II describes the development of titania-supported iridium catalysts with high loading weight for the catalytic synthesis of amines by the multialkylation of aqueous ammonia with primary and secondary alcohols. Neither additional solvent nor high pressure or reduction atmosphere was required, and the reaction could be performed readily in an air or argon atmosphere at relatively low temperature without harmful output. Over Ir/TiO₂-10 catalyst, tertiary and secondary amines were synthesized in a yield of over 90% within 6 hours. To the best of our knowledge, this is the first example of a heterogeneous system that works under such very simple reaction conditions. Moreover, the crystal structure of titania supports of the iridium catalysts markedly affected their activities. Namely, the use of anatase as support showed the best results. Detailed characterization of the catalysts revealed that highly dispersed partially-reduced iridium nanoparticles of less than 2 nm in diameter would be responsible for the excellent activity. The NH₃-TPD and in-situ FTIR studies evidenced the presence of titania support further improved the adsorption of ammonia. The formation of the product smoothly proceeded in large-scale reactions. The catalyst could be easily recovered and reused at least five times without a significant loss of activity. The developed catalysis system surely meets the requirements of green chemistry principles.

Chapter III demonstrates the promotional effects of the use of phosphorus-modified titania as support of the catalysts for the synthesis of benzimidazoles. The

phosphorus-modified titania supports were prepared by the hydrothermal and wet impregnation methods. The use of these modified supports resulted in a marked enhancement of the catalytic activity towards the synthesis of benzimidazoles from 2-nitroaniline and primary alcohols via hydrogen transfer. The hydrothermal P-doping realized ca. 5 times promotion of the catalytic activity. The modification of high surface area titania such as JRC-TIO-7 with phosphoric acid by wet impregnation also increased the activity of the iridium catalysts. The hot filtration study indicates that the catalysis proceeded heterogeneously. These modified catalysts kept their activity even after the additional supply of the substrate, indicating their fair durability. H₂-TPR study revealed that phosphorus-modification facilitated the formation of iridium species reduced at higher temperatures and would stabilize the state of iridium species suitable for the present catalysis.

In chapter IV, titania-supported iridium catalysts were developed for the dehydrogenative synthesis of benzoxazoles from 2-aminophenol and primary alcohols. The titania supports prominently affected the activity of supported iridium catalysts: The catalysts supported on TIO-10 showing the highest activity. The use of [Ir(cod)Cl]₂ as an iridium precursor instead of Ir(acac)₃ further promoted the catalytic activity. The present catalysts could be recycled without a significant loss of activity. The hot filtration test and ICP results clearly indicated the heterogeneous nature of the present catalysis process. The catalysts enabled the conversion of 2-aminophenol and various benzylic alcohols with both electron-withdrawing and donating substituents as well as a simple aliphatic primary alcohol. The byproducts were only water and molecular hydrogen. Detailed characterization of the catalysts revealed that highly-dispersed, well-reducible iridium particles in the range of 1-2 nm predominantly formed on the

surface of the Ir/TiO-10 catalysts were responsible for the high activity.

As discussed above, titania-supported iridium catalysts that were successfully developed in the present study enable the catalytic synthesis of nitrogen-containing chemicals via hydrogen transfer and dehydrogenation pathways. The present results provide a greener and more economical organic synthetic method for nitrogen-containing chemicals. As expected, iridium catalysts exhibit excellent activity in the N-alkylation of ammonia or amine with alcohols as well as N-heterocyclization. XPS and TEM characterization reveals the high activity of iridium catalyst could be assigned to the high dispersion of iridium nanoparticles with a small diameter less than 2 nm and the suitable valence state of iridium species that were tunable by the selection of titania support.

In addition, titania support also contributed to the activity of iridium catalysts. NH₃-TPD results suggest the presence of weak acid sites on the surface of titania, and the weak adsorption and desorption of ammonia at low temperatures could promote the N-alkylation of ammonia. In-situ FTIR spectra evidenced the efficient adsorption and desorption of ammonia on the catalyst which realized rapid N-alkylation of ammonia with benzylic alcohols. H₂-TPR results indicate that the presence of phosphorus enhanced the interaction between iridium and titania. By means of this strong interaction, titania support promoted the dispersion of iridium species on its surface, thus forming well-dispersed iridium species smaller than 0.5 nm.

Overall, the results described above evidence that titania supported iridium is a promising catalyst for green organic synthesis. The catalyst can be used in hydrogen transfer and dehydrogenation reactions involving activation of N-H bonds and oxidation of alcohols. The particle size and valence state of iridium nanoparticles on

the surface can be controlled by adjusting the iridium loading amount, by choosing suitable titania support, and by modifying the surface of the support, so as to improve their activity to the corresponding reaction. The present results will provide guidance not only for further application of titania-supported iridium catalysts to various reactions but also for the controlled preparation of other supported transition metal catalysts.

In our next stages, we will proceed with the development of heterogeneous catalysis in the following strategies. Firstly, based on the present research results, the titania-supported iridium catalyzed hydrogen transfer route is green and efficient method for the synthesis of N-containing chemicals. The expanding of substrates to other environmentally benign nitrogen source is highly desired and reasonable. Secondly, the strong interaction between metal and support has been disclosed to have a significant effect on the distribution and size of iridium nanoparticles on the support surface. Therefore, the development of a support that effectively promotes the distribution of iridium nanoparticles is an attractive strategy. To this end, we will challenge the application of new materials to iridium heterogeneous catalyst support. Moreover, the application of iridium heterogeneous catalyst in the new green chemical reactions is also worth expecting.

Publications

Publications in journal

1. **H. Yu**, L. Ma, K. Wada, R. Kurihara, Q. Feng, S. Uemura, K. Isoda, Rapid Multialkylation of Aqueous Ammonia with Alcohols by Heterogeneous Iridium Catalyst under Simple Conditions, *ChemCatChem*. 13 (2021) 3588–3593.
2. **H. Yu**, K. Wada, T. Fukutake, Q. Feng, S. Uemura, K. Isoda, T. Hirai, S. Iwamoto, Effect of phosphorus-modification of titania supports on the iridium-catalyzed synthesis of benzimidazoles, *Catal. Today*. 375 (2021) 410–417.
3. **H. Yu**, L. Ma, K. Wada, R. Kurihara, Q. Feng, S. Uemura, K. Isoda, Development of Titania-supported Iridium Catalysts for the Acceptor-less Dehydrogenative Synthesis of Benzoxazoles, *J. Japan Pet. Inst.* 64 (2021) 271–279.
4. K. Wada, **H. Yu**, Q. Feng, Titania-supported iridium catalysts for dehydrogenative synthesis of benzimidazoles, *Chinese Chem. Lett.* 31 (2020) 605–608.
5. T. Fukutake, K. Wada, **H. Yu**, S. Hosokawa, Q. Feng, Development of titania-supported iridium catalysts with excellent low-temperature activities for the synthesis of benzimidazoles via hydrogen transfer, *Mol. Catal.* 477 (2019) 110550.

Conference

1. **余涵**, 和田健司, 福武龍宙, Effect of phosphorus-modified titania supports on the iridium-catalyzed synthesis of benzimidazoles, 第28回キャラクターゼーション講習会, 徳島大学, P-27, 2018/11/27.
2. **H. Yu**, K. Wada, T. Fukutake, Effect of phosphorus-modified titania supports on the iridium-catalyzed synthesis of benzimidazoles, 第123回触媒討論会, 大阪市立

大学, 1P06, 2019/3/20.

3. **H. Yu**, K. Wada, T. Fukutake, Effect of phosphorus-modified titania supports on the iridium-catalyzed synthesis of benzimidazoles, The 17th Korea Japan Symposium on Catalysis, Jeju Korea, YP03, 2019/5/20.
4. **H. Yu**, K. Wada, T. Fukutake, Development of titania-supported iridium catalysts for the synthesis of benzimidazoles: Effects of crystal facet of titania and phosphorous doping, 分子環境相関論サマーセミナー2019, 京都大学, 2019/7/29.
5. **H. Yu**, K. Wada, Q. Feng, Development of titania-supported iridium catalyst for the synthesis of benzoxazoles and trialkylamines, 第 126 回触媒討論会, 静岡大学, 3D01-A1, 2020/9/18
6. **H. Yu**, K. Wada, Q. Feng, Development of titania-supported iridium catalysts for the synthesis of trialkylamines from aqueous ammonia solution or urea, 第 127 回触媒討論会, 千葉大学, 1P03, 2021/3/16

Acknowledgment

The work presented in this thesis would not have been possible without warm assistance and collaboration from many people. The four years spent at Kagawa University will be one of the most priceless memories of my life.

First and foremost, I would like to sincerely thank my supervisor, Prof. **Qi Feng**, for offering me this precious opportunity to pursue a Ph.D. He essentially supported the progress of my doctoral course and provided me with important guidance in scientific research. He is always full of vigor and passion for scientific research. His never-ending exploration for new scientific areas and rigorous scholarship is my lifelong learning example. In those four years, I not only acquired knowledge but also reshaped my faith and purpose in life. Thank you, for always keeping your door open.

I would like to express my sincere thanks to Prof. **Kenji Wada** equally, for leading me into a new area in science. He always took time to patiently teach me various experimental techniques and had helpful discussions. He provided many important instructions for the experiment and supported the progress of the data analysis. He offered me a free space for scientific exploration and guided my efforts and directions productively with his knowledge. Thank you, for always replying to my E-mail at each break of dawn.

Second, I would like to express my heartfelt gratitude to my vice supervisors: Prof. Shinobu Uemura and Associate Prof. Kyosuke Isoda for their valuable advice, necessary support, and enthusiastic assistance to my doctoral study. In addition, I would like to express my special appreciation to Prof. Dengwei Hu (Baoji University of Arts and Sciences) for his recommendation, encouragement, and support throughout my study.

I am grateful to the technicians who guided and supported me in the utilization of the apparatus at Kagawa University. Special thanks to Ms. Ayami Nishioka. I really appreciate your professional technology in electron microscopy. In addition, I would

also like to thank Dr. Ryohsuke Kurihara (Faculty of Medicine) for offering me great help in the experiments and revision of the paper. My special thanks go also to the former and current administrative staff at Kagawa University, and Kagawa Prefecture International Exchange Association, for making great efforts to help foreign students better adapt to the life of studying abroad.

I am pleased to express my sincere thanks to former members of Feng's Lab: Dr. Linfeng Xu, Dr. Wenxiong Zhang, Dr. Weixing Zhao, Dr. Sen Li, and Miss. Yuanju Li for their timely assistance, the valuable suggestions to my doctoral study and daily life. I also owe my gratitude to my colleagues in our Lab, who gave me many helps and assistance. Thank you all very much for making my life easier and better in Japan.

Finally, I am forever indebted to the ceaseless support from my family, my parents, and my parents-in-law in all respects. Especially to my wife Lin Ma and daughter Zhaoge Yu, without your love and encouragement, I could not have the confidence and determination to complete the Ph.D. program.

Han Yu

Feng's Lab, Department of Advanced Materials Science

Faculty of Engineering and Design

Kagawa University, Kagawa, Japan

March 2022